FOREWORD

The work presented in this report was performed by Goodyear Aircraft Corporation, Akron, Ohio, under the authority of Project 6065, Task 606506, entitled "Feasibility Study for a Balloon Type Stabilization and Deceleration System for High-Altitude and High-Speed Recovery," and Air Force Contract No. AF33(616)-8015.

This is Part I of the contract. Mr. S. Metres, Flight Accessories Laboratory, Aeronautical Systems Division, served as contract monitor.

The authors and contributing personnel of Goodyear Aircraft Corporation who cooperated in the research and preparation of this report were F. R. Nebiker, project engineer; A. C. Aebischer, associate project engineer; J. Schlemmer, trajectory analysis; J. J. Graham, design; D. T. Wight, instrumentation and ground facilities; M. Davidson, telemetry; and Dr. R. S. Ross and F. Bloetcher, consultants.

ABSTRACT

Feasibility of using an inflatable sphere as an aerodynamic decelerator and stabilizer was previously established by experimental wind tunnel tests and limited free-flight tests. To acquire further full-scale test data, additional free-flight tests were conducted. These tests were in the subsonic, transonic, and supersonic speed regimes at altitudes ranging from 100,000 to 170,000 feet. This field test program included six missions demonstrating recovery of a 500-pound test missile utilizing a deployable fabric sphere with a nine-foot inflated diameter.

This report has been reviewed and is approved.

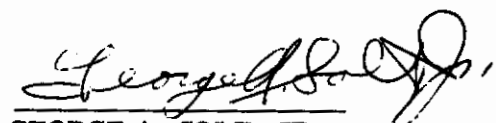

GEORGE A. SOLT, JR.
Chief, Retardation and Recovery Branch
Flight Accessories Laboratory

RECOVERY MISSION - BALLUTE AND PAYLOAD

TABLE OF CONTENTS

TABLE OF CONTENTS (Continued)

LIST OF ILLUSTRATIONS

LIST OF TABLES

SECTION 1

INTRODUCTION

Goodyear Aircraft Corporation (GAC), under Contract No. AF33(616)-8015 with Aeronautical Systems Division, Air Force Systems Command, has completed a study of inflatable balloon type drag devices for Mach 10 flight regime. The study is an extension of an applied research study to determine the feasibility of these drag devices for applications such as first-stage deceleration of emergency escape capsules, booster assemblies, missile components, and others.

High-speed, high-altitude flight dictates the need for new methods of stabilization and deceleration for successful recovery. Earlier investigations by GAC, including feasiblity study of an inflatable type stabilization system for high-altitude and high-speed recovery, indicate that this system is both feasible and practical for this use.

To establish more complete data and specify general requirements for these drag devices, the contract was issued for (1) a determination of the functional and performance characteristics in the transonic and supersonic speed regime and (2) a study supported by supersonic and limited hypersonic wind tunnel and laboratory tests to determine the feasibility of extending the operational capabilities into the Mach 10 flight regime.

The investigation was divided into two parts: Part I is concerned with functional and performance determination, and Part II is the preliminary Mach 4 to Mach 10 investigation. Part I, presented in this report, consists of a free-flight test program comprising four drop tests, using an Air Force test vehicle of the Cree type (overland recovery for transonic, overwater-boosted ground-launched for supersonic) to test the inflatable balloon type drag device, GA482-100, designed and manufactured by Goodyear Aircraft Corporation.

Test missions for the transonic speed test program were conducted at the Air Force Missile Development Center, Holloman Air Force Base, New Mexico. Four functional tests demonstrating deployment and operation consisted ot lifting the 500-pound test vehicle by stratospheric altitude balloons to floating altitude and releasing for a programmed descent. Deployment of the drag device above 75,000 feet was initiated by timing devices after a predetermined free-fall period. The test vehicles contained a four-channel telemetering system to measure and telemeter static pressure, ram pressure, internal balloon pressure, and balloon drag force.

Test missions for the supersonic speed test program were conducted at the Air Force Missile Test Range, Eglin Air Force Base, Florida. Two functional tests demonstrating deployment and operation consisted of propelling the test vehicle by booster rockets to the test altitude and speed. Test conditions were programmed to include Mach 1.5 at 135,000 feet and approximately Mach 4 at an altitude required to develop a dynamic pressure of 10 psf. Deployment of the drag device was initiated by a timing device during ascent. The test vehicles contained a five-channel telemetering system to measure and telemeter differential (dynamic minus static) pressure, shock force, drag force, test vehicle acceleration, and balloon pressure.

Work under the program started in April 1961 with preparation of drawings for fabrication of the Ballute assemblies, and awarding of subcontracts to Winzen Research for construction of the stratospheric balloons and to Cook Research for refurbishing of Cree Missiles and field test support at Holloman Air Force Base and Eglin Air Force Base.

Manuscript released by the author September 1962 for publication as an ASD Technical Documentary Report.

SECTION 2

FREE-FLIGHT TESTING OF INFLATABLE BALLOON TYPE DRAG DEVICES (BALLUTES) IN THE TRANSONIC VELOCITY RANGE

A. GENERAL DISCUSSION

1. Contract Requirements

In accordance with the specifications of the contract, which have been outlined in the introduction, the testing was accomplished at Holloman Air Force Base, New Mexico. The test item, a nine-foot-diameter Goodyear Aircraft Corporation Ballute, was packaged in a container attached to the aft part of a Cree test missile. This assembly, as well as ancillary equipment, was lifted to an altitude of 100,000 feet by a 134.6-foot diameter, 1,000,000-cubic-foot stratospheric balloon filled with helium. Upon reaching floating altitude, the test item was released and allowed to free-fall until a dynamic pressure of 10 psf had been developed. At this time the Ballute was deployed, and the operational data was acquired. Final recovery of the system was accomplished by an eight-foot-diameter parachute.

2. Trajectory Analysis

In accordance with contract requirements, the Ballute was to be deployed at a dynamic pressure of 10 psf at an altitude of not less than 75,000 feet. The weight of the test item was to be 500 pounds:

$V_0 = 0$

$H = 100,000$ feet

$W = 500$ pounds

$q = 10$ psf

To obtain the ballistic coefficient for the free-fall, subsonic drag data was taken from Reference 1. Using configuration $N_1\ B_2\ F_{20-4}$ from Reference 1, the total drag coefficient C_{D_T} based on a 9-inch diameter is

$C_{D_T} = C_{D_F} + C_{D_b} = 0.55 + 1.15 = 1.65$ at $M = 0.60$,

$A = 0.785\ (9/12) = 0.441$ square feet,

$$R_N \text{ at } 90,000 \text{ feet} = V\ell/\gamma = \frac{0.6(983)\ (9/12)}{5.8 \times 10^{-3}} = 7.6 \times 10^4$$

where γ is kinematic viscosity in ft^2/sec,

and $W/C_DA = 687$.

Using $W/C_DA = 700$, the free-fall trajectory shown on page 56, graph 29 of Reference 2 was used to determine the test point at $q = 10$ psf.

Altitude, velocities, and time from graph 29 of Reference 2 were used in computing the q value at various altitudes. From $q = (1/2)\rho V^2$, it was determined that $q = 10$ psf at 93,000 feet after 21.5 seconds of free-fall from 100,000 feet. Figure 1 depicts the plotted trajectory.

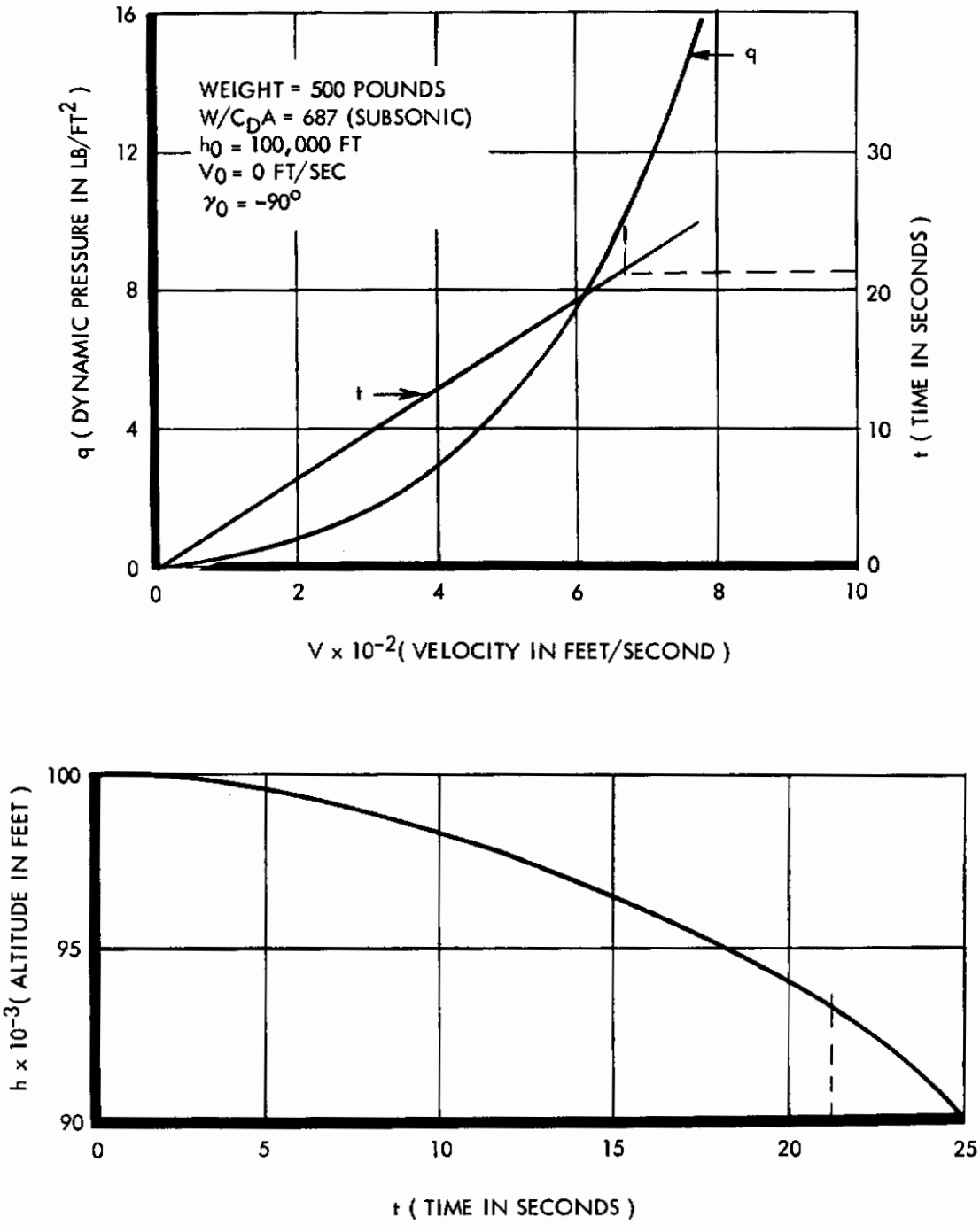

Figure 1. Vertical Drop Trajectory

3. Performance Parameters

The feasibility of Ballute stabilizer-decelerator in the transonic velocity regime is dependent upon a composite of several functional and performance parameters that are now defined for purposes of this report.

a. Stability. Stability is the aerodynamic characteristic of a Ballute that causes it to follow the line of flight of the payload. It is measured in terms of the amplitude and frequency of its deviation from this line of flight and the degree of aerodynamic stability or instability thereby imparted to the payload.

b. Drag Coefficient. Drag coefficient is the decelerating efficiency of the Ballute defined in terms of percent of the product of the dynamic pressure and the area of the Ballute.

c. Inflation and Deployment. Inflation and deployment are the functional and performance characteristics of the Ballute from the time of initiation to steady-state operation. This parameter is measured in terms of

(1) The reliability of the system which frees the Ballute from the launch canister.

(2) The speed with which the Ballute inflates.

(3) The speed with which the Ballute is deployed to its maximum distance aft of the payload.

(4) The ratio of the weight and volume of the inflation components to the weight and volume of the payload.

(5) The stability of the complete system during this period.

d. Effective Trajectory Segment. Effective trajectory segment is that portion of the recovery trajectory during which the Ballute system satisfies the mission requirements. This parameter may be measured in terms of

(1) Initial and terminal velocities

(2) Altitude range limits

(3) Structural integrity of the Ballute

B. DATA ACQUISITION

1. Stability

Stability of the system is recorded optically by the on-board camera which covers the first 36 seconds of the Ballute operation. By analyzing the film from this camera, these items can be expressed numerically:

(1) Ballute rotation rate in rps

(2) Deviation from flight line in degrees

(3) Frequency of oscillation in cps

(4) Stability of Cree missile with respect to "fixed" reference points such as the ascension balloon and ancillary equipment parachute.

The ground-based tracking cinephototheodolite cameras also afford examination of the same performance characteristics in so far as the resolution of the film allows.

2. Drag Coefficient

The efficiency of the drag device is expressed in terms of drag coefficient (C_D), which is equated

$$C_D = \frac{2F_D}{\rho V^2 A}$$

where

F_D = drag force in pounds,

ρ = atmospheric density in slugs per cubic foot,

V = velocity in feet per second,

A = πR^2, area of the drag device in square feet

where R is the radius of the Ballute at its equator.

The drag force is obtained by telemetered values of the loads being applied to the tensiometer by the drag of the Ballute.

The density is computed as described on page 41.

The velocity is determined by the position versus time data acquired by the cinephototheodolite and radar installations.

The area (A) of the fully inflated Ballute is measured prior to the test.

3. Inflation and Deployment

The on-board camera records the following events:

(1) The flash of the shaped charge canister separation explosion

(2) The opening characteristics of the Ballute canister

(3) The rate of inflation of the Ballute

(4) The rate of deployment by the reel

(5) The stability characteristics of the Ballute during this period

4. Effective Trajectory Segment

The Ballute is performing its mission properly only as long as inflation is complete. A determination of the fullness of the Ballute is obtained optically and recorded by both the cinephototheodolite and on-board camera films. Another indication of inflation is the telemetered internal pressure of the Ballute compared to the external static and dynamic pressures.

C. AIRBORNE EQUIPMENT

The complete airborne package for the Holloman Air Force Base drop tests consisted of the ascension balloon, ancillary equipment, a Cree Missile, and the GAC package as shown in Figures 2 and 3. A description of package items and a programming sequence are presented in the following paragraphs.

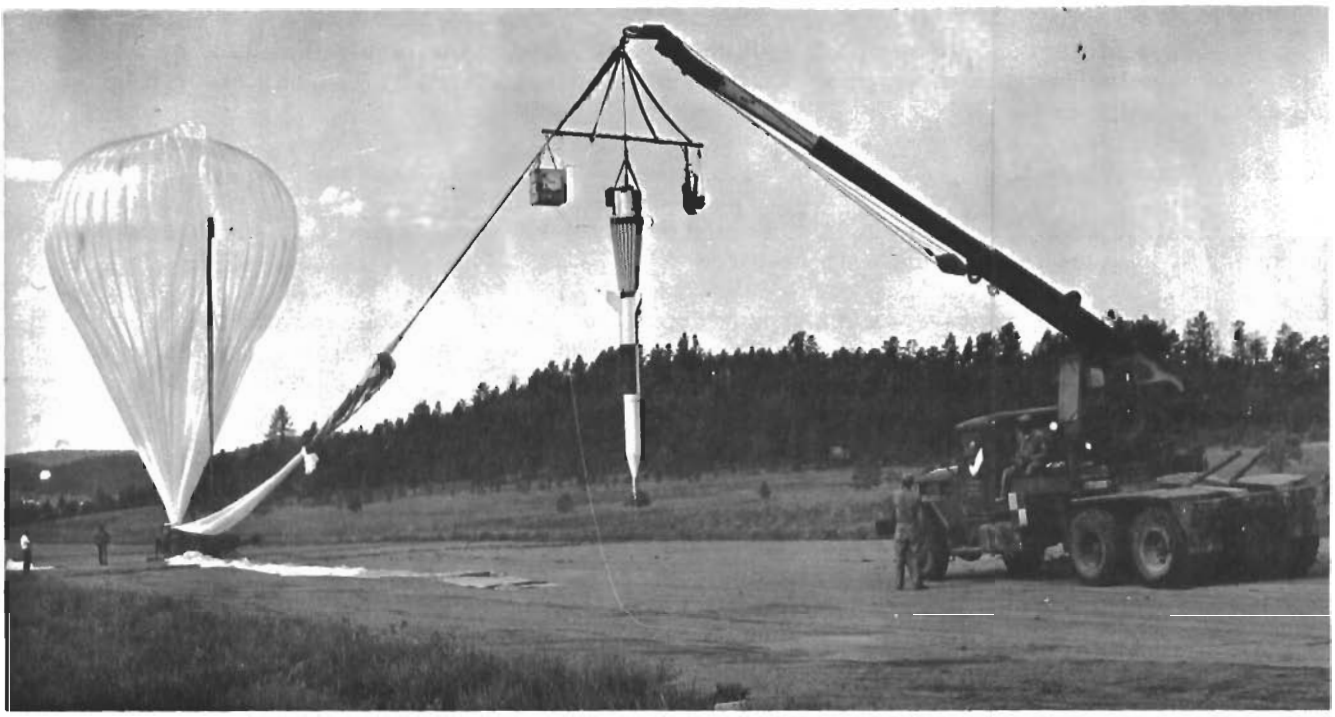

Figure 2. Airborne Package Ready for Launch

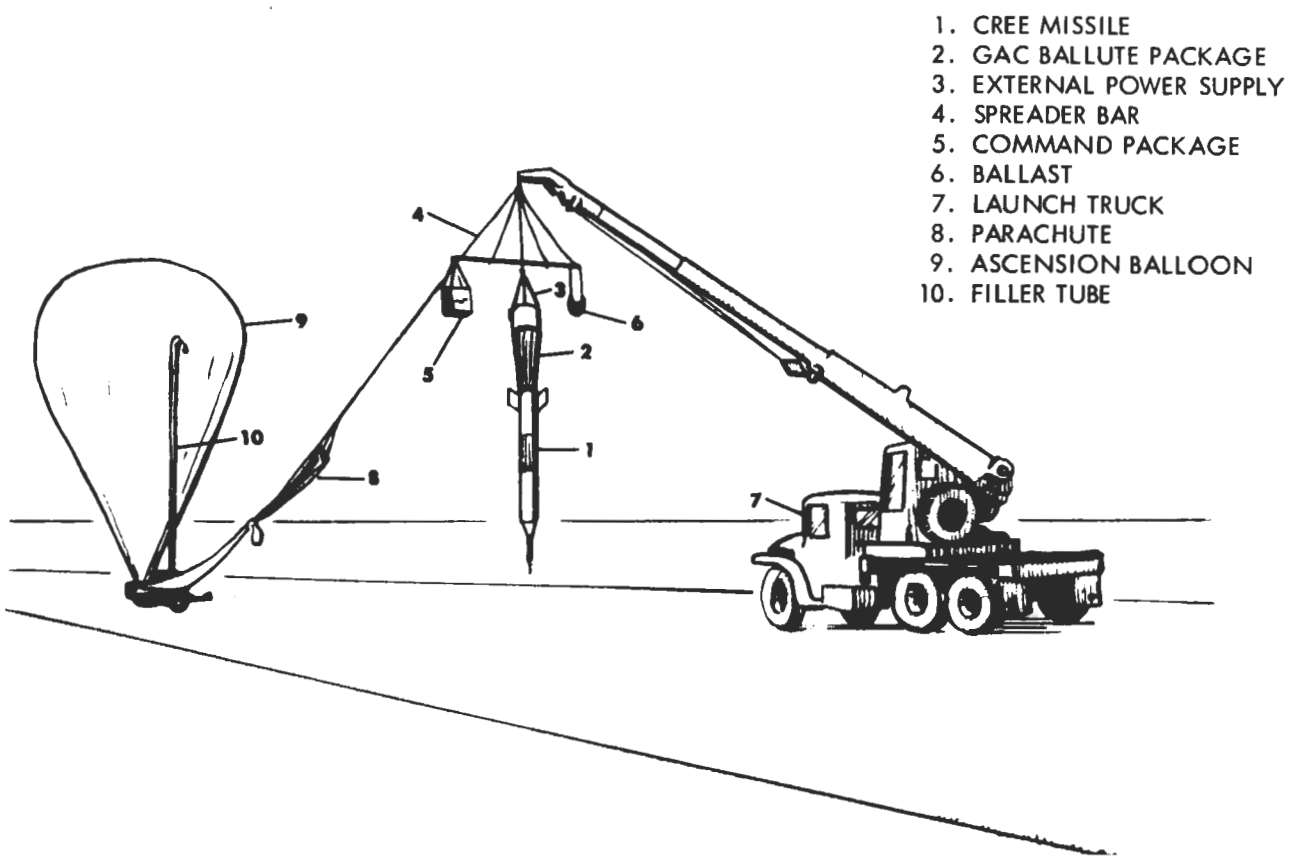

Figure 3. Launch Configuration

1. Ascension Balloon

The test item and its auxiliary equipment were lifted to the required altitude by a 134-foot-diameter polyethelene balloon weighing 315 pounds and manufactured by Winzen Research Inc of Minneapolis, Minnesota.

2. Ancillary Equipment

In addition to the test item, a command package, an external power supply, and a separate recovery system for these items were required.

The command package was suspended from one end of a spreader bar and balanced by ballast at the other end. The external power supply was mounted at the center of the spreader bar.

The command package consisted of a radio receiver and relays; its function was

(1) To close the external power circuit five minutes prior to release of the test item.

(2) To switch to internal power one minute before release of test item.

(3) To signal timer initiation and fire shaped charge separation. The shaped charge is part of GAC package.

(4) To signal release of ancillary equipment from the ascension balloon.

3. Cree Missile

The Cree Missile was the payload for purposes of these tests and is described dimensionally in Figure 4. The gross weight of the Cree is 363 pounds. The major components of this missile are

(1) Airborn instrumentation

(2) Ballast

(3) Recovery system

a. Airborne Instrumentation

(1) Description. The airborne instrumentation system was supplied to the contract as Government Furnished Equipment (GFE) and encompassed the following major subsystems:

(1) Transducers

(2) Programmer and Control Circuitry

(3) Telemetry Set

(4) Antenna

(5) Camera

(6) Power Supply

(a) Transducers. Test data obtained during the subsonic drop test series included shock force, internal Ballute pressure, dynamic pressure, and altitude.

Shock force data was obtained from a circular ring tensiometer developed by Cook Research Laboratories for parachute load measurement. The tensiometer formed a mechanical linkage

between the Cree missile and the aerodynamic decelerator. Bonded strain gages, Type C12-141-B, were used to convert the shock force experienced by the tensiometer into an equivalent electrical signal. A current schematic for the shock force channel is shown in Figure 5. A strain gage oscillator is employed to supply 8-kc, 3-volt power to the strain gage bridge circuit. Resistors R_1 and R_2 are used as calibrate resistors. The carrier amplifier is operated as a differential amplifier to provide 0 to 5 volt signals to the subcarrier oscillator.

Internal pressure of the Ballute was obtained from a Bourns pressure transducer, Model 409B20-0-2-502, with an operating range of 0 to 2 psi. The signal output voltage is of high level (0 to 5 volts dc) and is used for direct modulation of a subcarrier oscillator.

The remaining two phenomena measured during the test and telemetered to the receiving stations were static and dynamic pressures. These potentiometric transducers were Bourns Model No. 509.

(b) Programmer and Control Circuitry. A block diagram of the programmer and control system is presented in Figure 6. Command signals are received from the ground control center by the command receiver. The first of three received signals energizes a relay which in turn applies 28-volt d-c power to the telemetry instrumentation system. The second signal to be received actuates another relay which permits power to be supplied to the camera mounted external to the payload. The third received signal actuates a pyrotechnic device which results in separation of the payload from the balloon. At time of separation, the arming switch is closed, resulting in a changeover from external power to internal power, and the programmer is initiated. Schematic diagrams of the programmer and power control circuits are shown in Figures 7 and 8 respectively.

When the arming switch (S-4) is closed, power is applied to the timer motor and to one side of the control switches (T-2, T-3, T-5, T-7, T-8, and T-10) for the calibration sequence to the internal camera and for the pyrotechnic devices D_1 through D_6.

Timer switch contact T-10 remains closed until the timer has completed its cycle; then T-10 opens, removing internal power from the instrumentation system.

Referring to Figure 8, external power is supplied to the telemetry system through relay contacts 7 and 8 (filament supply) and contacts 11 and 12 (d-c converter supply). At time of payload separation from the balloon, the arming switch closes, removing external power and permitting the instrumentation system to be operated by the internal supply.

(c) Telemetry Set. The telemetry set was a standard four-channel system utilizing FM/FM techniques. A block diagram of the system is shown in Figure 9. Major components of the telemetry set were manufactured by Teledynamics Incorporated. The subcarrier oscillators were standard voltage controlled units of the Type 957. The crystal-controlled FM transmitter was Type 1001A, which provided three-watt power measured at the output. The Unerac Type 1401A functioned as a summing amplifier, a calibrator, and a regulator. It provided the 150-volt d-c regulated plate voltage for the oscillator units and +5 volts dc for transducers and distributed unregulated high voltage to the transmitter.

(d) Antenna. The transmitting antenna for the telemetered signals was a 1/4-wave end-fed stub which also doubled as a pitot tube for static and dynamic pressure measurements.

(e) Camera. Photographic coverage of Ballute deployment was provided by a Fairchild motion analysis camera, Model HS100, mounted inside the Cree Missile with the lens looking aft toward the aerodynamic decelerator. This camera provided approximately 20 seconds of observation during deployment of the Ballute.

A Fairchild 16-mm gun camera was attached to the side of the external power supply package to obtain photographic observation of the Cree Missile as it separated from the balloon mechanism.

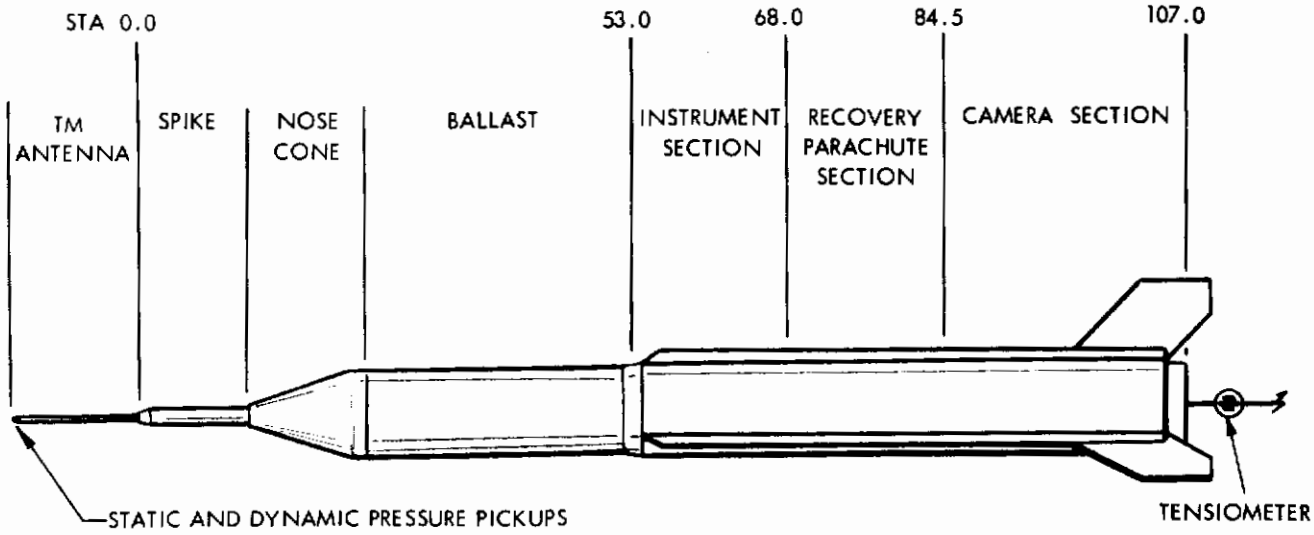

Figure 4. -57 Cree Missile

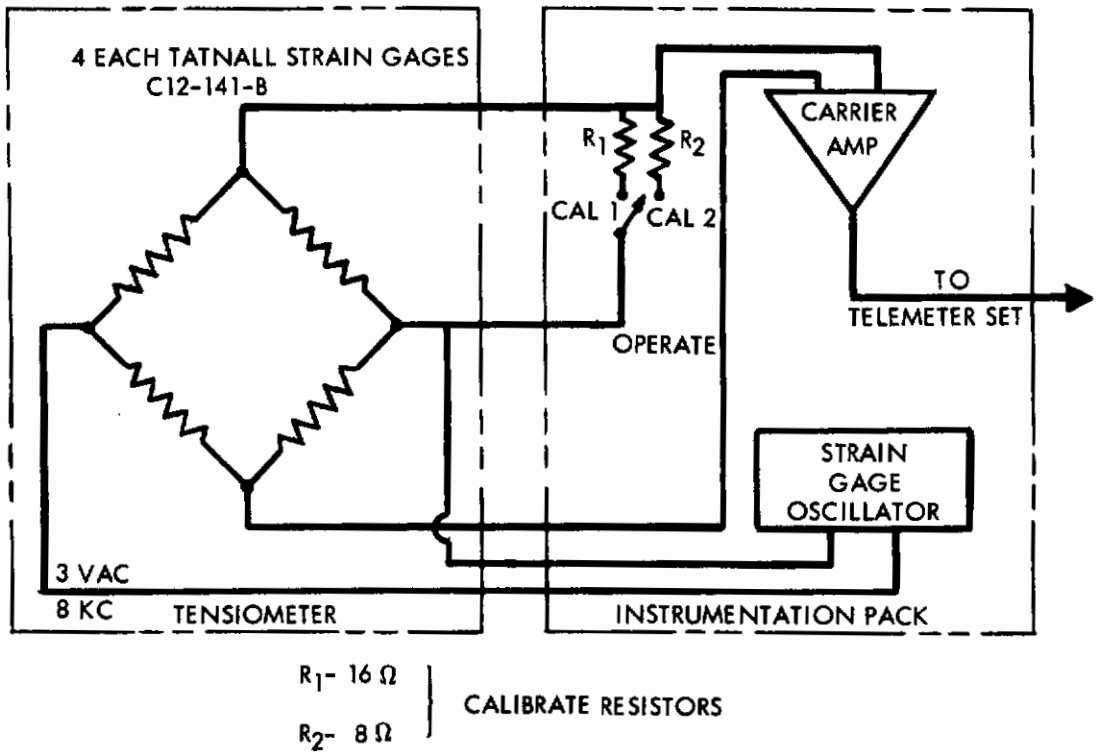

Figure 5. Shock Force Signal Conditioning Schematic

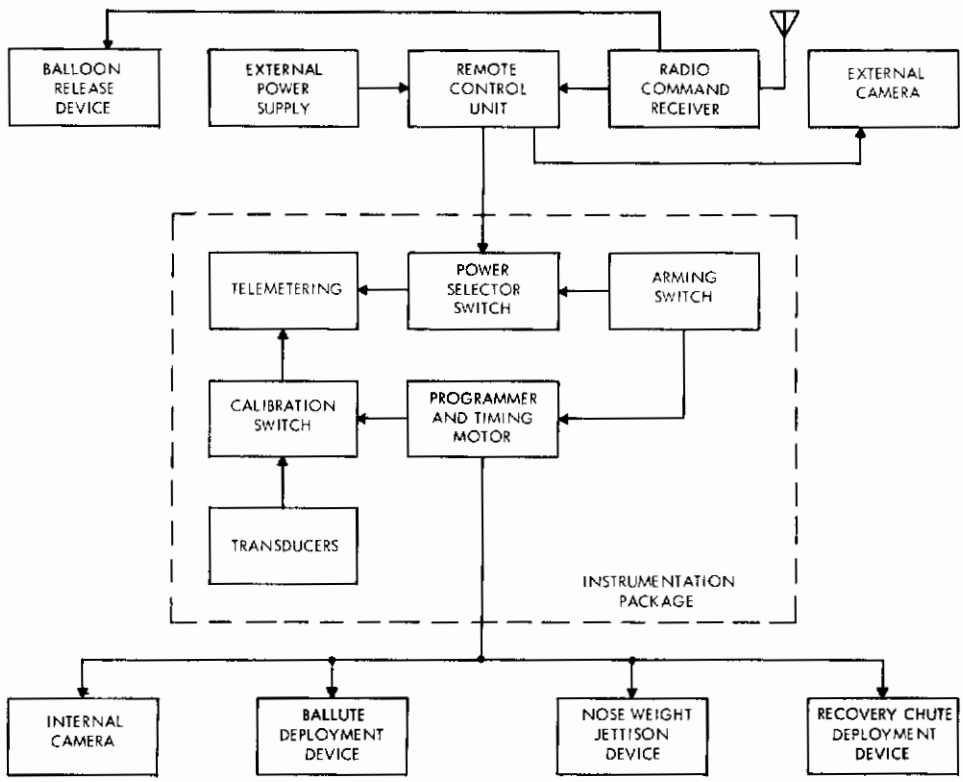

Figure 6. Control System Block Diagram

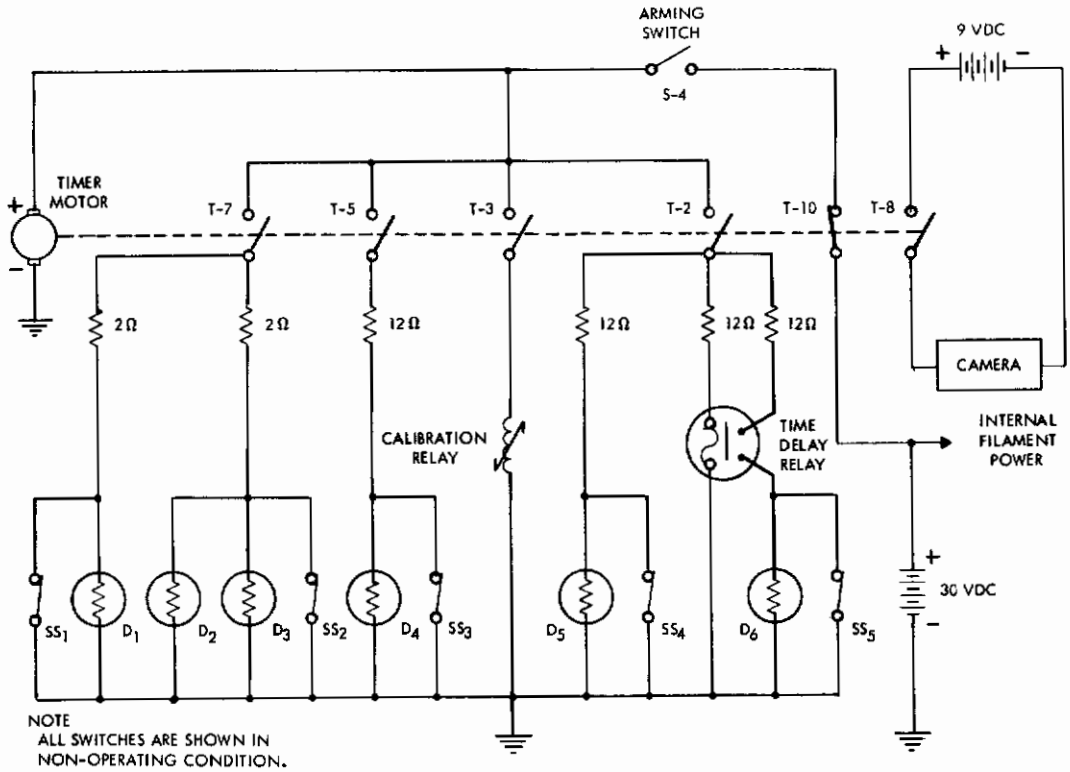

Figure 7. Programmer Schematic Diagram

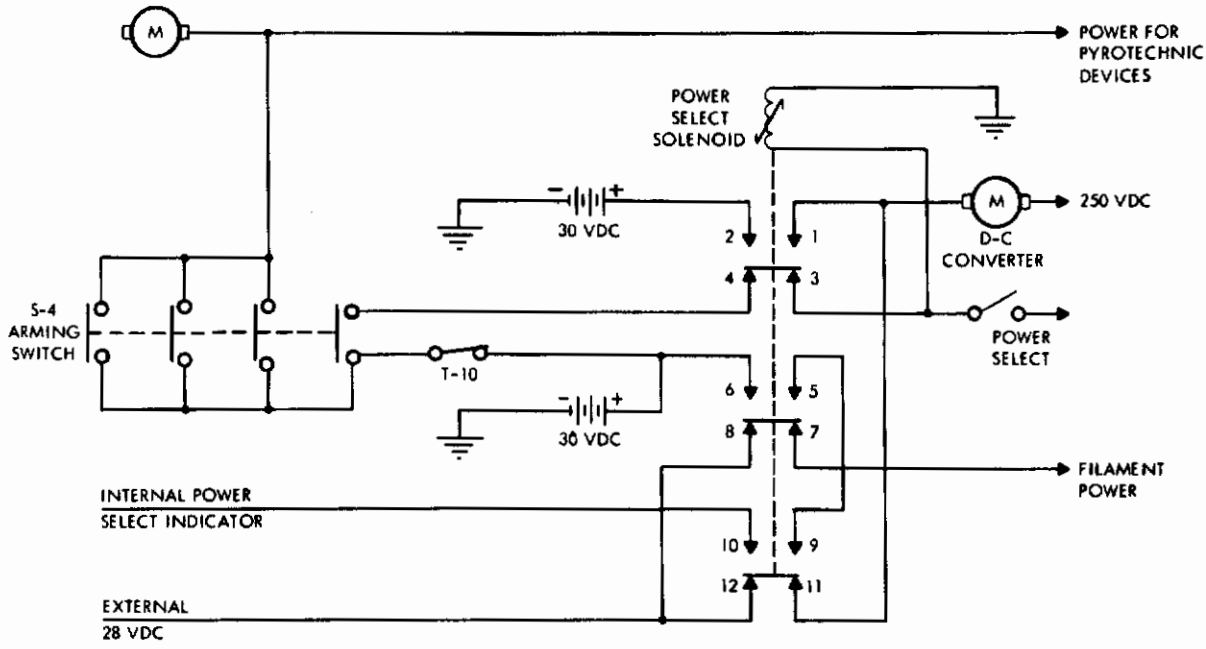

Figure 8. Power Control Schematic Diagram

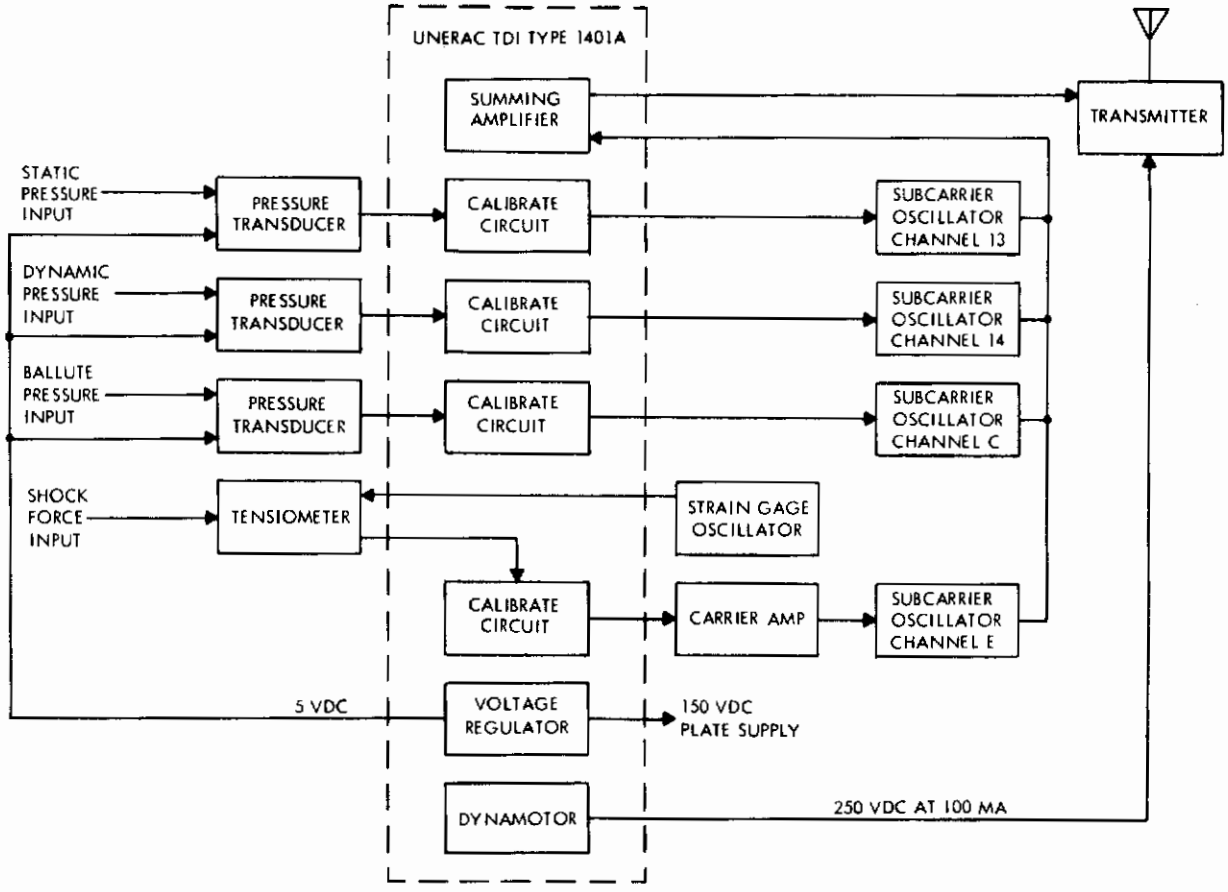

Figure 9. FM/FM Telemetry Set Block Diagram

(f) Power Supply. Electrical power for the battery heaters during balloon ascension and for the instrumentation system from T minus 5 minutes to T minus 0 was provided by a 28-volt d-c aircraft storage battery. The battery was housed in a metal container and surrounded with insulating material. The internal power supply consisted of a series of sealed nickel-cadmium batteries. Three separate battery packs were employed. One supplied 30-volts dc at 0.75 a-h power for filaments and transducers of the instrumentation system and for the pyrotechnic devices. A second battery pack supplied 30 volts dc at 1.75 a-h power for the d-c to d-c converter, which in turn provided the necessary high voltages for plate supplies. The third battery pack supplied the 9 volts dc required to operate the internally mounted camera.

(2) Tests and Performance. Prior to assembly of the instrumentation system into the Cree Missile, a functional test of individual components was made. Included in these laboratory tests were linearity and stability checks of the voltage-controlled subcarrier oscillators and carrier amplifier, frequency stability, distortion and power output of the transmitter, camera film speed, and timing accuracy of the program timing motor.

After installation, each channel of the telemetry system was calibrated by providing stimulus to the transducers and measuring the output frequency of the subcarrier oscillators.

Following system calibration for each channel of telemetered data, the output voltage from each oscillator unit was adjusted to obtain proper pre-emphasis and transmitter frequency deviation. When several subcarrier oscillators are used to transmit data over a common r-f link, the combined outputs are mixed in a summing amplifier. The composite output signal from the amplifier is then used to modulate the transmitted carrier frequency. Since in the presence of white noise *, interference increases as the 3/2 power of the subcarrier frequency, it is necessary to adjust the outputs of the higher frequency subcarrier oscillators for greater amplification than the lower frequency subcarriers. At the same time, distortion in the transmitted signal will occur if overdeviation of the transmitter is permitted, thereby limiting the output level from the subcarrier oscillators to approximately 2 volts rms. The nominal deviation recommended for TDI Model 1001A transmitter is ±125 kc. To determine the proper pre-emphasis for each channel, the following parameters were observed:

(1) Maximum signal level for highest channel was 2.0 volts rms.

(2) Minimum signal level for lowest channel was 0.5 volts rms.

(3) Maximum deviation of transmitter was ±125 kc.

Using the above guide lines, the output level (E_0) from each oscillator was established using the following equation:

$$E_0 = 1.5 \frac{f}{f_n} \sqrt{\frac{f_r}{f_{rn}}} + 0.5$$

where

f = subcarrier oscillator frequency,

f_r = intelligence frequency (modulation index = 5),

f_n = highest subcarrier frequency,

f_{rn} = highest subcarrier intelligence frequency.

Final adjustment for ±125 kc deviation of the transmitter was made at the output of the summing amplifier.

---

*Random noise in which the instantaneous amplitudes of the components of the noise are distributed in time in accordance with normal Gaussian distribution.

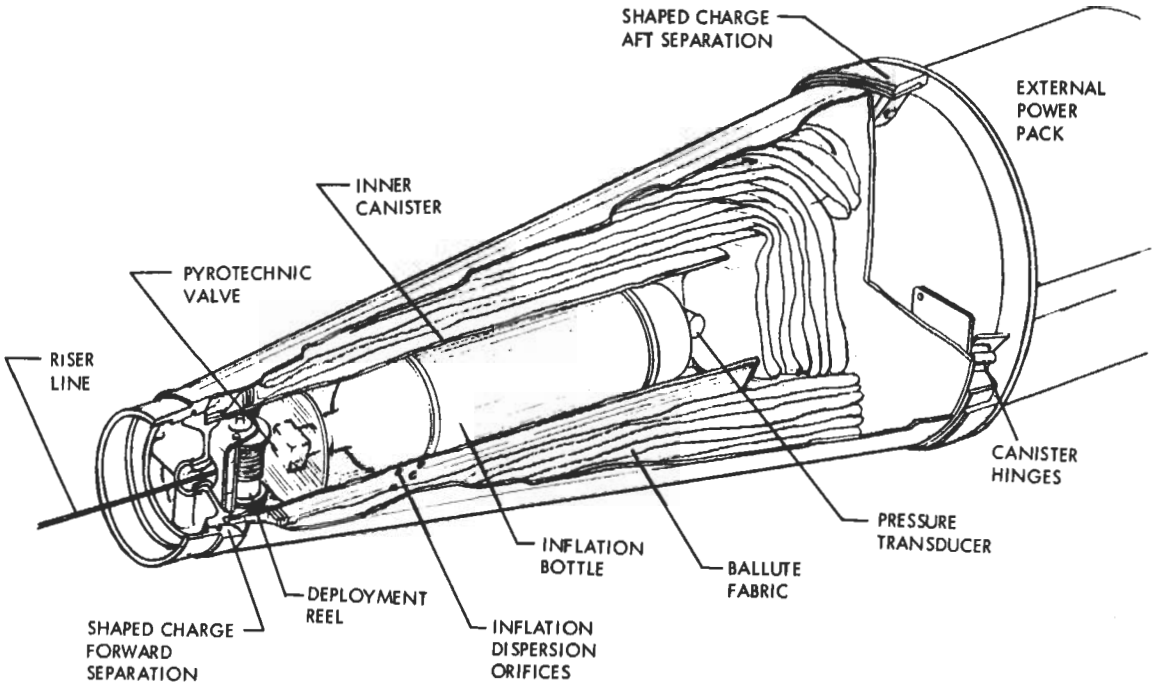

Figure 10. Test Item - GAC Ballute

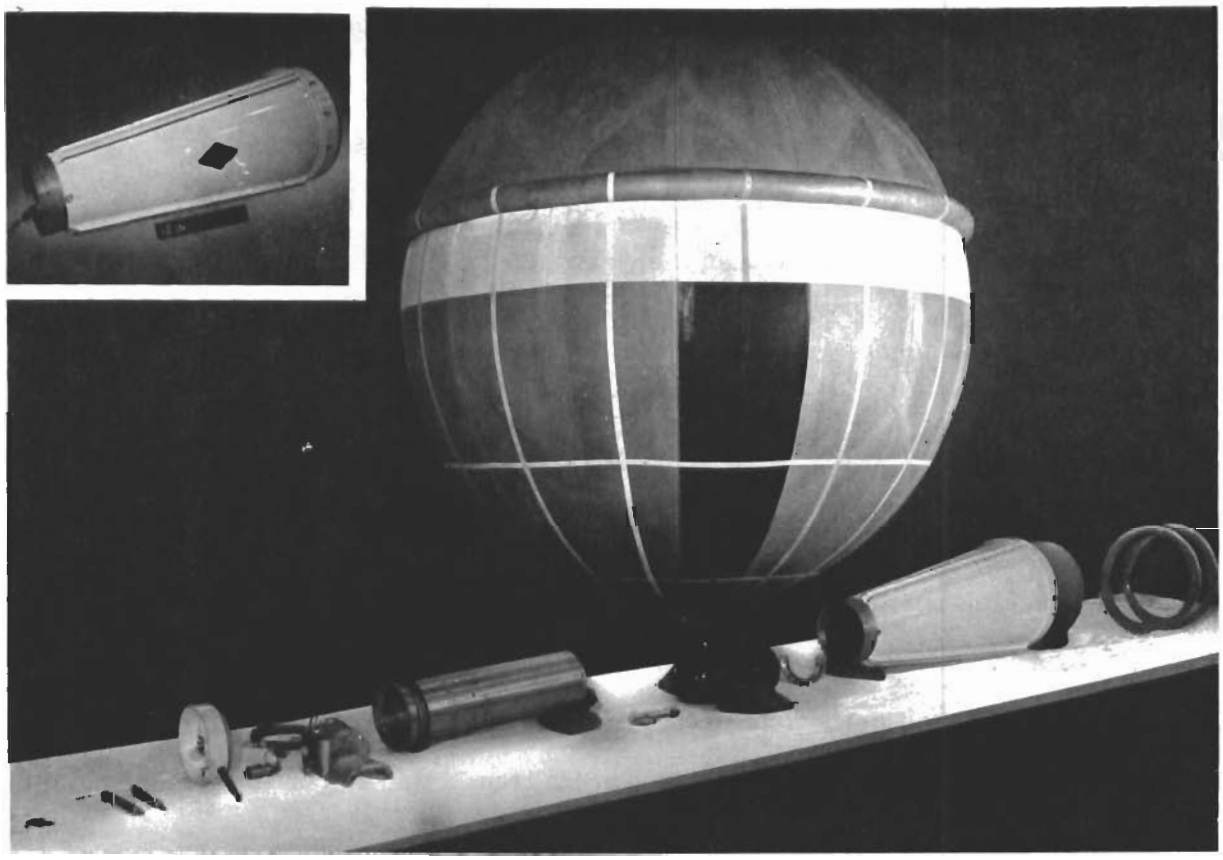

Figure 11. Components - GAC Package

An on-range test of the telemetry system was made just prior to the marriage of the missile to the lifting balloon. These tests were made utilizing AFMDC's mobile telemetry ground station facility. During the test, calibration signals were applied to the airborne instrumentation system. These were in turn received and recorded at the ground station.

The frequency limits of each subcarrier were set for a 6-1/2 percent deviation in lieu of the normal 7-1/2 percent. This was done to preclude loss of data due to oscillator drift causing full-scale signals to exceed band limits of the discriminators in the data processing equipment.

b. Ballast. The nose weight, 175 pounds, forms the forward portion of the missile and provides the ballistic coefficient necessary to develop a dynamic pressure of 10 psf within a predetermined time after test item release. The nose weight is pyrotechnically jettisoned after the test mission has been completed.

c. Missile Recovery. The same signal that releases the Cree ballast also pyrotechnically opens the parachute compartment in the side of the missile from which is deployed an eight-foot ribbon chute. The resultant impact velocity is approximately 90 to 100 fps.

4. GAC Ballute Package

The GAC Ballute package consists of a canister and Ballute (see Figures 10 and 11). Description and function of components are presented in the following paragraphs.

a. Canister. The enclosure that contains the packaged Ballute also provides a structural transition between the Cree Missile and the external power supply (see Figure 12). The aft portion of this canister contains a shaped charge that provides the means of separating the test package from the lighter-than-air system. The canister shell consists of three 120-degree segments of a truncated cone which are hinged to a common plate at the aft end as shown in Figure 12. Upon separation of

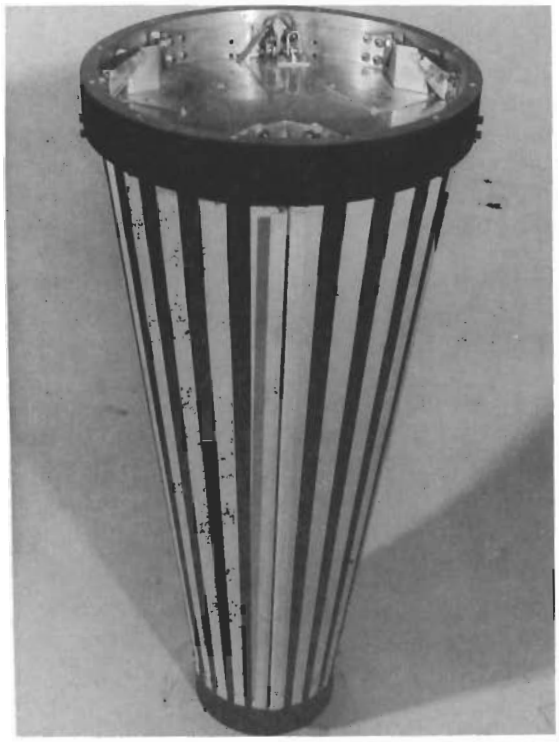

Figure 12. Canister

these segments from the Cree by another shaped charge, the canister is forcibly unfolded into a three-bladed aerodynamically stable shape (see Figure 22). The fabric of the Ballute is separated from the canister wall by a cotton sheath which is jettisoned upon deployment. The GAC Ballute package does not contain heaters; therefore, a thermodynamic investigation concerning temperatures at the drop test altitudes was made. As a result the missile was painted with 1/2-inch black stripes and 3/4-inch white stripes. This was necessary to control the heat absorption during exposure to solar heat. The complete thermodynamic investigation is presented in Appendix I.

b. Ballute. The Ballute comprises several major components which will be discussed separately:

(1) The fabric skin

(2) The suspension system

(3) The deployment reel

(4) The inflation system

(5) The pressure transducer

(1) Fabric Skin. The material is a neoprene-impregnated Dacron cloth with a gross weight, including hardware, of approximately 40 pounds. The spherical shape is fabricated in 16 axial gores and inflates to nine feet in diameter (see Figure 13). The "burble fence" or laminar flow separator, a 6-1/2 inch diameter torus located 15 degrees aft of the equator, serves as a stabilizing device in the subsonic velocity range.

(2) Suspension System. The Ballute is enclosed in an axial network of 16 stranded steel meridian cables that converge at each pole (see Figure 14). A single steel cable or riser line connects the Ballute to the tensiometer at the aft end of the Cree Missile. Prior to deployment this riser line is stored on the deployment reel inside the Ballute.

(3) Deployment Reel. The deployment reel (see Figure 14) allows the Ballute to move aft of the payload at a controlled rate without acceleration, thereby reducing the shock or snatch loads. The reel transfers the linear motion of the riser line to rotary motion in the drum. This rotary motion is converted again to linear motion in the form of piston motion within the drum. The piston pressure causes compression of a series of brake discs. The whole system is controlled by the flow of hydraulic fluid from one side of the piston to the other in such a way that the braking force rises in proportion to the rotation rate of the drum.

(4) Inflation System. Compressed nitrogen at 1950 psia is stored in a 300-cubic-inch bottle inside the balloon (see Figure 10). The bottle is equipped with a cartridge-actuated valve that is ignited as programmed by the timer within the Cree.

(5) Pressure Transducer. In order to provide continuous monitoring of the internal pressure of the Ballute, a pressure transducer is mounted on the aft end of the pressure bottle canister. The signal from this transducer is fed into the instrumentation section of the Cree, and the data is telemetered to the ground station.

5. Programmed Sequence

After a complete check-out of all systems within the test vehicle, the ancillary equipment and the test item are suspended from the quick-disconnect fitting at the end of the launch truck boom by a yoke of nylon straps (see Figure 3).

The ascension balloon is unrolled away from the launch truck with the ancillary equipment recovery chute and a length of riser line between the balloon and the suspension yoke. The ascension balloon is filled with helium through a six-inch-diameter polyethylene tube. When approximately

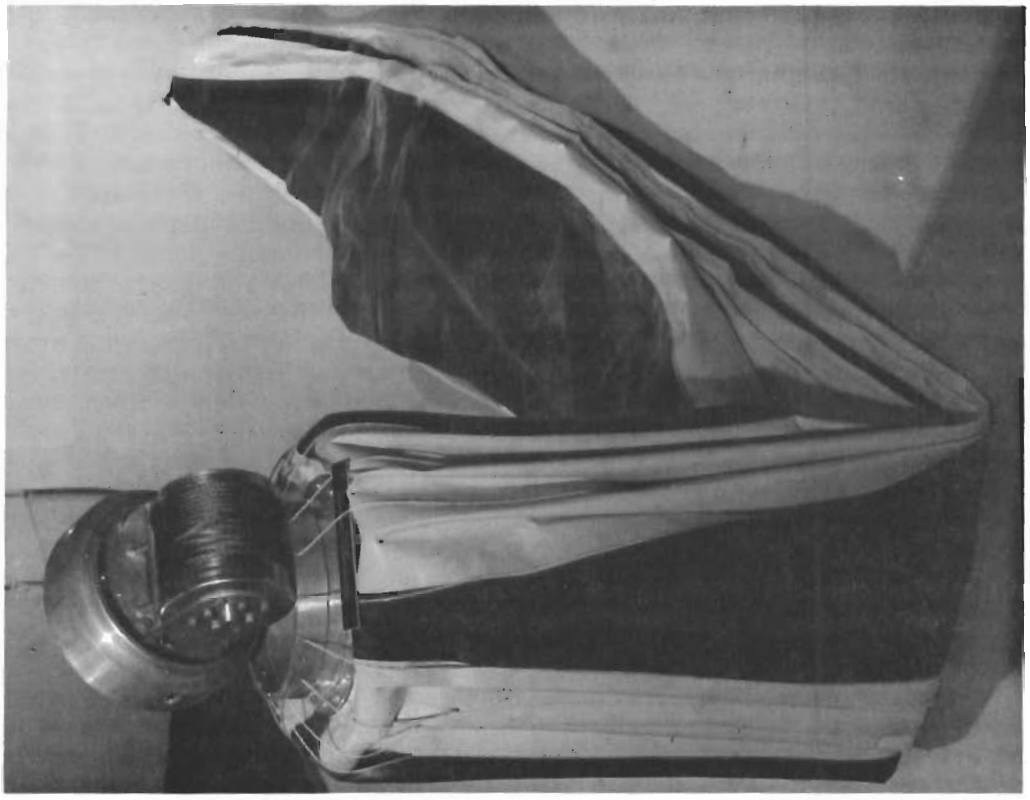

Figure 14. Deployment Reel and Ballute

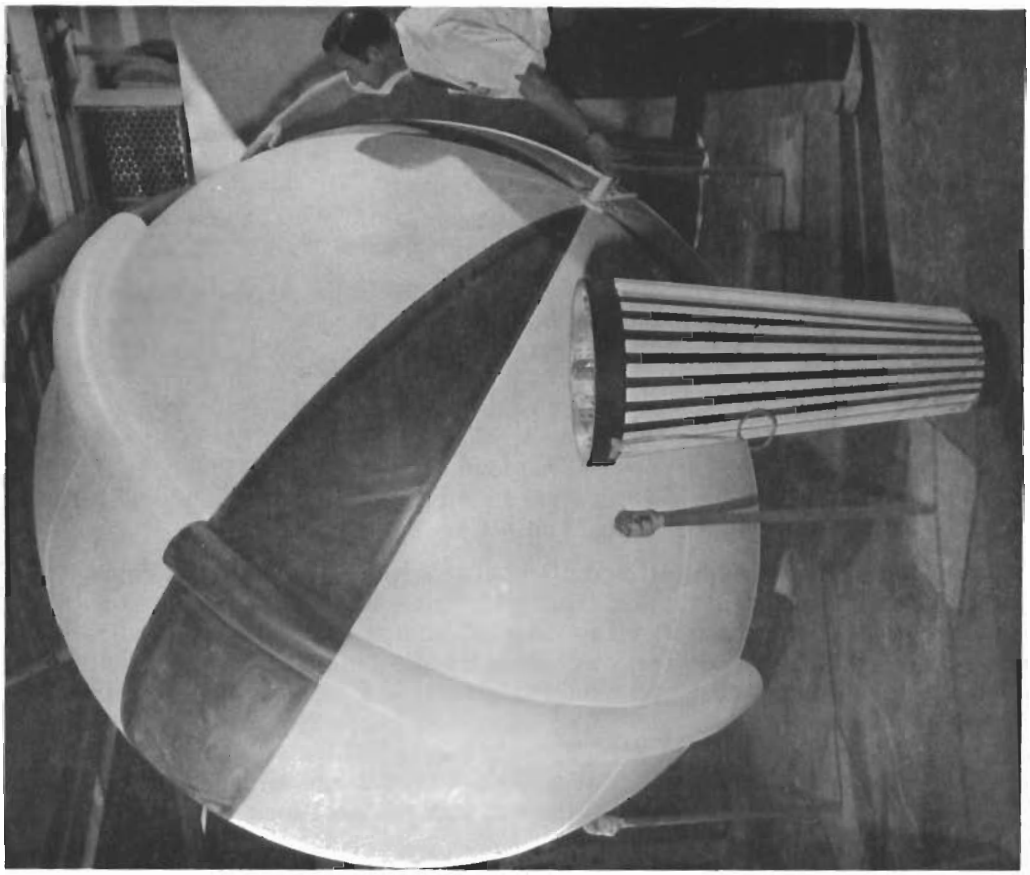

Figure 13. Inflated Nine-Foot Ballute and Canister

50,000 cubic feet of helium has been pumped into the balloon, the balloon is released and begins to rise, carrying with it the parachute and riser line (see Figure 15).

When the lift of the balloon has relieved the launch truck of the weight of the test item and when the riser line is almost vertical, the quick-disconnect is disengaged and the complete system begins its ascent at about 1000 feet per minute (see Figure 16). During ascent to float altitude, which requires about 90 minutes, a transmitter in the command package monitors the altitude. Skin-tracking radar and cinephototheodolite installations are now plotting the position of the system. When the system reaches float altitude (see Figure 17) and is approaching the desired impact area, five minutes prior to the test item release the command package is signalled to close the external power supply circuit. The telemetry is now energized and the signals calibrated. One minute prior to launch, the command is given to switch to internal power. At T - 0 the command is given to release the test item. The shaped charge is ignited, and the test item is severed from the external power supply package (see Figure 18). Within a reasonable time after T - 0, the command is given to cut down the ancillary equipment from the ascension balloon. This equipment is then recovered by its own parachute (see Figure 19). At the release of the test item, the timers in the Cree are activated and now control the remainder of the programming. The test item free-falls for 21.5 seconds until the dynamic pressure is approximately 10 psf (see Figure 20). After the predetermined free-fall, the timer activates the Ballute canister separation charge and the cartridge actuated inflation valve (see Figure 21).

The canister separates and "cloverleafs" behind the Ballute in an aerodynamically stable configuration whose ballistic coefficient is significantly lower than that of the test item (see Figure 22). As the Ballute inflates, aerodynamic drag builds up and unreels the riser line to its full length. The test point has now been reached, and the next 60 to 70 seconds of the flight will provide the required functional and operational data as depicted in Figure 23.

The nose weight of the Cree is jettisoned and the recovery chute deployed (see Figure 24), decelerating the missile to a terminal velocity of approximately 90 to 100 feet per second (see Figure 25). The impact shock is partially absorbed by ground penetration of the nose spike (see Figure 26). Chase planes and trucks are used for the final acquisition of the test item.

D. QUALITY ASSURANCE

1. Functional Testing and Shaped Charge Separation Systems

One forward and one aft separation ring was functionally tested; the aft separation ring was loaded with a ten-grain-per-foot charge. The charge proved excessive and resulted in multiple fracturing of the ring rather than cutting (see Figures 27, 28 and 29).

Upon the recommendation of GAC, the second specimen (forward separation ring) was loaded with a five-grain-per-foot charge. A good clean break was obtained (see Figures 30, 31, and 32), and this concentration proved satisfactory in all four drop tests.

2. Functional Testing of Deployment Reels

Tests were performed at various temperatures to functionally check reel operation for different valve settings and to ensure a constant deployment velocity. A 500-pound load was used for functional checks; however, to assure structural integrity, a drop was made with 1000 pounds. Test results are presented in Figure 33 and Table 1.

The drop test arrangement utilized a ±5g accelerometer which was connected to an oscillograph recorder and an electrically tripped timing circuit. The reel was cooled with dry ice. The quantity of dry ice was varied as required to maintain temperature. Temperature was maintained for one hour prior to performing the test. A thermocouple installed between the stationary portion of the reel and the mounting bracket was used to determine a monitor temperature.

a. Reel No. 1. The reel was filled with 30-weight oil, and the valve was set at zero or fully closed. The 200-pound load was raised 12 feet, 9-5/8 inches and attached to the reel cable. The load was released and fell approximately 20 inches, and the reel locked.

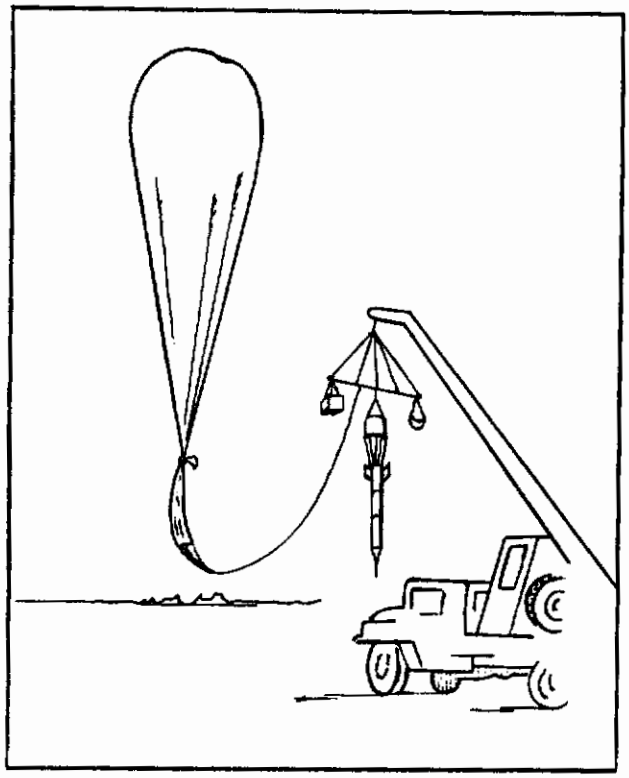

Figure 15. Ascension Balloon Release

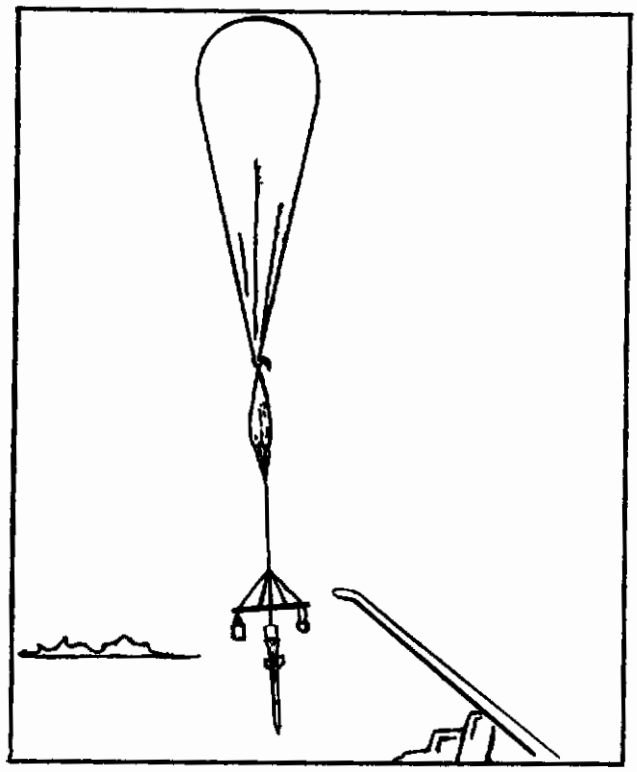

Figure 16. Launch

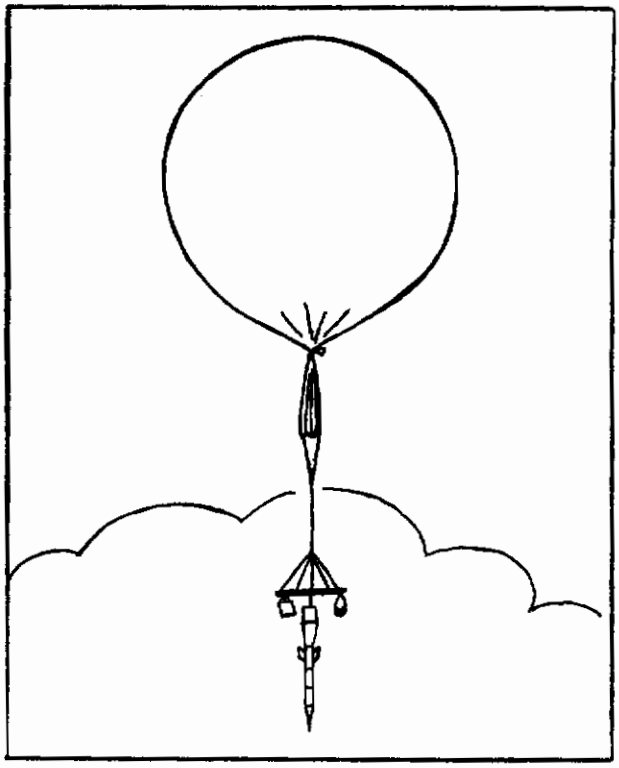

Figure 17. Float Altitude

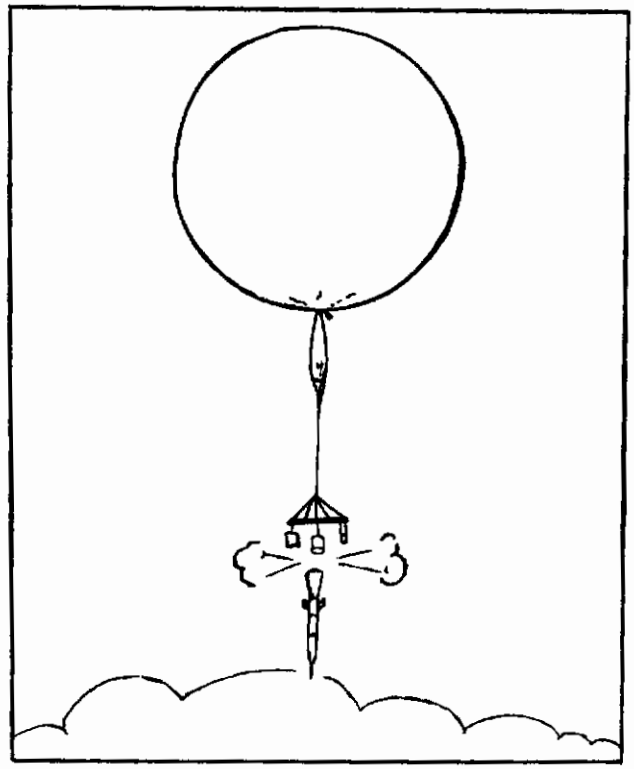

Figure 18. Test Vehicle Release

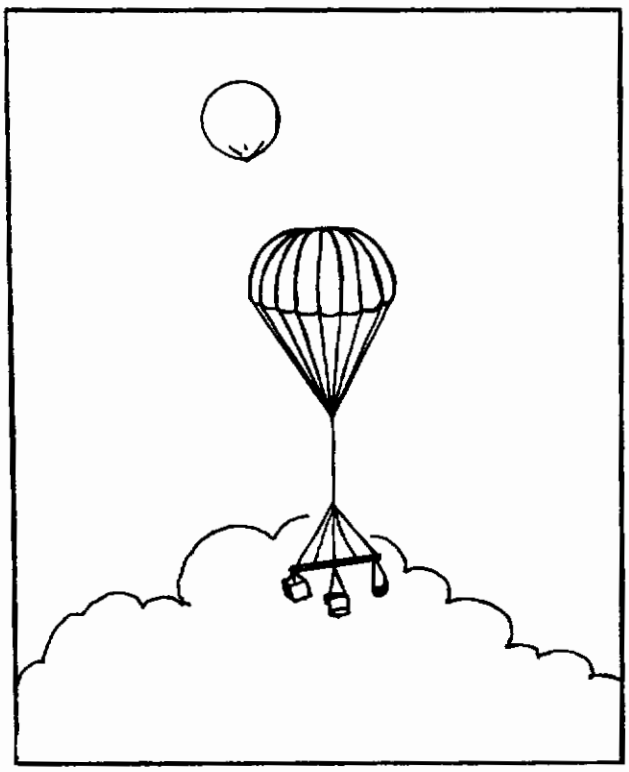

Figure 19. Command Package Recovery

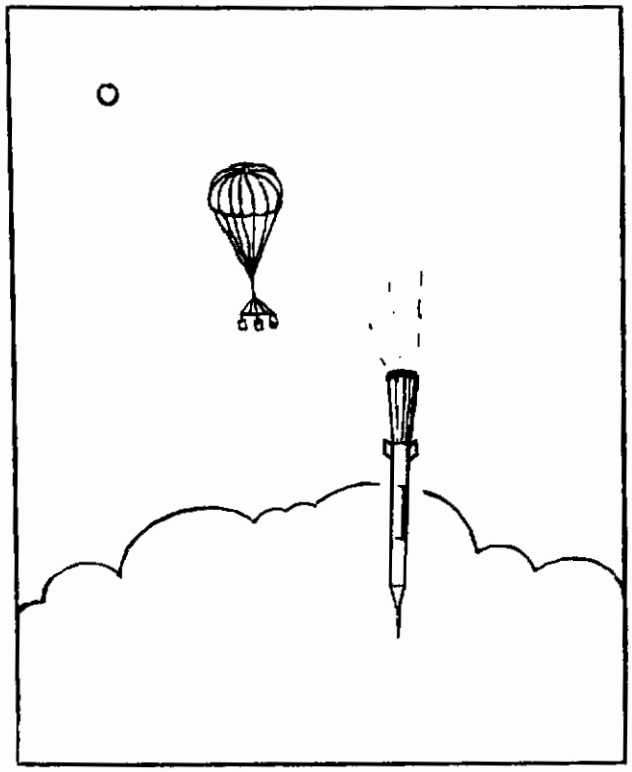

Figure 20. Free-Fall

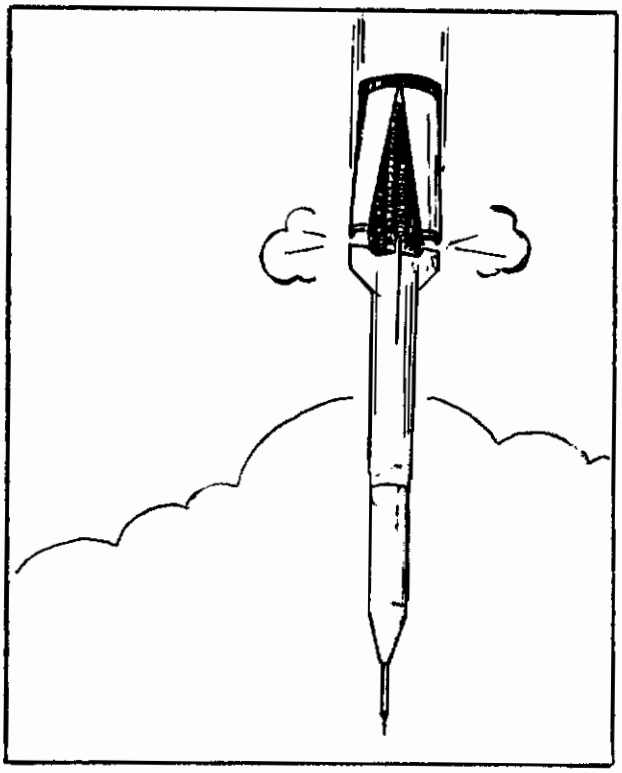

Figure 21. Canister Separation

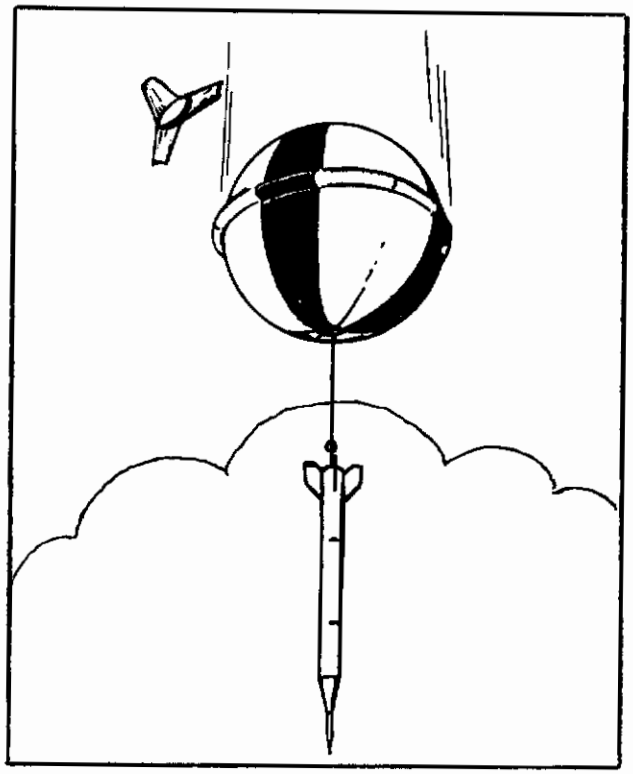

Figure 22. Inflation and Deployment

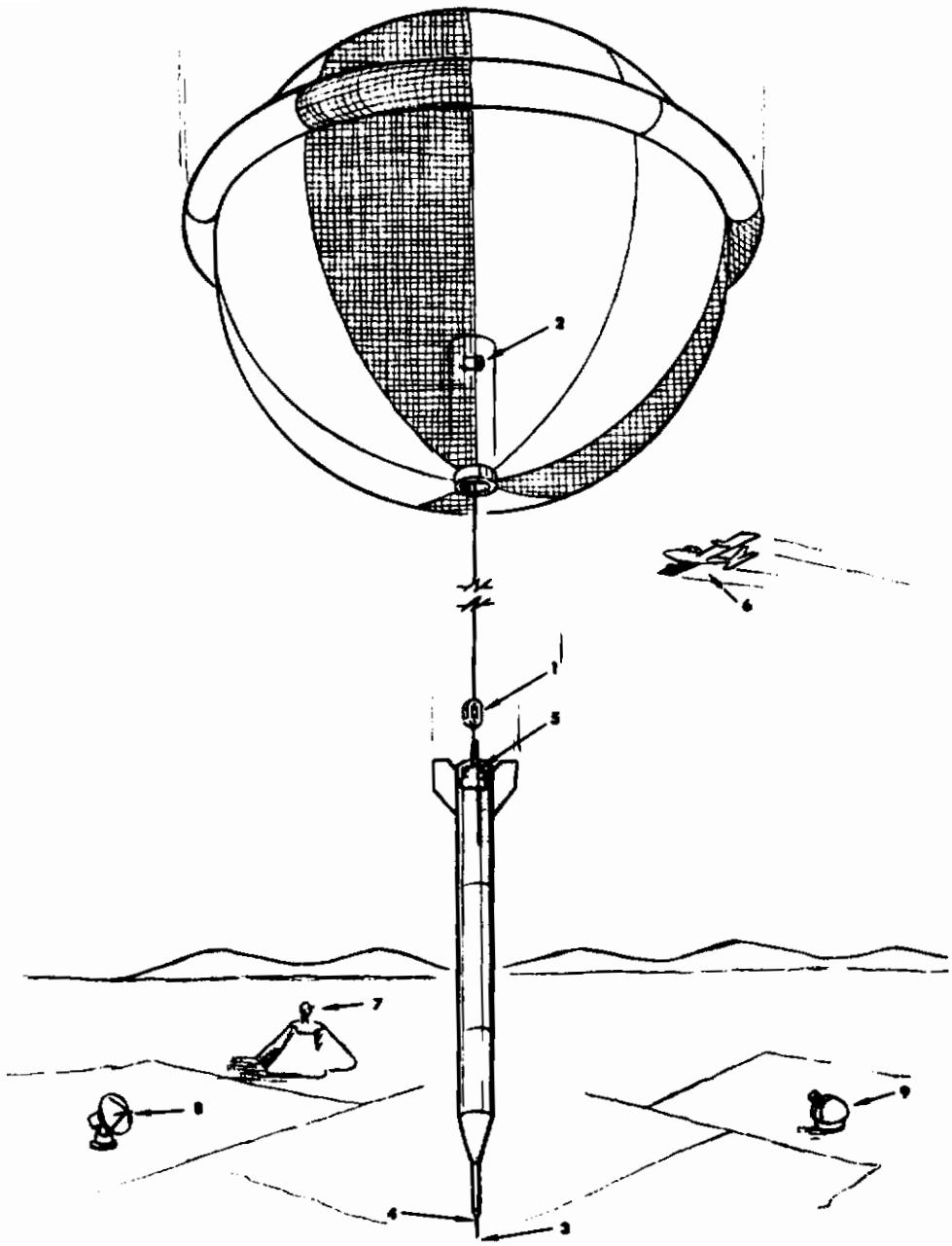

1. TELEMETRY DRAG FORCE, TENSIOMETER
2. TELEMETRY INTERNAL PRESSURE, TRANSDUCER
3. TELEMETRY DYNAMIC PRESSURE, PITOT TUBE
4. TELEMETRY STATIC PRESSURE, ORIFICE
5. ON-BOARD CAMERA
6. CHASE AIRCRAFT
7. TELEMETRY RECEIVER
8. RADAR - SKIN TRACKING
9. CINEPHOTOTHEODOLITE

Figure 23. Functional and Operational Data

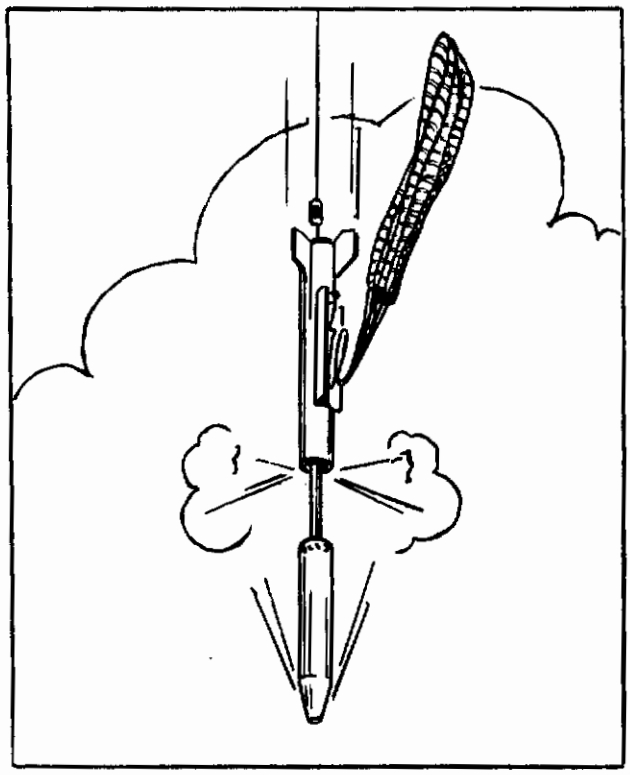

Figure 24. Ballast Release and Parachute Recovery

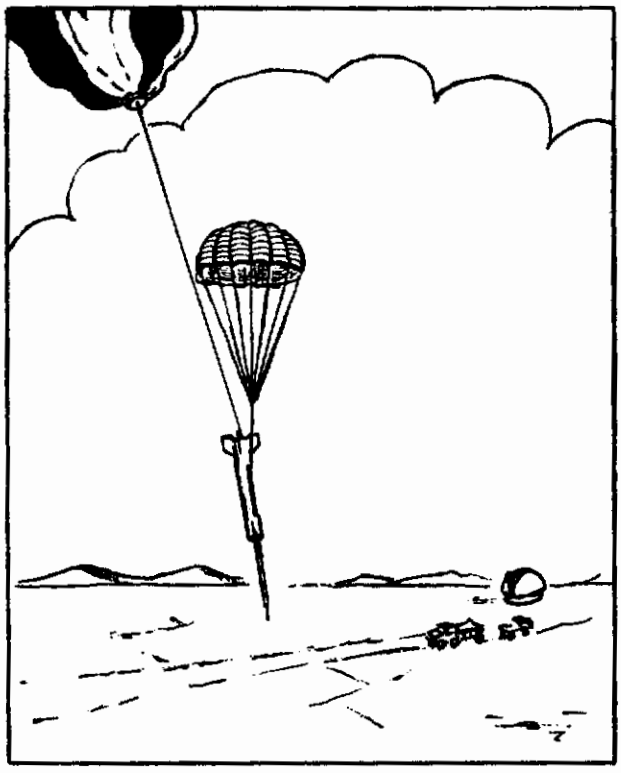

Figure 25. Cree Recovery

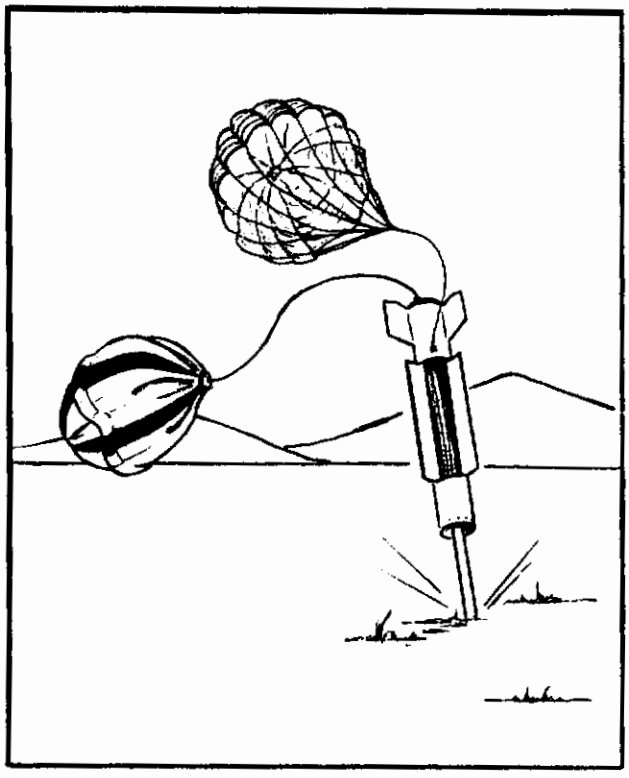

Figure 26. Impact

Figure 27. Aft Backup Ring

Figure 28. Forward Part of Aft Mounting Ring

Figure 29. Aft Part of Aft Mounting Ring

Figure 30. Forward Backup Casting

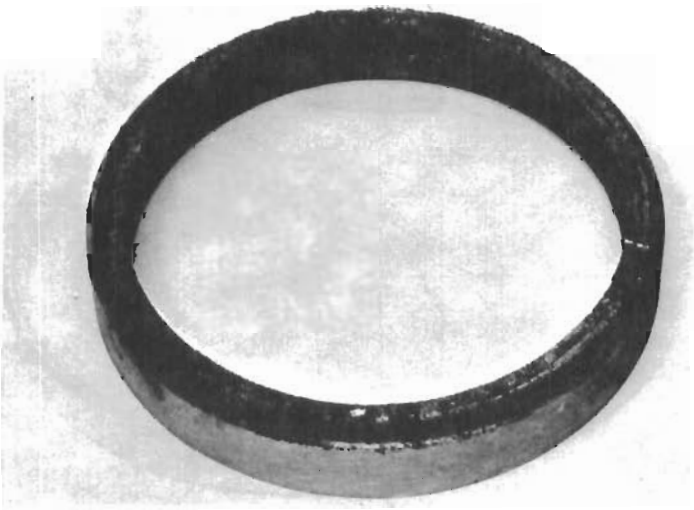

Figure 31. Forward Part of Forward Splice Ring

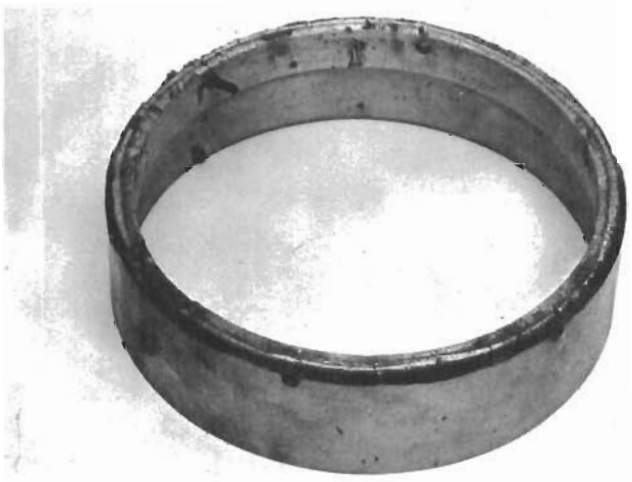

Figure 32. Aft Part of Forward Splice Ring

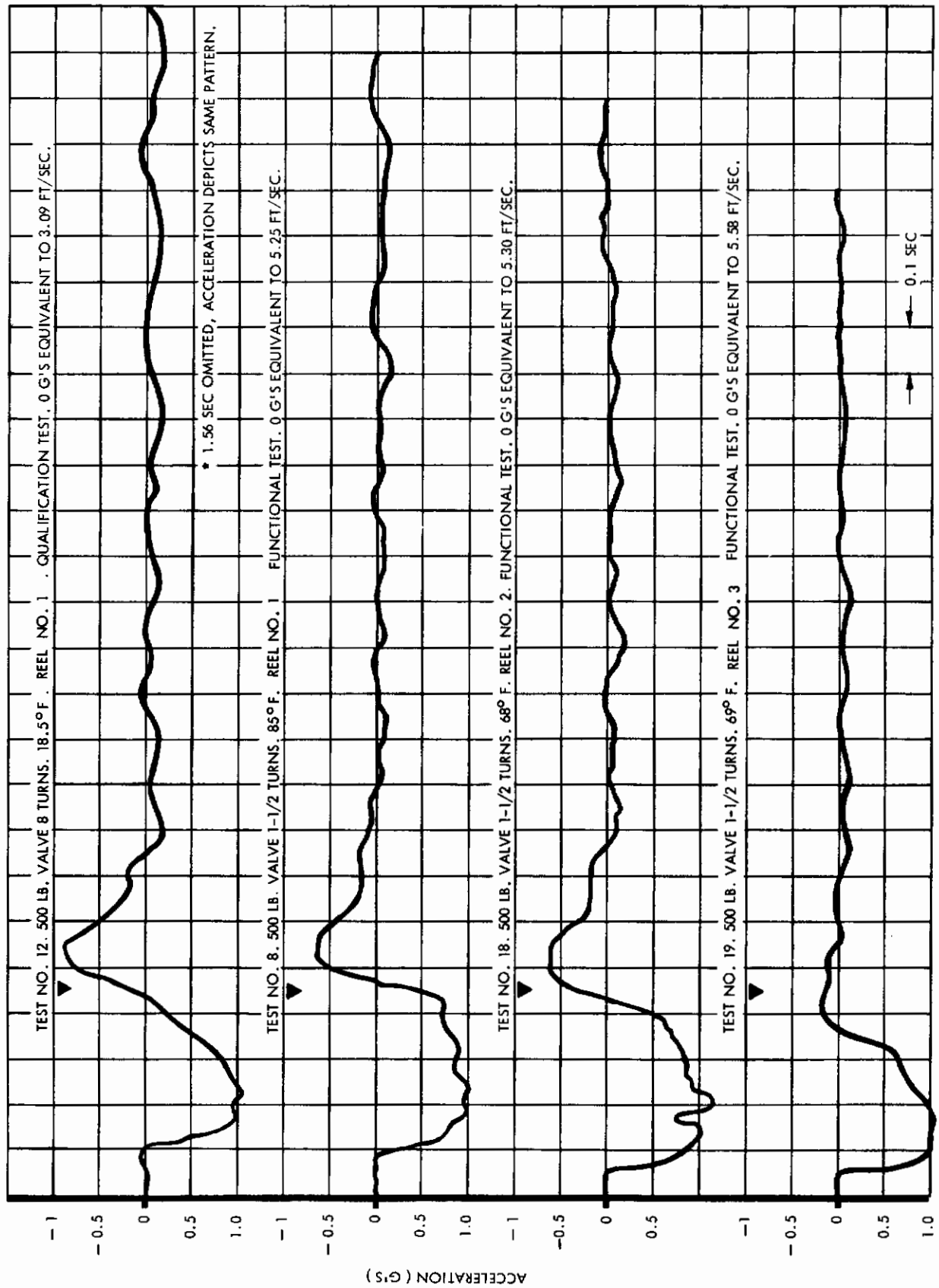

Figure 33. Acceleration Curves - Deployment Reels

Table 1. Functional Tests of Deployment Reels

TEST NO.	REEL NO.	FLUID	VALVE SETTING	TEMP	LOAD (pounds)	TIME (seconds)	VELOCITY (ft/sec)
1	1	30-weight oil	Closed	Ambient	200	**	0
2	1	30-weight oil	1 turn	Ambient	200	**	0
3	1	30-weight oil	≈ 8 turns	Ambient	200	**	0
4*	1	Brake fluid	2 turns	Ambient	200	3.95	3.23
5	1	Brake fluid	1 turn	Ambient	200	4.99	2.56
6	1	Brake fluid	0.5 turn	74°F	500	≈ 3.5	3.64
7	1	Brake fluid	1 turn	76°F	500	3.4	3.60
8	1	Brake fluid	1.5 turns	85°F	500	2.33	5.25
9	1	Brake fluid	1.5 turns	-34°F	500	28.43	0.43
10	1	Brake fluid	1.5 turns	-20°F	500	No data	No data
11	1	Brake fluid	1 turn	81°F	1000	2.65	4.62
12	1	Brake fluid	8 turns	18.5°F	500	3.96	3.09
13	1	Brake fluid	8 turns	30°F	500	3.33	3.68
14	1	Brake fluid	10 turns	25°F	500	3.65	3.35
15	1	Brake fluid	12 turns	29°F	500	3.3	3.71
16	3	Brake fluid	1.5 turns	69°F	500	1.88	6.5
17	3	Brake fluid	1.5 turns	73°F	500	1.81	6.77
18	2	Brake fluid	1.5 turns	68°F	500	2.31	5.3
19	3	Brake fluid	1.5 turns	69°F	500	2.19	5.58

*The piston was reworked; 0.004 inch was removed from the outer diameter.
**Load only dropped approximately 20 inches; the timing circuit was not tripped.

The cable was rewound, and the load was raised to drop height. The valve was opened one turn, and the load was released. The load again traveled approximately 20 inches, and the reel locked.

The cable was rewound, and the load was attached. The valve was opened until the screw was flush (approximately eight turns) with the housing. The load was released and traveled approximately 20 inches.

The reel was disassembled, and inspection was made of the piston, the reel housing, and the thread fit between the piston and the shaft. The brass and steel friction discs were checked for scoring. The parts were found to be dimensionally correct, and the friction discs were in a functional condition. It was decided that the outside diameter of the piston be turned down 0.004 inch.

The reel was reassembled, filled with brake fluid, and installed on the test fixture. The load was attached, and the valve was opened two turns. The load was released and traveled 12 feet, 8 inches in 3.95 seconds (3.23 feet/second).

The reel was rewound, the valve was opened one turn, and the load was dropped again. The load traveled the 12 feet, 8 inches in 4.99 seconds (2.56 feet/second).

The load was increased to 500 pounds, and the valve was opened 0.5 turn. The load was released and traveled the 12 feet, 8 inches in approximately 3.5 seconds (3.64 feet/second). The time is based on the acceleration trace of the oscillographic record.

A timing height of 12 feet, 5 inches was maintained for the remaining tests.

The valve was opened one turn, and the 500-pound load traveled the distance in 3.4 seconds (3.6 feet/second).

The reel was rewound, and the valve was opened 1.5 turns. The load was released and traveled the measured distance in 2.33 seconds (5.25 feet/second).

The reel was cooled with dry ice to -34°F. The load was released with a valve setting of 1.5 turns; the time required for the drop was 28.43 seconds (0.43 foot/second).

The same test was run at -20°F, but the timing line broke and no data was recorded.

The reel was allowed to return to ambient temperature, the load was increased to 1000 pounds, and the valve was opened one turn. The time required for the load to travel the measured distance was 2.65 seconds (4.62 feet/second).

The load was reduced to 500 pounds, and the reel was cooled to 18.5°F and allowed to soak at this temperature for approximately one hour. The valve was opened eight turns, and the load was released. At these conditions, the time required for the load to travel the set distance was 3.96 seconds (3.09 feet/second).

The reel was rewound, the temperature was maintained at 30°F, and the load and valve settings were not changed from the previous drop. The drop time was 3.33 seconds (3.68 feet/second).

The valve was opened to 10 turns. The temperature was stabilized at 25°F. The time for the drop with a 500-pound load was 3.65 seconds (3.35 feet/second).

With the same load, with the temperature maintained at 29°F, and with a valve setting of 12 turns open, the drop time was 3.30 seconds (3.71 feet/second).

b. Reel No. 2. The reel was filled with brake fluid and installed on the test fixture. The valve was set at 1.5 turns, and the 500-pound load was attached. The load was released, and time for the drop was 2.31 seconds (5.3 feet/second).

c. Reel No. 3. The reel was filled with brake fluid and mounted on the test fixture. The 500-pound load was attached to the cable, and the valve was set at 1.5 turns. At a temperature of 69°F, the load was dropped at an approximate 6.5 foot/second rate (1.88 seconds). The time was determined from the oscillograph record.

The test was rerun, and the recorded drop time was 1.81 seconds (6.77 feet/second).

The reel was drained and then filled with brake fluid. The 500-pound load was dropped with a valve setting of 1.5 turns at a temperature of 69°F. The time required was 2.19 seconds (5.58 feet/second).

d. Conclusions. This functional test program demonstrated that the reels can be adjusted by valve setting to provide the desired constant velocity deployment of 5 feet per second for the free-flight tests. For the same settings, differences in velocity are attributed to machining tolerances on the needle valve and its orifice. The function of the needle valve is to be able to adjust to the desired deployment velocities. The reels are structurally adequate to deploy loads up to 1000 pounds. The steel roller was used for eight drops, and there were no signs of wear.

3. Environmental Chamber Tests - Ballute Inflation

Questionable degree of inflation of the Ballute during the third drop test at Holloman Air Force Base led to mutual agreement between ASD and GAC to conduct tests in the altitude chamber at Wright-Patterson Air Force Base prior to the fourth drop test. Conditions simulated those encountered during a Holloman drop:

a. Test No. 1 - 22 August 1961 - 83,200 Feet at 30°F. The Ballute was suspended from the top of the chamber. Inflation at 83,200 feet was to be accomplished using the complete Ballute package, excluding the outer canister. The bottle, installed within the inner canister, was pressurized to 2025 psi. Circuitry to fire the 3 to 4 ampere squib was as similar to the Cree Missile circuitry as practical. A transducer was installed within the inner canister to measure internal pressure. The wire cables from the squib and pressure transducer were routed out of the test chamber through access vents, and the electrical connection was made outside the chamber as shown in Figure 34. A Century recorder oscillograph was used to record the pressure signal from the Bourns Transducer, which was calibrated in the test chamber in increments from 1.907 psia at 47,500 feet to 0.404 psia at 80,000 feet (see Figure 35).

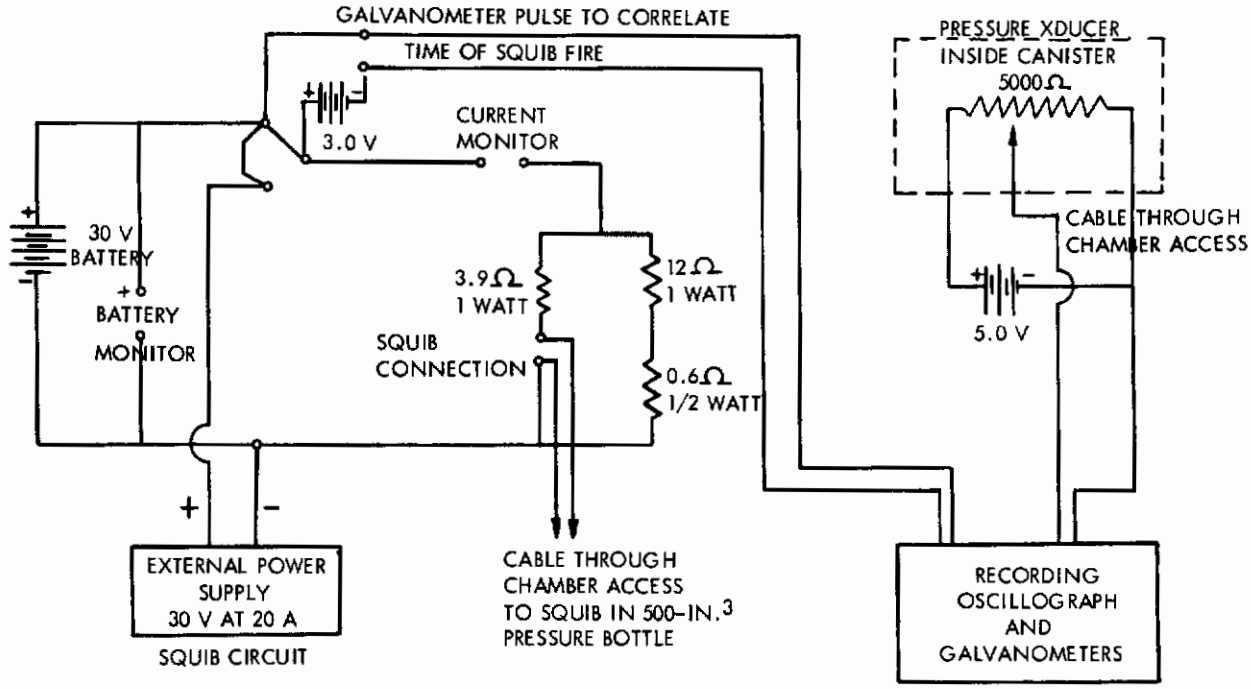

Figure 34. Circuitry for Chamber Tests

The first attempt to fire the squib failed. Approximately 2.2 amperes were delivered to the squib. This particular squib requires approximately 2.7 to 3.0 amperes to fire.

A second source of power, capable of delivering 20 amperes, was used. Using this power source, the squib fired and the Ballute inflated. Conditions at the time of inflation were

Altitude - 83,000 feet

Pressure (ambient) - 0.35 psi

Temperature (chamber) - 34°F

Time required for Ballute to develop a spherical shape was visually timed to approximately seven seconds.

The internal Ballute pressure indicated 1.5 psia with a rise to 1.6 as shown in Figure 36. Apparently there was some fault in the test recording setup.

The altitude in the chamber was lowered to 53,000 feet, where ambient pressure is 1.46 psi, to determine that the Ballute would retain shape and that internal pressure was approximately equal to the ambient pressure. At 53,000 feet the Ballute retained its shape.

b. Test No. 2 - 23 August 1961 - 115,000 Feet at 70°F. At 115,000 feet the Ballute expanded to a nearly full spherical shape from residual air trapped inside the Ballute. A vacuum cleaner had

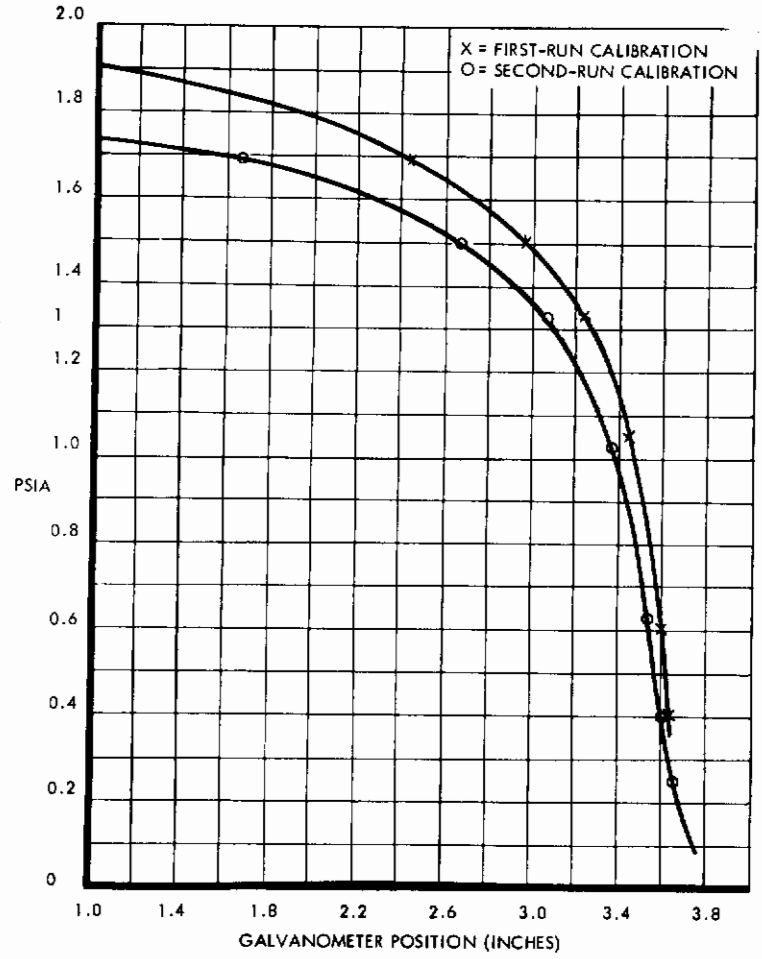

Figure 35. Internal Ballute Pressure Calibration - Chamber Tests

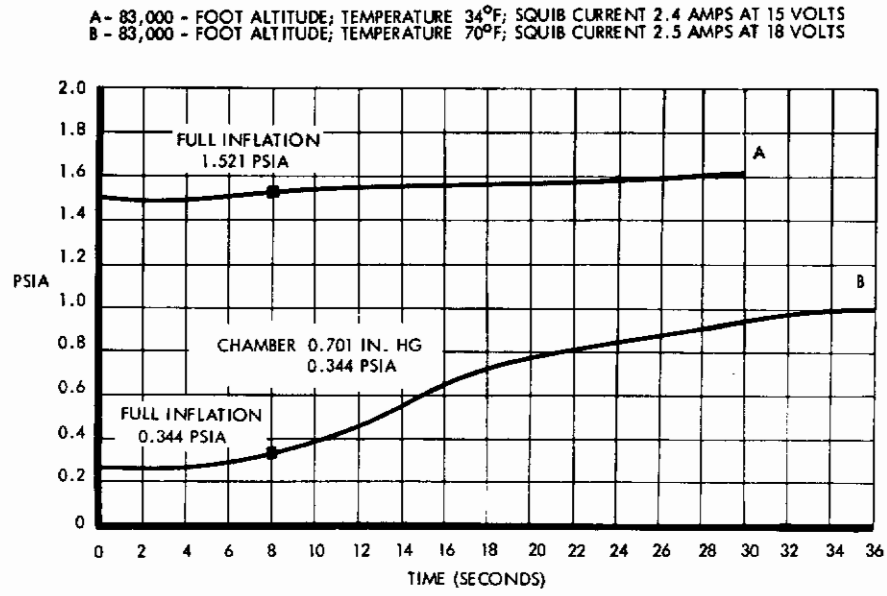

Figure 36. Internal Ballute Pressure versus Time

been used in both tests to evacuate residual air. At the beginning of the tests the Ballute was evacuated until completely collapsed, and there was no visual space between the inside of the gores.

The 115,000-foot test simulated the 155,000-foot altitude tests, taking dynamic pressure into consideration.

This test was then changed to nearly repeat test No. 1; conditions at time of inflation were as follows:

Altitude - 83,000 feet

Temperature - 70°F

Time required for Ballute to develop a spherical shape was visually timed to be approximately six seconds. As shown in Figure 36, the time to inflate to full shape was eight seconds. The test was terminated after approximately 36 seconds.

Altitude was also reduced to demonstrate that the Ballute retained its shape at 53,000 feet.

c. Conclusions. Ballute inflation was satisfactory; however, the following changes were made prior to the fourth drop test:

(1) Squib was changed from 3 or 4 amperes to 750 milliamperes.

(2) Complete electrical check was made on the missile and Ballute package by duplicating sequences during test. The check included telemetry operation, camera operation, etc. Amperage delivered to the bottle squib at 19 seconds of the time sequence was measured with two amperes as minimum acceptable. A 750-ma squib was connected into the circuit to demonstrate firing.

(3) A nylon lanyard was added as a secondary measure to assure recovery of the Ballute.

E. TRANSONIC DROP TESTS

1. Drop Test No. 1 - 28 June 1961

The telemetry was checked out by closed loop prior to departing for the launch site. Channels were used as follows:

Ballute internal pressure - 14.5 kc

Ram air pressure - 22 kc

Tensiometer (shock load) - 40 kc

Tensiometer (steady drag load) - 70 kc

In addition, the temperature was measured at the reel within the Ballute package.

The test unit was launched at 0810 hours. The balloon ascended at a rate of approximately 1025 fpm to about 89,000 feet. During the latter part of the flight, the rate of ascent decreased and the maximum altitude reached was 94,800 feet. The flight duration was one hour and forty minutes. The test unit was released at 0950 hours at 94,800 feet. The balloon was inflated with helium to approximately seven percent, and the total weight lifted is as follows:

Balloon - 315 pounds

Test unit - 506 pounds

External battery, camera, water bottles - 151 pounds

Holloman command, 64-foot chute, ballast, and bar - 231 pounds

Total - 1203 pounds

Prior to release the telemetry receiving station, Jig 1, advised that the telemetry signals were too weak for good data reception. The authorization to drop without telemetry was given by the GAC representative as per previous discussions with ASD representatives. A review of the telemetry records after test offered no explanation as to why good telemetry signals could not be received. All telemetry equipment was checked after test and found to be operating satisfactorily. The

transmitter was tuned and rated at 3.5 watts. All sequences functioned properly, but the Ballute did not inflate. No part of the Ballute package was recovered.

After recovery of the missile, all circuitry was checked and found to be functioning properly. The timer was originally set at 21.5 seconds for separation of the outer canister. The post-flight test revealed that the timer initiated canister separation at 23.6 seconds. This does not have any bearing on the non-inflation problem.

A review of the optical data indicated that due to non-inflation the missile encountered a pendulum effect and the camera within the missile indicated twisting. The wire to the pressure bottle was broken due to twisting about some object. It was then concluded that the broken wire had prevented squib ignition.

Corrective action taken was the extension of the squib wire to a length of 15 feet and the removal of the 0.35-time delay between canister separation and Ballute inflation. Removal of the time delay also ensures that the wire will not break during the explosion for ring separation. There were several areas of powder burns on the tensiometer and the camera lens within the aft end of the missile. However, there was no conclusive evidence that the explosion broke the wire to the squib.

Three time delays were checked to determine if they could have failed or if the time delay was excessive. The time delays checked averaged out to be 0.19 second.

At the time of missile preflight check-out, the squib circuitry was checked by wiring in a 12-volt, 2-cp bulb, When current was applied, as programmed by the timer, this bulb burned out. This is normal check-out procedure.

2. Drop Test No. 2 - 6 July 1961

Telemetry was checked out by closed loop and also checked out at the launch site. Channels were used as follows:

Static air pressure - 14.5 kc

Ram air pressure - 22 kc

Ballute pressure - 40 kc

Tensiometer - 70 kc

The test unit was launched at 0720 hours. Immediately after launch, the test unit was prematurely released by explosive separation of the aft ring on the Ballute package. When dropped, the lanyards pulled the timer pins, thus engaging the timer. The test specimen cycled through the various stages as programmed by the timer.

An investigation was conducted, but firm evidence could not be established as to the reason for the premature release. The wires from the battery, mounted on the aft end of the Ballute, to the Holloman command package had been damaged in two places. Shorting in these damaged areas could have closed the circuit and caused the after ring to separate. This wire could have wrapped around one corner of the command package. The wire was bent, and the shielding was cut in two places. However, it could not definitely be ascertained that this happened when the packages were swinging at launch or when the packages hit the ground. A check of all other circuitry did not reveal any discrepancy that could have triggered or shorted the circuit to cause release.

Dismantling of the Ballute package revealed that the pressure bottle squib did not fire. Thus, there was no inflation of the Ballute. An investigation was made to determine why the squib did not fire. The circuitry in the missile to the squib was checked and found to be satisfactory. A package of nickel-cadmium batteries was installed in the missile, and a check of the squib measured two amperes. The battery used was not up to full charge of 30 volts but was measured to be 24 volts. A squib was connected directly to the battery and exploded immediately. A squib was connected in the missile circuitry, but it would not explode. Using a 30-volt battery with the 12-ohm resistor in the circuit, as used in the missile, the amperage should be approximately 2.5 amperes. According to the squib manufacturer, the squib was to explode at 1.3 to 1.6 amperes. Another squib was tested by adding current at the rate of 0.5 ampere for a duration of one second. This squib was exploded

when the amperage reached 2.67 amperes. A check with the squib manufacturer resulted in his recommendation to use approximately 4 amperes for sure-fire results.

To ensure firing of the squib for the third drop test, the 12-ohm resistor in the missile was replaced with a 4-ohm resistor. With 30 volts the squib circuit draws approximately 7-1/2 amperes.

3. Drop Test No. 3 - 20 July 1961

The launch for the third drop test was accomplished 20 July 1961. Launch time was 0540 hours. The polyethelene balloon was inflated to approximately seven percent. Weight lifted was as follows:

Balloon - 313 pounds

Test specimen - 505 pounds

External battery, camera, and water bottles - 143 pounds

Holloman command, chute, ballast, and bar - 233 pounds

Total - 1194 pounds

The telemetry was checked out prior to launch at the launch site. Channels were as follows:

Static air pressure - 14.5 kc

Ram air pressure - 22.0 kc

Ballute internal pressure - 40.0 kc

Tensiometer - 70.0 kc

The test specimen was released at 0745 hours over the west side of the 50-mile impact area. The release altitude was approximately 94,400 feet. Prior to release, the first command had external power on, and the telemetry reception at Jig 1 was very good. The missile remained on external power for five minutes. The second command switched the power from external to internal, and during the one minute duration of internal power, telemetry reception remained very good. At the third command when the specimen was released, telemetry reception ceased. This test was apparently very similar to test No. 1. However, a substantiated increase in free-fall time was accomplished. The Ballute appeared to inflate more than test No. 1, although complete inflation was not accomplished.

The Ballute was not recovered. Without recovery of the Ballute, it is very difficult to determine if there had been a malfunction. The missile was recovered; it was quite damaged. A check on the circuitry within the missile indicated that the sequence had functioned satisfactorily. Since the Ballute was not recovered, it could not be determined if the partial inflation was due to trapped residual air or due to nitrogen in the pressurized bottle.

From an analysis of available evidence, the sequence of events for both tests No. 1 and 3 was as follows:

(1) After the balloon train had reached its float altitude of about 96,000 feet, the telemetry was turned on external power. In both cases the system appeared to be functioning normally, and the signal was loud and clear.

(2) Telemetry was switched to missile, or internal, power shortly before missile release. All channels were run through a calibration sequence. Telemetry system appeared to be functioning normally, and the signal was good.

(3) At the instant of release of the missile from the balloon, the ground receiving stations lost telemetry signal on both tests.

(4) After recovery of the test missiles, careful checks of the telemetry system revealed it to be in perfect working condition. It was not possible to duplicate the failure even though extensive laboratory tests were conducted.

An attempt was made to explain the loss of signal. Some of the possible causes are

(1) The telemetry receiving station antennas are highly directionally sensitive, and the movement of the test missile caused reduction in signal strength.

(2) The missile power selector was switched to the external position by the same signal that effected missile releases.

(3) An electrical short in the missile caused the power selector switch to step to external power.

It does not appear possible that the small angular change the missile position would assume relative to the ground antenna orientation could cause even a minor reduction in signal strength. Therefore, possible cause No. 1 can probably be eliminated. Possible cause No. 2 appears to be a distinct possibility until the missile power selection system is analyzed. This system employs a rotary solenoid which, upon receipt of an electrical impulse, will transfer the missile telemetry system from external power to internal power or vice versa. The system is so arranged that, in the event that the missile should inadvertently be released while on external power, the solenoid would automatically step to internal power. This function is controlled by the arming switch, which is lanyard-actuated at the time of missile release.

Thus it can be seen that if the radio command signal that effected missile release also caused the power selector switch to step to external power, the system would have returned to internal power almost immediately. This then seems to eliminate possible cause No. 2 from consideration.

The third possible cause appears to offer the only explanation for telemetry signal loss. However, when the missiles were examined in the laboratory after the missions, no evidence of electrical shorts could be found. Thus, if a short did exist, it must have been of such a nature that it existed only at the instant of missile release from the balloon train. Such a short would necessarily have to be external from the missile.

Investigation of the umbilical cable, which is pulled free from the missile at release, revealed no flaws. However, it was determined that if a momentary short could be induced across two of the umbilical connector pins, the rotary solenoid would step once to the external position. Furthermore, as long as the short was maintained, the solenoid would remain energized. If the arming switch is actuated while the short is in effect, the solenoid will be held in the energized position indefinitely even though the short was removed. An inherent feature of the rotary solenoid used is that in order for it to restep after once being energized it is necessary to first de-energize the circuit so that the solenoid can reset.

Thus, there appears to be one possible explanation for the failures. If at the time of missile release a short is applied across pins of the umbilical connector and while this short is in effect the arming switch closes, the power selection system will switch to and be held in the external position. Thus, the telemetry signal would fail at missile release.

The only possibility for creating a short at the umbilical connector is by means of the helical spring which forces the connector apart. While it cannot definitely be established that such an event occurred, no other logical explanation can be advanced.

4. Drop Test No. 4 - 31 August 1961

The following changes were made to the test specimen prior to drop test No. 4:

(1) Added a rubber coating to the surface of the helical spring which forces the umbilical connector apart.

(2) Rearranged the umbilical connectors so that it was not possible for the spring, at the time of release, to contact pins carrying voltage or any part of the power system.

(3) Increased the length of the lanyard to delay actuation of the automatic power select.

(4) Changed pressure bottle squib from an E-92 to an S-68 to obtain the following results:

	S-68	E-92
No fire	30 milliamperes	1.5 amperes
Minumum fire	--	2.0 amperes
Average minimum fire	0.5 amperes	3.5 amperes
All fire	2.0 amperes	5.0 amperes

(5) Added a backup circuit to fire the valve squib, as shown in Figure 37. Circuitry was added so that if the squib was not fired by the 30-volt, 0.75-ampere/hour battery, then approximately three seconds later current would be delivered to the squib from the camera battery. Switch T-7 remains closed for three seconds; then if the squib is not fired, switch T-A closes and delivers approximately four amperes for about three seconds. With the squib fired, current is not delivered to the open squib circuit by the camera battery.

(6) Added a 4000-pound nylon lanyard from the missile to the Ballute. This lanyard was approximately 10 to 12 inches longer than the reel cable.

Prior to the ground tests, the mechanical timer was set and checked out as follows:

T + 0 (seconds) - timer started.

T + 3.19 - telemetry calibrate

T + 7.64 - telemetry calibrate

T + 12.21 - telemetry operate

T + 17.54 - camera in missile on

T + 19.01* - release outer canister and inflate Ballute

T + 22.6 - backup circuit for Ballute inflation

T + 112.8 - drop nose weight

T + 114.8** - deploy recovery chute

*Desired - 19.00

**Desired - 120.00 (timer limit approximately 116 seconds)

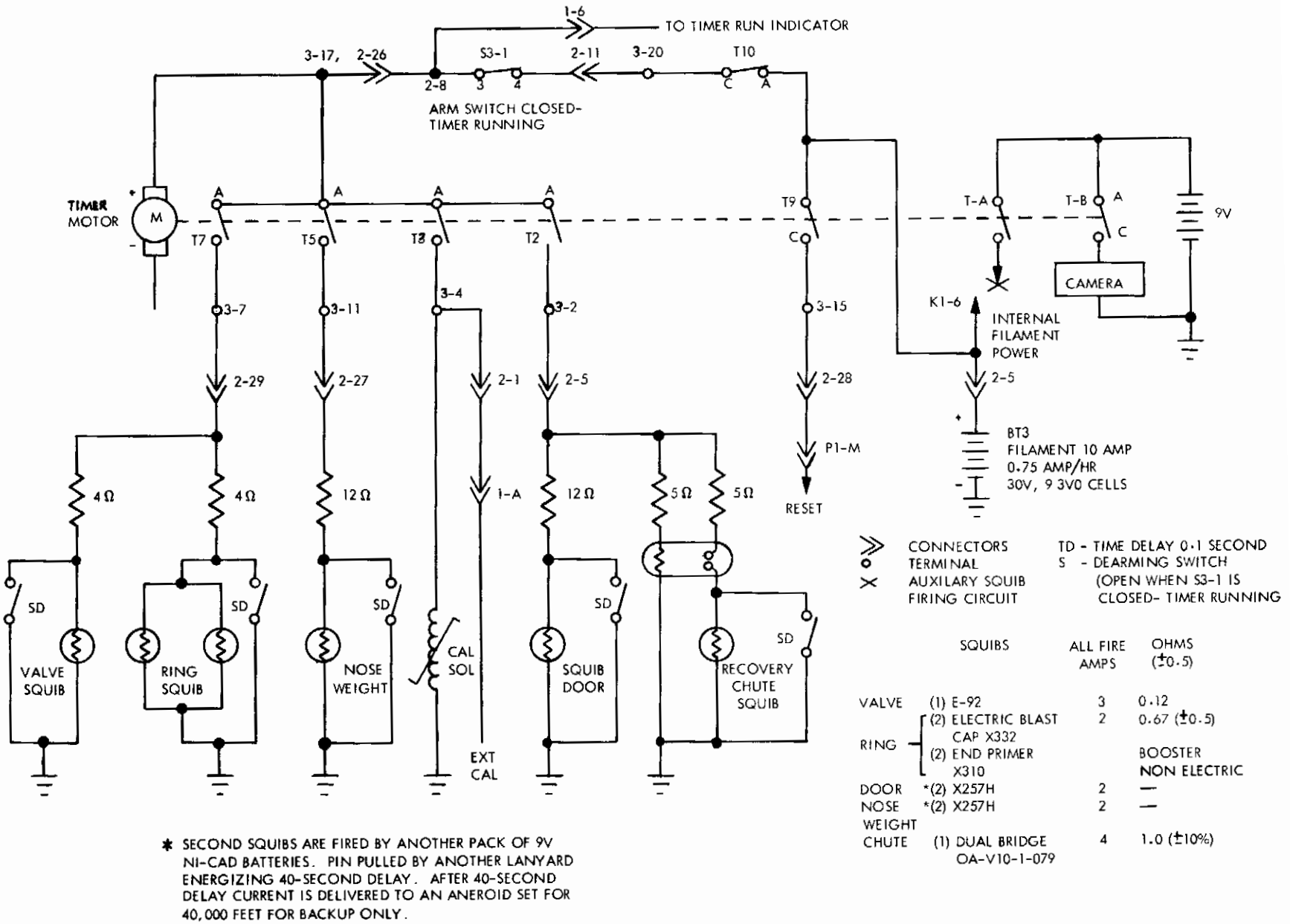

SQUIBS		ALL FIRE AMPS	OHMS (±0.5)
VALVE	(1) E-92	3	0.12
RING	(2) ELECTRIC BLAST CAP X332	2	0.67 (±0.5)
	(2) END PRIMER X310		BOOSTER NON ELECTRIC
DOOR	*(2) X257H	2	—
NOSE WEIGHT	*(2) X257H	2	—
CHUTE	(1) DUAL BRIDGE OA-V10-1-079	4	1.0 (±10%)

* SECOND SQUIBS ARE FIRED BY ANOTHER PACK OF 9V NI-CAD BATTERIES. PIN PULLED BY ANOTHER LANYARD ENERGIZING 40-SECOND DELAY. AFTER 40-SECOND DELAY CURRENT IS DELIVERED TO AN ANEROID SET FOR 40,000 FEET FOR BACKUP ONLY.

Figure 37. Timer Programmed Circuitry Schematic

The preflight ground tests were to completely check out the time of sequence of events and particularly ascertain that sufficient amperage was delivered to the bottle valve squib. Circuitry is shown in Figure 37. During the following tests, the circuitry was the same as that to be used during the actual drop test including missile circuitry and Ballute circuitry. As shown, the 30-volt, 0.75-ampere/hour, ni-cad battery operates the telemetry filaments and timer motor and ignites the squibs for canister separation, presure bottle valve, nose weight, chute door, and chute ejection. Figure 38 depicts the equipment run by the 30-volt, 1.75-ampere/hour, ni-cad battery package.

For preflight test No. 1, three 1-ohm resistors in parallel were wired in the circuitry instead of the two X332 squibs with a resistance in parallel of 0.33 ohm. Two 1-ohm resistors in parallel were wired in the circuitry instead of the S-68 pressure bottle valve squib. Resistance of the S-68 squib is approximately 0.67 ohm. As a result, the 30-volt internal battery was disconnected and a 28 volt d-c external power source was used in place of the internal battery. An amperage of 3.8 was measured at the valve squib, and 4.0 was measured at the ring squib. The amperage was measured when the timer reached T + 19.

Preflight Test No. 2 was run as in test No. 1. Results show that, at T + 19, 3.8 amperes were measured in valve squib circuitry and 4.1 amperes were measured in ring squib circuitry.

In addition to changes made for test No. 1, the following changes were made for test No. 3: the missile battery (30-volt, 0.75 - ampere/hour) was connected, and prior to starting the timer, the telemetry filaments were on for 2-1/2 minutes to simulate time on this battery used for telemetry check-out in the field. In addition, the telemetry was on for one minute to simulate time on the battery during flight prior to release. Results show that, at T + 19, 3.8 amperes were measured in the valve squib circuitry and 4.25 amperes were measured in the ring circuitry. During T + 19 the battery measured 27 volts.

For preflight test No. 4, the S-58 squib was installed and the three 1-ohm resistors were removed; the E-92 squib was installed, and the two 1-ohm resistors were removed; and the telemetry filaments were run for 2-1/2 minutes prior to starting timer. The result was that both squibs fired simultaneously at T + 19.

For preflight test No. 5, the ring squib circuitry was shorted out to simulate a bare wiring in the circuit shorting to ground, an E-92 dual bridge squib was installed, and the telemetry filament was run for 30 seconds. At T + 19 the dual bridge squib did not fire.

Only one bridge of the E-92 squib was connected for preflight test No. 6, and as a result the squib fired at T + 19.

Preflight test No. 7 was the same as No. 6 except that a squib was not used in the valve squib circuitry. An ammeter was connected to check amperage to the valve squib when the ring squib was shorted to ground. At T + 19, 3.6 amperes were measured at the valve squib circuitry. The missile internal battery measured 28.5 volts.

To check the backup circuitry to the valve squib, preflight test No. 8 was made to measure amperage delivered at T + 22.8. The 9-volt ni-cad battery pack was connected to the valve squib circuitry. This was a permanent change to be used during the actual drop. At T + 22.8, four amperes were measured across the valve squib circuitry. The camera speed was considerably reduced for approximately three seconds when current was being delivered to the squib circuitry. If the squib is fired by this backup circuit, this should be apparent during projection of the camera film.

Preflight test No. 9 consisted of testing the complete missile in the environmental chamber at Holloman Air Force Base (see Figure 39). Results are shown in Table 2. The two 1-ohm resistors in parallel and three 1-ohm resistors in parallel were used in place of squibs (same as test No. 1). At T + 19, 3 amperes were measured at the valve squib circuitry. The battery heaters were disconnected during this test. However, the battery heaters were checked in this chamber prior to this test. This check verified that the battery heaters came on at 30°F.

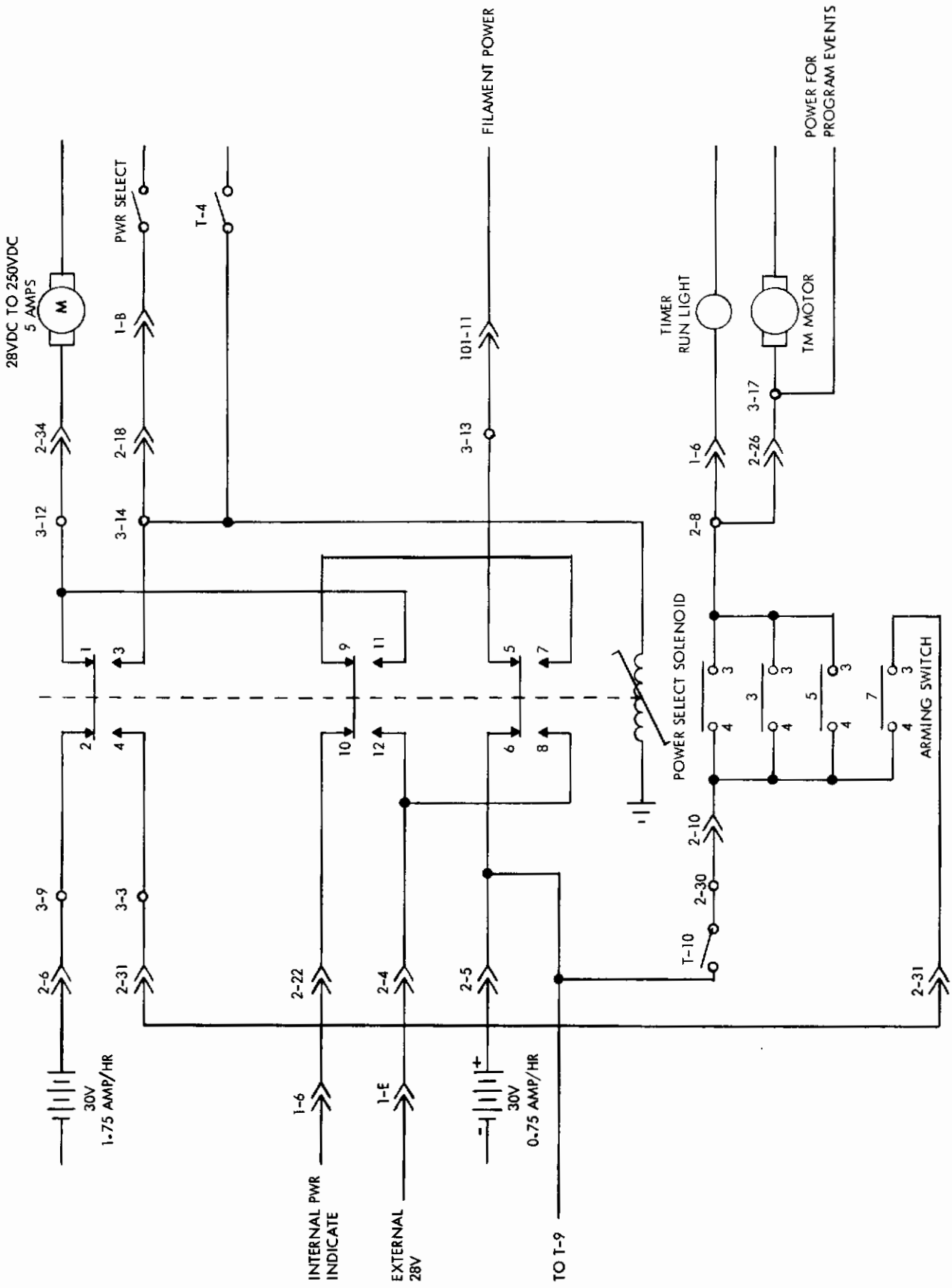

Figure 38. Ni-Cad Battery-Operated Equipment

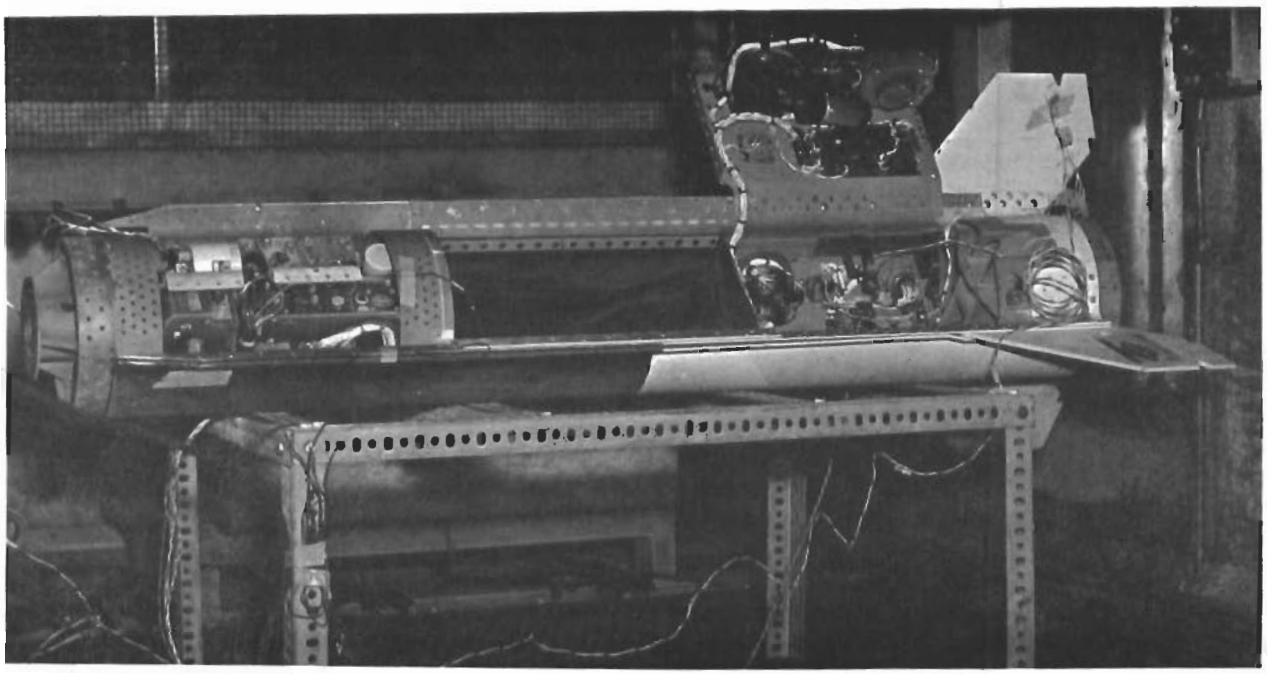

Figure 39. Testing Complete Missile in Environmental Chamber

Table 2. Environmental Test of Cree Instrumentation System

TIME	ALTITUDE x10^{-3} FT	DRY BULB TEMPERATURE (^{O}F)	BATTERY TEMPERATURE (^{O}F)	
09:25	5	- 1	65	63
09:30	5	- 5	61	59
09:35	5	- 7	55	52
09:40	5	-10	54	50
09:45	5	-12	49	46
09:50	5	-14	44	40
09:55	5	-16	40	36
10:00	5	-17	36	33
10:05	5	-18	35	31
10:10	5	-19	30	26
10:15	5	-20	27	24
10:20	5	-22	25	22
10:25*	5	-22	21	18
10:30	5	-30	17	14
10:35	5	-38	14	10
10:40	5	-40	10	7
10:45	5	-43	6	3
10:50	5	-41	3	1
10:55	5	-43	0	-2
10:55	5	-43	0	-2

* Instrumentation Started

Table 2. Environmental Test of Cree Instrumentation System (Continued)

TIME	ALTITUDE $x10^{-3}$ FT	DRY BULB TEMPERATURE (°F)	BATTERY TEMPERATURE (°F)	
10:56	7	-44	-4	-7
10:56	16	-49	-5	-10
10:56	21	-51	-2	-8
10:57	25	-48	-1	-5
10:57	33	-48	0	-4
10:57	42	-51	1	-2
10:58	52	-53	2	-1
10:58	53	-52	3	0
10:58	77	-51	3	0
10:59	85	-50	4	1
10:59	92	-48	4	1
10:59	97	-47	4	1
10:59	94	-45	4	1
11:00	--	-44	5	1
11:00	95	-43	5	2
11:00	97	-41	5	2
11:01	97	-41	5	2
11:01	97	-40	5	2
11:01	97	-39	5	2
11:01	97	-39	5	2
11:02	97	-36	5	2
11:02	97	-36	5	2
11:03	97	-38	5	2
11:03	97	-37	5	2
11:03	97	-37	5	2
11:03	97	-37	5	2
11:04	97	-36	5	2
11:05	97	-36	5	2
11:08	97	-34	5	2
11:08	97	-34	5	2
11:08	97	-34	5	2
11:09	97	-34	4	2
11:09	97	-34	4	2
11:09**	97	-34	4	2
11:10	97	-34	5	2
11:10	97	-33	5	2
11:10	97	-33	5	2
11:11	97	-33	5	2
11:11	97	-33	5	2
11:11	97	-33	5	2
11:12	97	-33	5	3
11:12	97	-33	5	3
11:12	97	-33	6	3
11:13	97	-33	6	3
11:15	97	-32	8	5
11:20	5	-32	9	6
11:23	5	-34	13	9
11:25	5	-33	13	10

**Timer Ignition

A final test was made when the test specimen was prepared for the drop test. Light bulbs (12-volt) were connected to the squib circuitry for nose weight, chute door, and chute ejection. A 300-milliampere squib was used in the canister separation, and an S-68 squib was connected to the valve squib circuitry. The telemetry filaments were turned on two minutes prior to starting the timer. The timer was started, and the complete sequence of events was timed. The sequence of events functioned as programmed; the light bulbs lighted and burned out to simulate firing of squibs. The valve and canister squibs fired simultaneously at T + 19 seconds. The missile camera motor started at approximately 17.5 seconds and continued until T + 115 seconds when the timer stopped. The auxiliary circuit was not required to fire the valve squib.

Prior to the drop test, the 500-cubic-inch pressure bottle was pressurized to 2050 psi on 23 August 1961. At room temperature (74°F) the bottle was checked on 24 August 1961 to be 1950 psi; also at room temperature on 28 August 1961 the pressure was checked to be 1940 psi. To inflate the Ballute to 1.5 psi, the bottle should be pressurized to 1950 psi.

Information received from Gulton Industries concerning the 3V0-.750 (9 in series) 3/4 ampere/hour, 10-ampere/peak, 30-volt battery pack. Typical thermal characteristics for a ni-cad battery are

70°F	2 minutes at 7C*	25 volts
32°F	2 minutes at 7C	18 volts
0°F	30 seconds at 7C	18 volts**

*Discharge rate **Very marginal

The balloon for the fourth drop test was launched at 0747 hours. Release time over the range was 1015 hours. Weight lifted is as follows:

Polyethelene balloon - 307 pounds

Test specimen - 501 pounds

Battery (external) and control box - 141 pounds

Holloman command package - 70 pounds

Holloman bar - 48 pounds

64-foot chute - 68 pounds

Ballast (4 bags at 15 pounds each) - 60 pounds

Total - 1195 pounds

Several optical stations were instructed to remain on the Ballute in case it parted from the missile.

The telemetry was checked out at the base and at the launch site and was working properly. Telemetry functioned properly on external and during the one minute on internal prior to release. After release it was reported from Jig 1 that telemetry reception was good.

The missile impact point was north of the northwest corner of the 50-mile impact area. The Ballute remained with the missile and was recovered at the impact area. The 4000-pound nylon strap, added as a safety measure for recovery, was not attached to the missile when recovered. The nylon strap was sewed inside the Ballute package to the reel mount plate, but it was not possible to sew it to the missile. The reel cable was still attached to the missile and to the Ballute. There

was no apparent damage to the reel cable. Photographs taken at the impact by Army photographers are shown in Figure 40. All reports received subsequent to the test indicated that the test was successful. A review of the film from Tear 15 showed that the Ballute properly inflated and all events functioned as programmed. Test result data are graphically illustrated in "Test Results" of this section.

F. TEST RESULTS

1. Test Data

Data acquired from Drop Tests No. 1, 3, and 4 are shown graphically in Figures 41 through 44.

2. Computational Procedures

In the left-hand rectangular coordinate geoditic system employed, the origin is the mean sea-level projection of the drop point. This system is based on the Clarke Spheroid of 1866. The XY plane is perpendicular to the plumb line that passes through the origin. The X axis is positive true north. The Y axis is positive east 90 degrees clockwise from the positive X axis, and the Z axis is positive upward. The origins for AFMDC Holloman are at the intersection of 35^{o} 05'00.00 north and longitude 106^{o} 20'00.00 west. This system is primarily used for reporting instrumentation points and their respective orientation systems.

An N-station least-square solution was used to compute the position data. The line of sight from each station was defined from observed azimuth and elevation angles. The computed position was then determined as that point for which the sum of the squares of the perpendicular distances to each line of sight was a minimum. Additional smoothing techniques were not applied.

The altitude (H) above mean sea level was computed for each position. The formula used for this computation is $H = Z + (X^2 + Y^2)/2(R + Z)$, where R is the average radius of the earth for this vicinity (20,897,038 feet) and X, Y, and Z are the position coordinates in the basic AFMDC coordinate system.

Each component velocity and acceleration was obtained by evaluating the first and second derivatives respectively of the second-degree least squares curve fitted to seven consecutive position points having their midpoint at the position of desired velocity and acceleration. Tangential velocity was computed as the magnitude of the vector sum of the component velocities. Tangential acceleration was computed by evaluating the first derivative of tangential velocity.

Upper air data was correlated with the flight data by relating the corresponding altitude components. The altitude component of the flight data was taken as the altitude (H) above mean sea level. The altitude component of the upper air data was a corrected altitude computed from pressure information. With the exception of the ambient density, all interpolations were linear. The density of the ambient air (ρ) was computed in grams per cubic meter at each altitude.

The following equation was derived using the perfect gas law equation modified by AFMDC to provide constants representative of the atmospheric conditions at Holloman Air Force Base:

$$\rho = 348.38 \frac{P - 0.0231\ F\ 10^{n}}{K}$$

where $n = 7.5C/(C + 237.3)$, C is the temperature in ^{o}C, K is the temperature in ^{o}K, F is the relative humidity, and P is the ambient pressure in millibars.

True airspeed (TAS) was computed as the absolute value of the vector difference of the velocities of the wind and the Cree. The vertical component of the wind velocity was assumed to be zero.

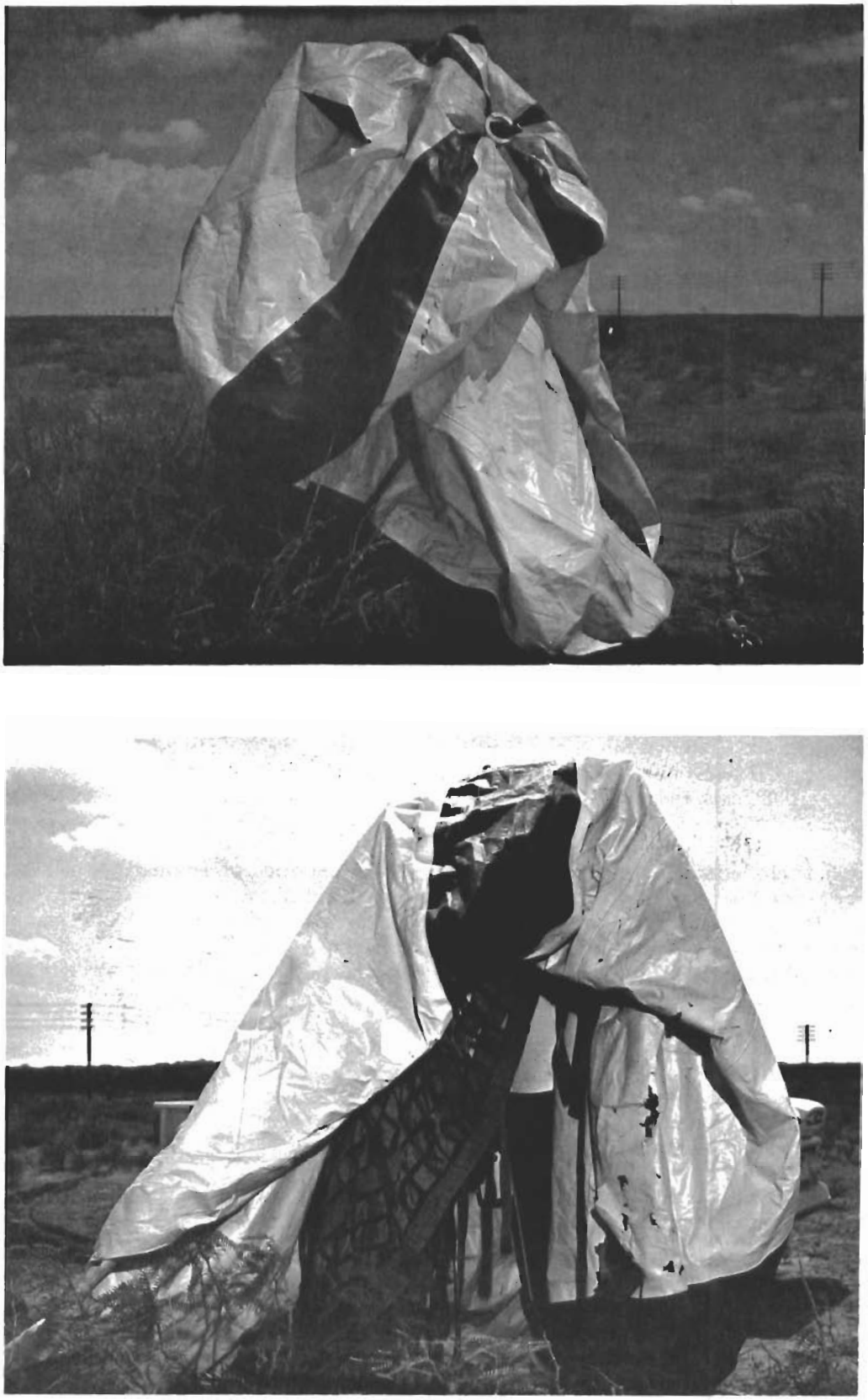

Figure 40. Impact - Drop Test No. 4

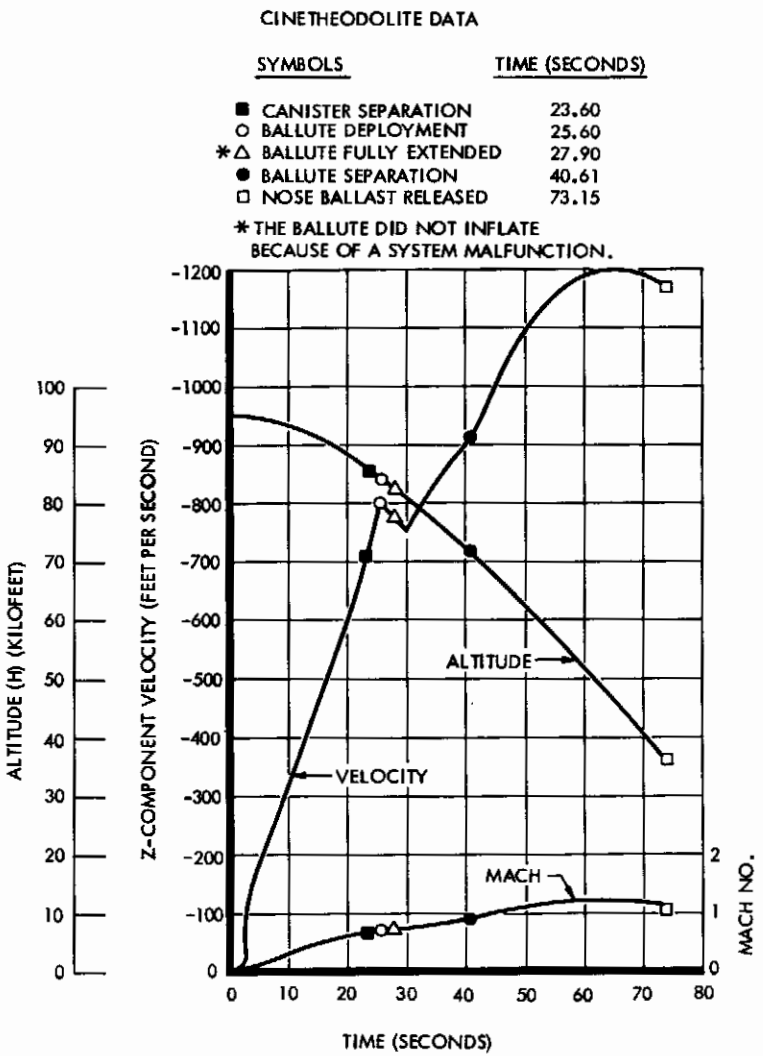

Figure 41. Drop Test No. 1

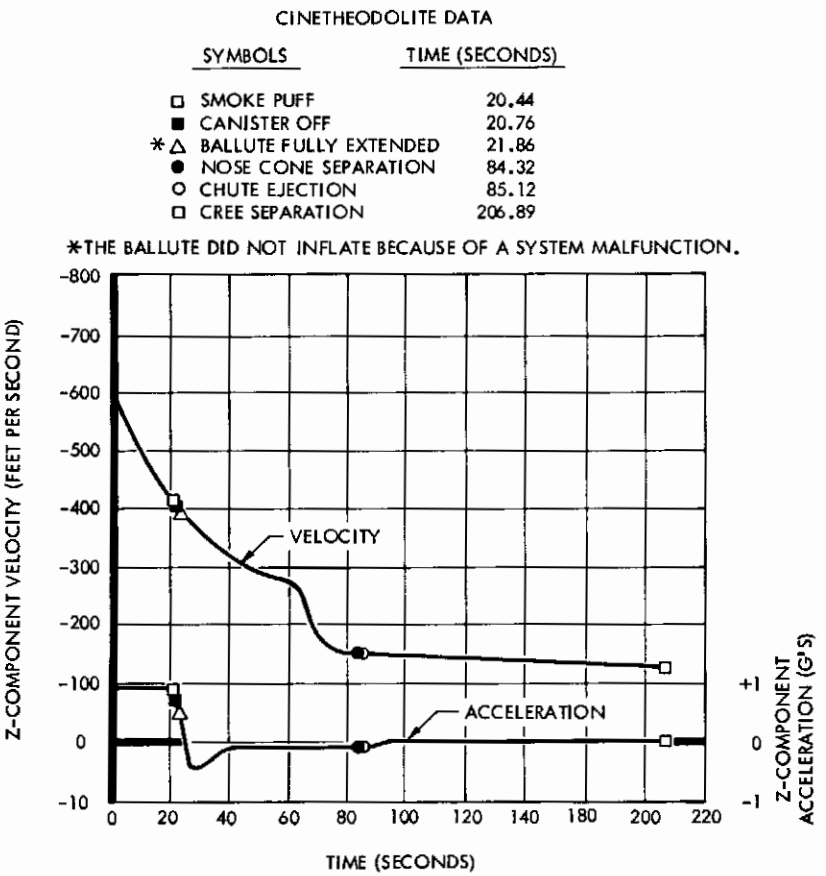

Figure 42. Drop Test No. 3

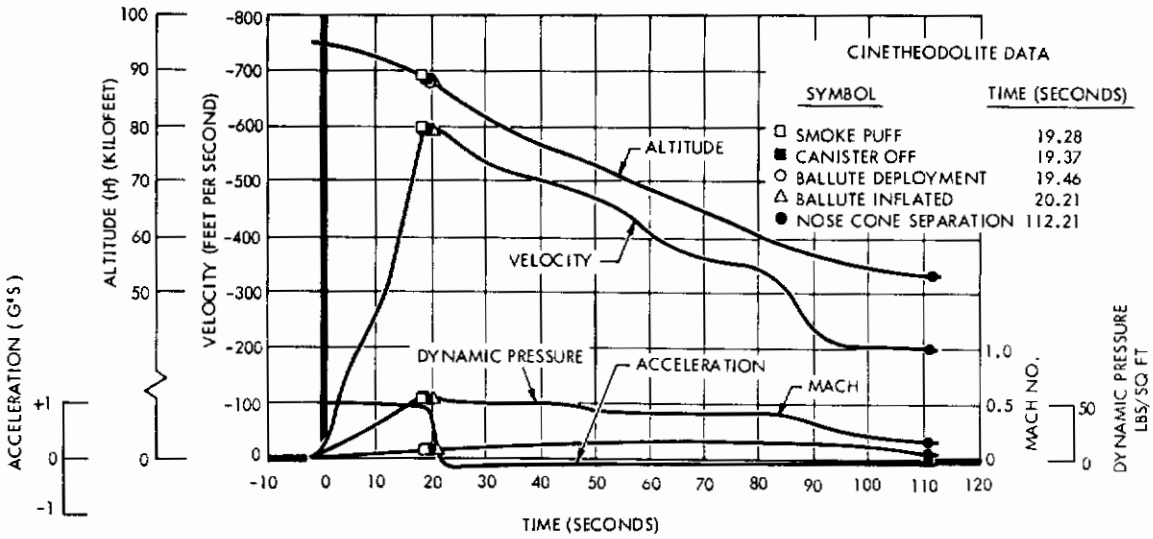

Figure 43. Drop Test No. 4

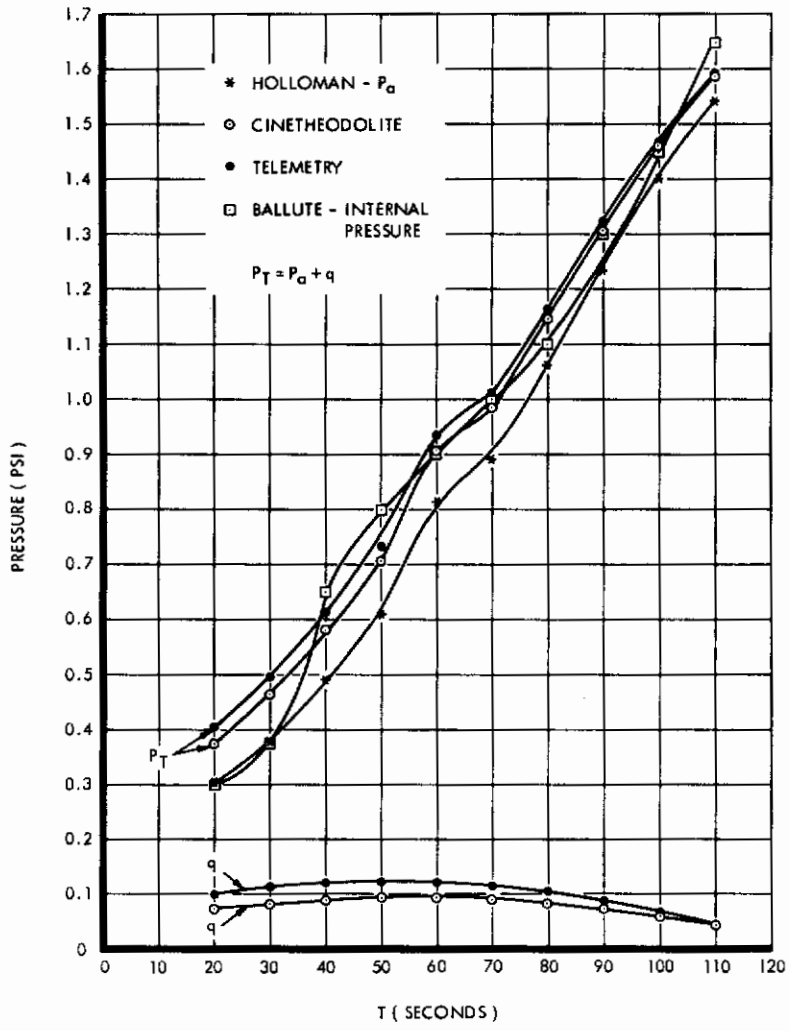

Figure 44. Pressure versus Time - Drop Test No. 4

Indicated airspeed (IAS) was computed using the equation

$$IAS = (TAS)\sqrt{\rho/\rho_0}$$

where ρ_0 is the density of the air at sea level elevation (NACA standard).

Mach number (M) was computed using the equation

$$M = 0.0152(TAS)/\sqrt{K.}$$

Position data was corrected for wind conditions. Wind data was correlated with position data by relating the corresponding altitude components. The wind velocity components were numerically integrated with respect to time and subtracted from X and Y to obtain a corrected position, U and V.

In the left-hand rectangular coordinate system employed for these position data, the UV plane coincides with the XY plane as defined above. The origin is the projection on the UV plane of a point in space moving relative to the ground, but fixed relative to its surrounding air mass and defined at zero time as the MSL projection of the drop point. The U axis is the same as the X axis; the V axis is positive 90 degrees clockwise from the positive U axis; and the W axis is positive upward.

3. Telemetry - Drop Test No. 4

Drop test No. 4 was accomplished by releasing the payload package from a 1,000,000 - cubic-foot balloon at an altitude of 96,415 feet. Telemetry data channel assignments were made as shown in Table 3.

Table 3. Telemetry Data Channel Assignments - Drop Test No. 4

INTER-RANGE INSTRUMENTATION GROUP CHANNELS	NORMAL SUBCARRIER LIMITS			DATA ITEM
	Upper Limit (cps)	Center Frequency (cps)	Lower Limit (cps)	
13	15,588	14,500	13,412	Altitude
14	23,650	22,000	20,350	Dynamic Pressure
C	46,000	40,000	34,000	Internal Pressure
E	80,500	70,000	59,500	Shock Force

The telemetry data was received and recorded on magnetic tape. Figure 45 shows panoramic displays of the recorded telemetry multiple signal at various flight times from X + 17 seconds to X + 90 seconds. From Figure 45, considerable low-level background noise and a relatively strong spurious signal of approximately 52.5 kc are noted. The signal on channel C is sufficiently separated from this signal to prevent interference during playback. The strange signal does interfere with channel E on several occasions during flight. The areas of interference are noted on the data playout of shock force in Figure 46. A brief discussion of each telemetry data channel follows:

a. Altitude - IRIG Channel 13. Pressure altitude telemetry data was recorded during the entire flight. Interference from background noise and possibly the noisy signal on channel 14 caused some spikes and data dropouts. The general trend of the data agrees fairly well with the photometric data.

b. Dynamic Pressure - IRIG Channel 14. No dynamic pressure data was obtained due to interference from an undetermined source. The interfering signal has a greater amplitude than any of the telemetry signals and is conspicuous by its deviation from the preemphasis of the telemetry composite signal. When a ground station FM discriminator is faced with two signals within its limits, it

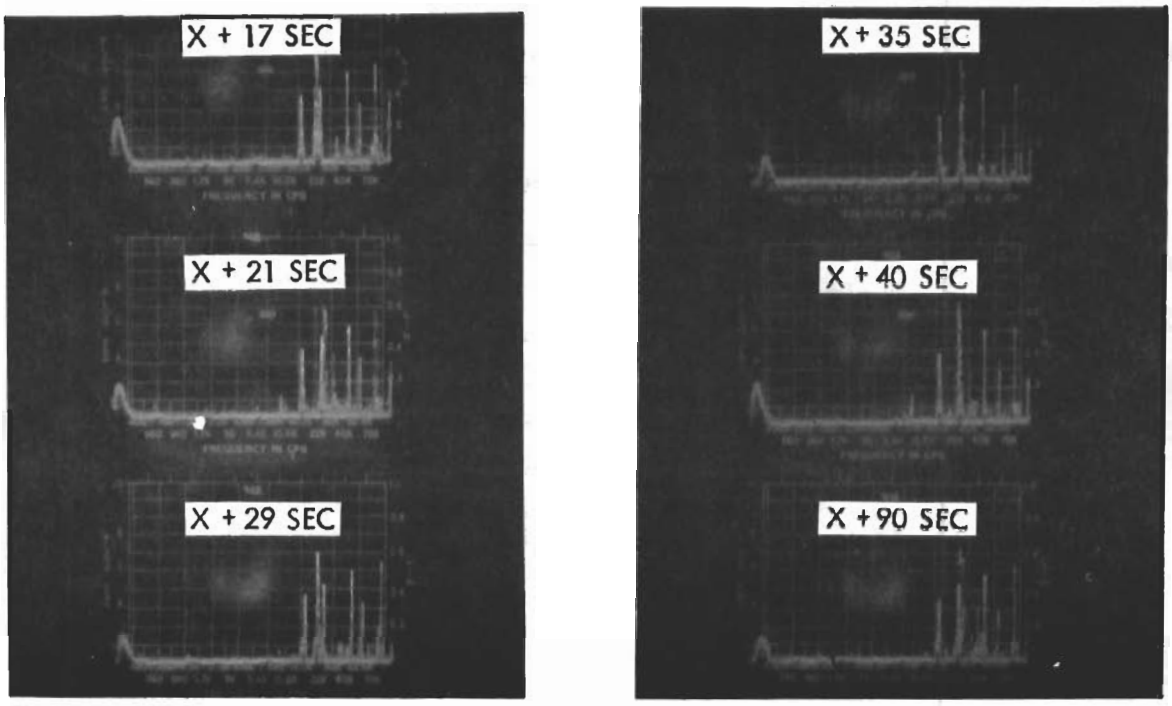

Figure 45. Holloman Drop No. 4 Telemetry Composite Signal Panoramic Display

generally tries to follow the stronger signal, but when the frequency separation is small and the amplitudes are within a few decibels of each other, it may not follow either signal.

From a comparison of Figures 45 and 46 it is concluded that

(1) The telemetry signal was fairly steady.

(2) The interfering signal was noisy and shifted back and forth in frequency through the telemetry signal.

(3) The trace in Figure 46 is essentially that of the interfering signal and does not represent dynamic pressure data.

(4) The telemetry data cannot be unscrambled from the interfering signal ordinary ground station playout equipment.

c. Internal Pressure - IRIG Channel C. Ballute internal pressure data was recorded from Ballute deployment until the pressure transducer reached its mechanical stop at approximately 2.5 psi. The telemetry signal was of good quality; a small amount of noise occurred from approximately X + 20 seconds until X + 40 seconds. The Ballute pressure remained slightly above atmospheric pressure during the drop.

d. Shock Force - IRIG Channel E. Shock force data was recorded from Ballute deployment until shortly after nose cone separation. At approximately 115 seconds, the force dropped to zero. The telemetry signal experienced some interference from the signal present in the channel 17 band. The nearness of this signal to channel E caused momentary losses of data subsequent to Ballute deployment. A curve is easily faired through the noisy areas, defining the general trend of the shock forces.

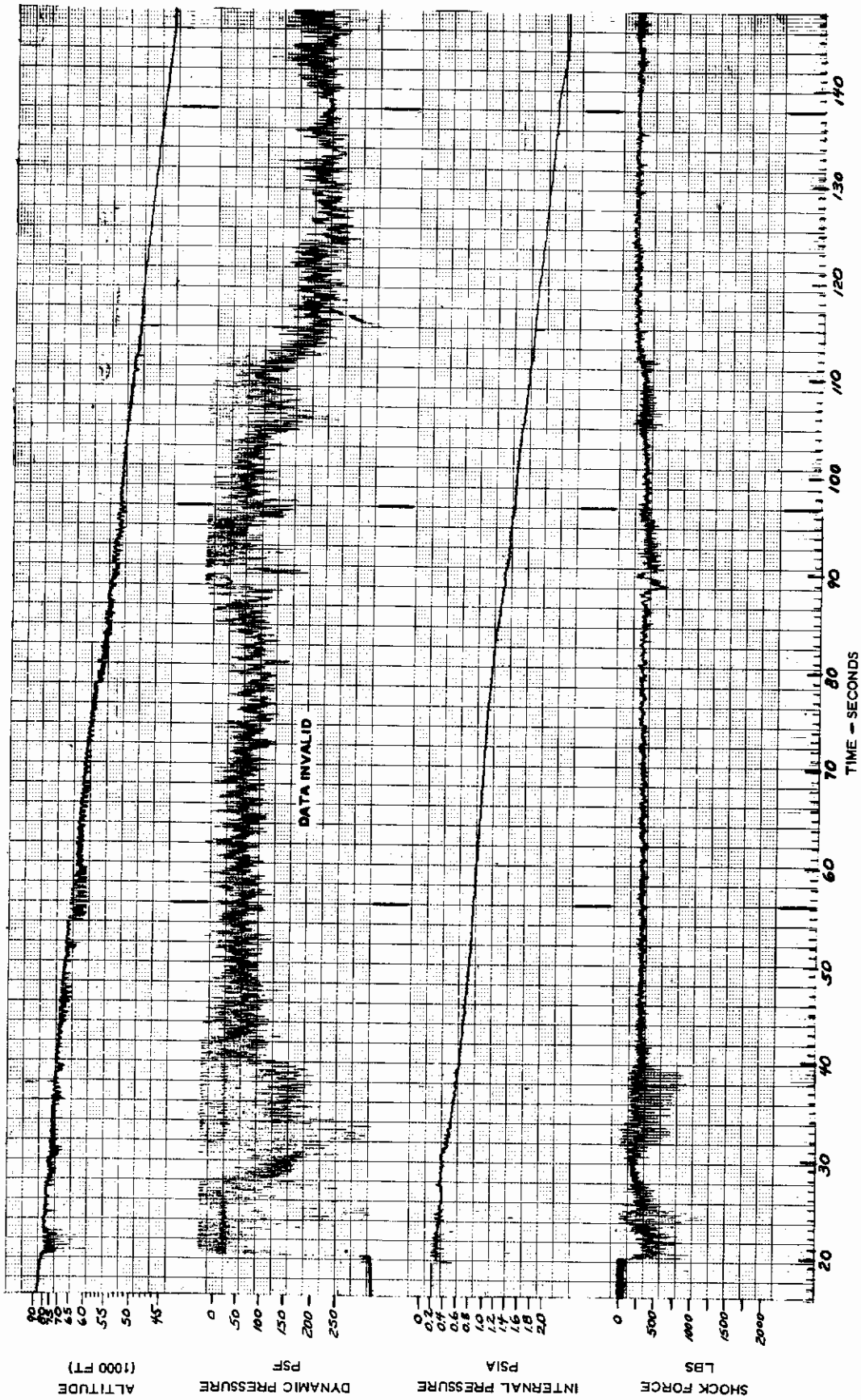

Figure 46. Aerodynamic Decelerator - Holloman Drop Test No. 4

4. Data Reduction

a. Mathematical Implementation. To determine drag effects from the available flight test data requires certain mathematical manipulations.

(1) Tracking Data. The optical tracking data was initially obtained in terms of altitude and range histories. This raw data was then smoothed by a least squares-fit to a polynomial, thus minimizing the data point scatter. Velocity and acceleration were then determined by evaluating the first and second derivatives of the polynomial.

The subsequent analysis to determine the aerodynamic effects reflects the inaccuracies due to smoothing and any bias in the raw tracking data. The resulting magnitude of error depends on the particular case; therefore, the solution gives a domain rather than an absolute value.

The parasite drag of the Ballute deceleration system can be approximated directly from acceleration data.

Developing the tangential equation of motion of the system in Figure 47 gives

$$(M_1 + M_2)\,\dot{V} = -D_1 - D_2 - (M_1 + M_2)\,g_0 \sin\gamma. \tag{1}$$

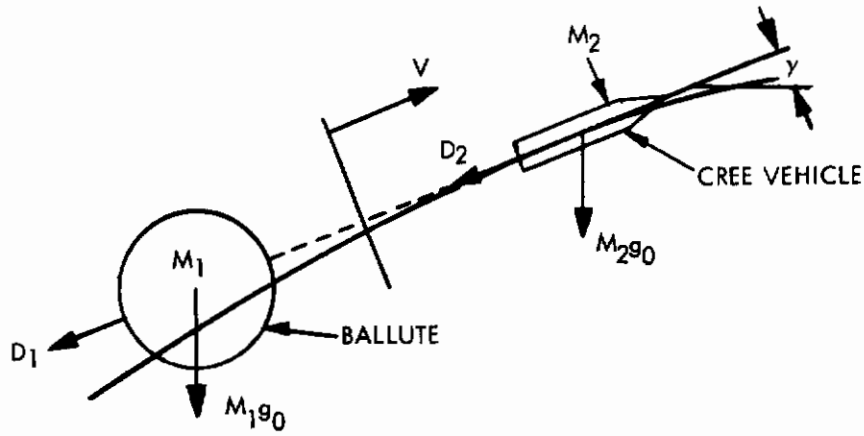

Figure 47. Free-Flight Forces

Now, assuming that the drag ratio (D_2/D_1) is equal to the area ratio since the drag of the Cree vehicle is minute compared to that of the Ballute, i. e.

$$\frac{D_2}{D_1} = \frac{A_2}{A_1} = \frac{0.44}{63.6} = 0.007, \tag{2}$$

and substituting this value into Eq 1 gives

$$(M_1 + M_2)\,\dot{V} = -1.007\ D_1 - (M_1 + M_2)\,g_0 \sin\gamma\ . \tag{3}$$

Rearranging and solving for D_1,

$$D_1 = -\frac{1}{1.007}\ (M_1 + M_2)\,(\dot{V} + g_0 \sin\gamma). \tag{4}$$

However, since $\dot{V}$ is negative, Eq 4 may be written:

$$D_1 = \frac{1}{1.007} (M_1 + M_2) (\dot{V} - g_0 \sin \gamma). \tag{5}$$

Drag can also be expressed as a function of velocity as follows:

$$D_1 = \frac{1}{2} \rho C_D A_1 V^2 \tag{6}$$

where ρ is the atmospheric density which is obtained readily from concurrent flight test data or Reference 3. The drag coefficient slope is now obtained directly from

$$C_D = \frac{2D_1}{\rho A_1 V^2} \tag{7}$$

(2) Telemetry Data. Drag data is also obtained from telemetry recordings from a strain gage mounted on the cable connecting the Ballute to the Cree vehicle. To determine the Ballute parasite drag this data is analyzed as follows:

Observing Figure 48, Eq 8 and 9 are formulated:

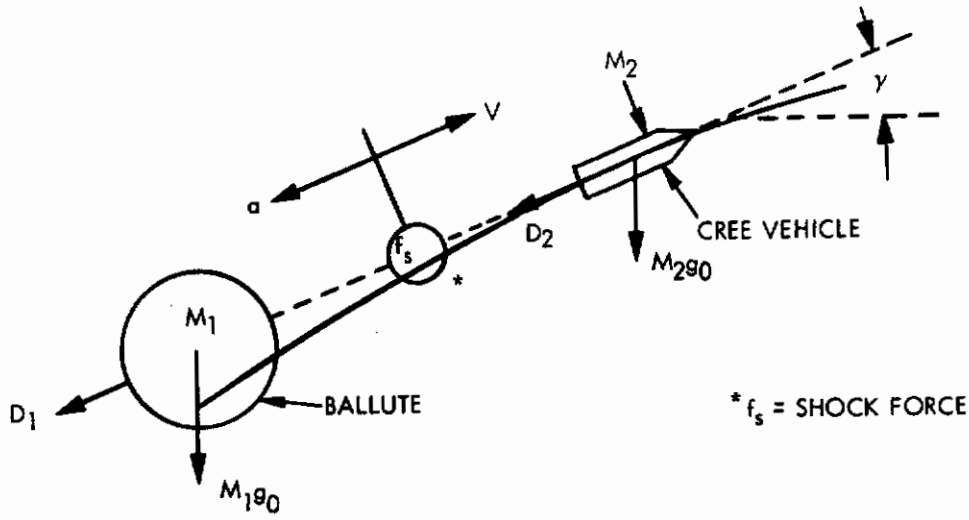

Figure 48. Free-Flight Forces with Tensiometer

$$M_1 a = -D_1 - M_1 g_0 \sin \gamma + f_s \tag{8}$$

and

$$M_2 a = -D_2 + M_2 g_0 \sin \gamma \; f_s . \tag{9}$$

Now, assuming that the drag ratio (D_2/D_1) equal to the area ratio (Eq 2) and solving these simultaneous equations (8 and 9) for drag (D_1) gives

$$D_1 = f_s \frac{M_2 + M_1}{M_2 - 0.007 M_1} . \tag{10}$$

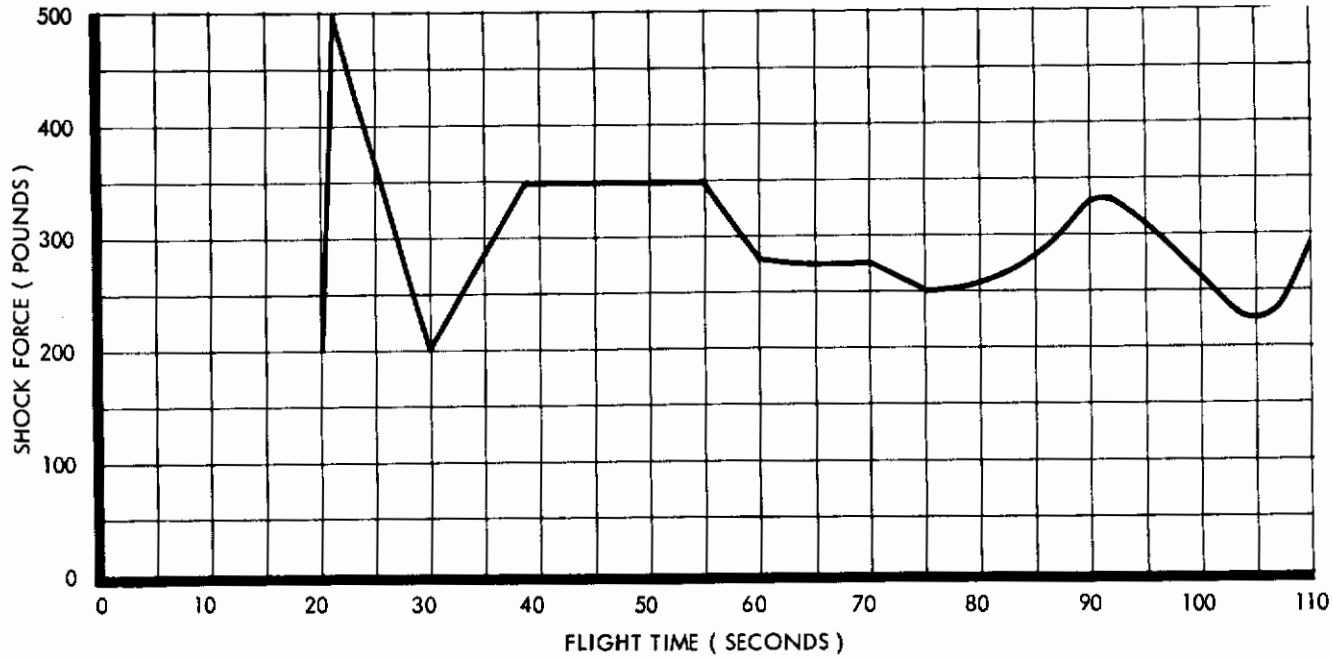

Figure 49. Telemetry Shock Force Data (Cree Drop Test No. 4)

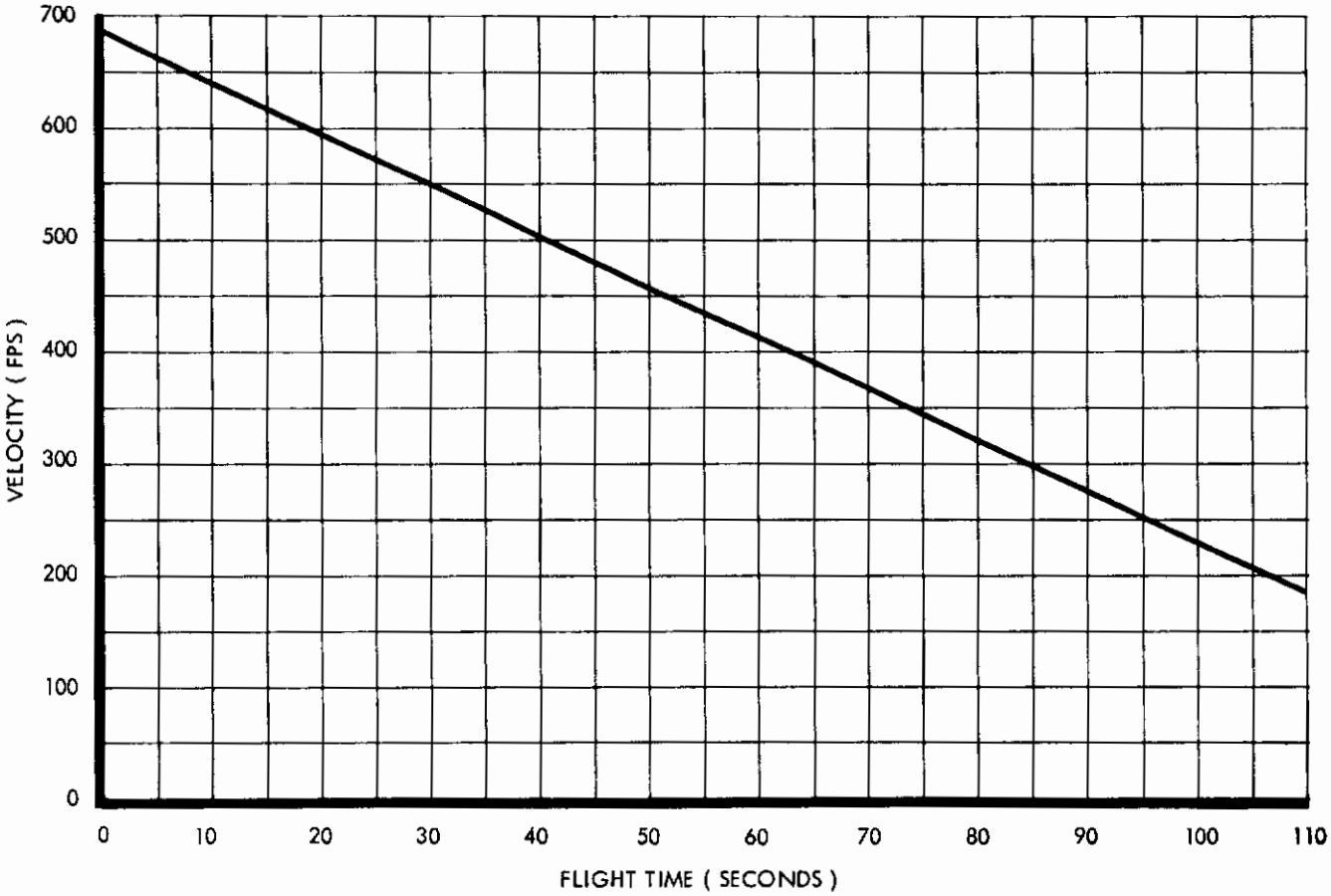

Figure 50. Theodolite Tracking Data (Cree Drop Test No. 4)

The drag coefficient can be determined by the same method used for the tracking data (utilizing Eq 7). This involves a correlation between telemetry and tracking data since the velocity term (V) in Eq 7 must be obtained from tracking data. However, the fundamental concepts differ, thus according independent results.

b. Data Analysis. Telemetry shock force data and velocity data interpolated from phototheodolite tracking are given in Figures 49 and 50 respectively for the Holloman Cree drop test No. 4. From these data, drag coefficient slopes were developed (see Table 4) for both telemetry and tracking flight test results. The resulting slopes are depicted in Figure 51.

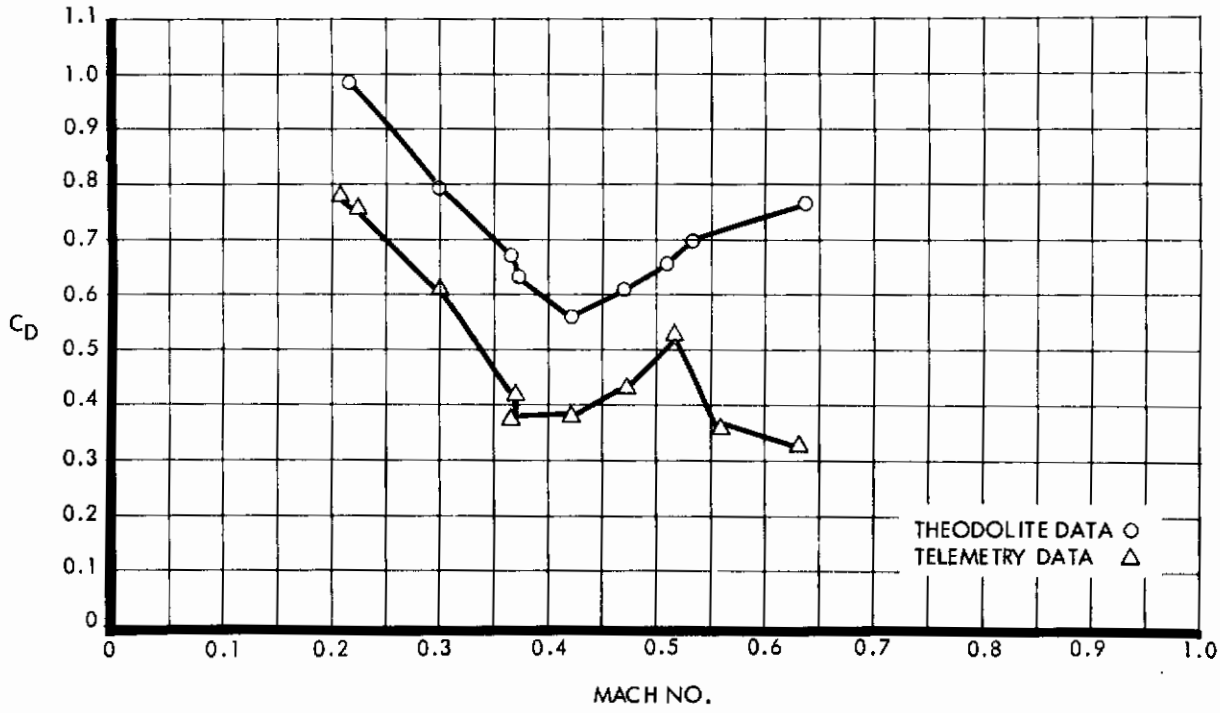

Figure 51. Drag Coefficient Slope Derived from Cree Drop Test No. 4

Table 4. Cree Drop Test No. 4 (Parametric Data)

t	V	$1/2\ \rho AV^2$	D*	D**	M	C_D*	C_D**
20	4.54	688.50	528.28	218.05	0.635	0.767	0.317
30	4.54	750.89	528.28	272.46	0.532	0.704	0.363
40	4.54	844.29	528.28	401.21	0.508	0.626	0.475
50	4.54	859.68	528.28	376.02	0.470	0.614	0.437
60	4.54	940.83	528.28	359.77	0.422	0.562	0.382
70	4.54	834.43	528.28	353.63	0.370	0.633	0.424
80	4.54	780.88	528.28	294.70	0.365	0.677	0.377
90	4.54	668.31	528.28	409.61	0.300	0.790	0.613
100	4.54	535.57	528.28	400.12	0.218	0.986	0.747
110	4.54	383.89	528.28	301.66	0.205	1.376	0.786

* Drag as calculated from theodolite data.
** Drag as calculated from telemetry data.

c. On-Board Camera Data. The high-speed camera mounted in the Cree Missile looking aft toward the Ballute began operating just prior to Ballute deployment (T + 19.28 seconds). The camera speed was 100 frames per second and covered the first 37 seconds of Ballute operation. The reference point used to synchronize the filmed sequence with the other data was the flash of the ignition of the forward shaped-charge canister separation which was clearly visible in two frames of the film. The upper portion of the photographs are obscured throughout the sequence by an unexplained obstacle, possibly residue from the explosion or a piece of tape from the wire bundle. Figures 52 through 63 show some of the significant stages of the deployment and operation of the Ballute.

The film data was analyzed by using two "fixed-position" references to determine the attitude of the missile. The motions of the Ballute with respect to the missile were determined by the position and attitude of the Ballute in the field in view of the camera. The "fixed-position" reference used were the ascension balloon and the ancillary equipment parachute. As previously mentioned, the film was obscured; therefore, the data are limited to the pendulus motion of the missile, rotation and amplitude of the Ballute oscillations. The film analysis determined that the maximum motions occurred as shown in Table 5.

Table 5. Ballute Stability - Drop Test No. 4

SYMBOL	VALUE	POSITION REFERENCE
a	13 Degrees	Parachute and Ascension Balloon
f_b	1.3 cps	Parachute and Ascension Balloon
θ	3 Degrees	missile
f_a	5.4 cps	missile
x	62.0 inches	missile
f_c	5.9 cps	missile

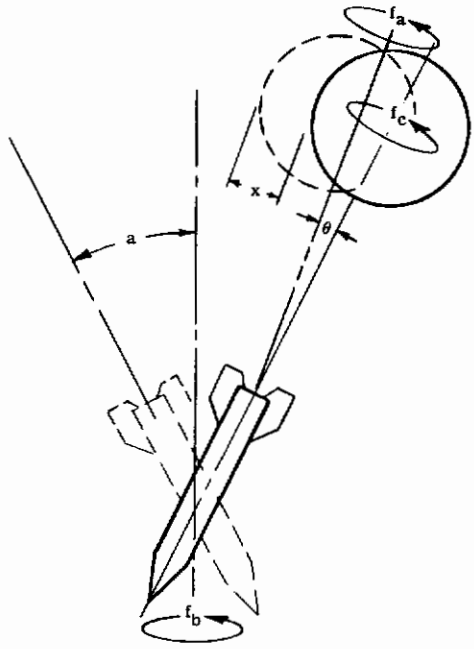

SYMBOL DESIGNATION

a = half angle of missile axis deviation from flight path (degrees)

f_b = coning rate of missile axis with respect to flight path (cycles per second)

θ = half-angle of Ballute excursion about missile (degrees)

f_a = Ballute excursion rate with respect to the missile (cycles per second)

x = total of Ballute excursions with respect to the missile

f_c = Ballute rotation with respect to the missile (cycles per second)

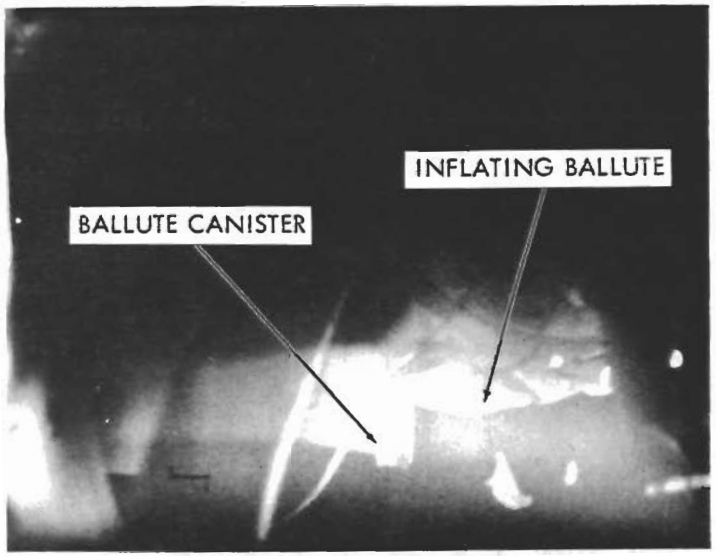

Figure 52. Ballute and Canister at
T + 20.36 Seconds

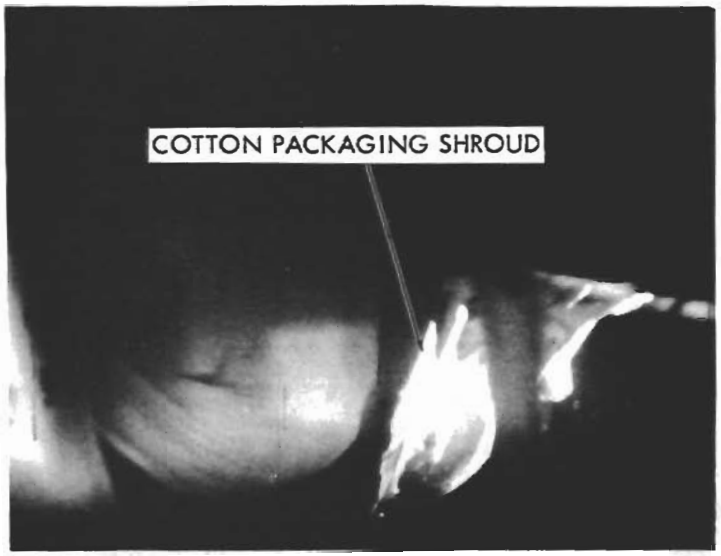

Figure 53. Packaging Shroud at
T + 20.40 Seconds

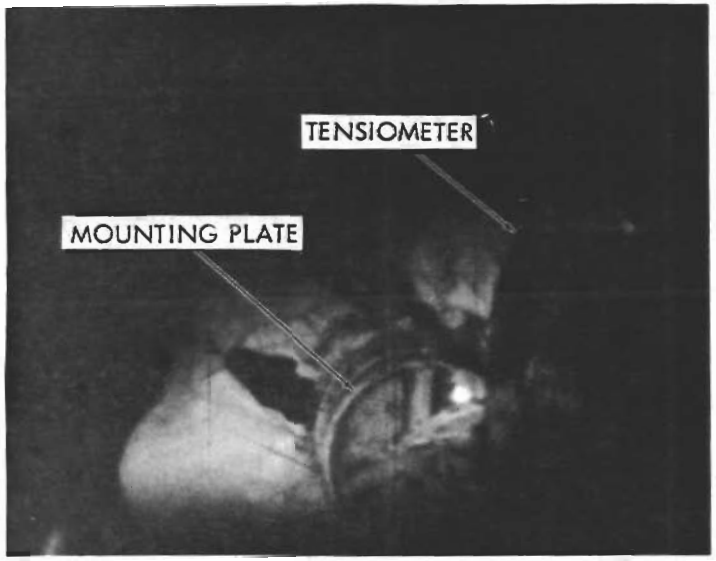

Figure 54. Mounting Plate and Tensiometer
at T + 20.74 Seconds

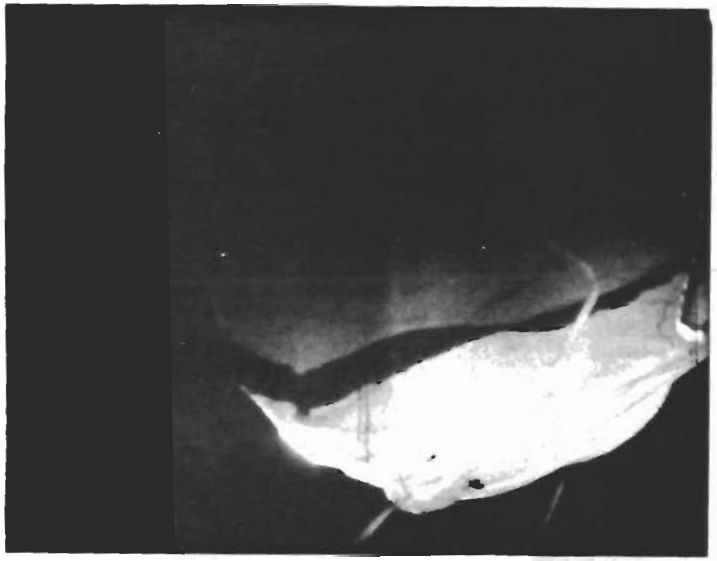

Figure 55. Partially Inflated Ballute
at T + 22.48 Seconds

Figure 56. Jettisoned Canister
at 23.45 Seconds

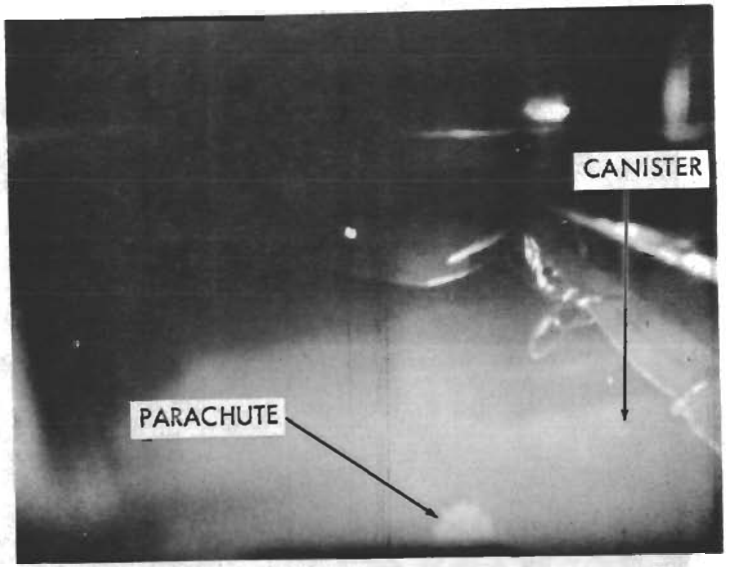

Figure 57. Ancillary Equipment Parachute
at T + 29.72 Seconds

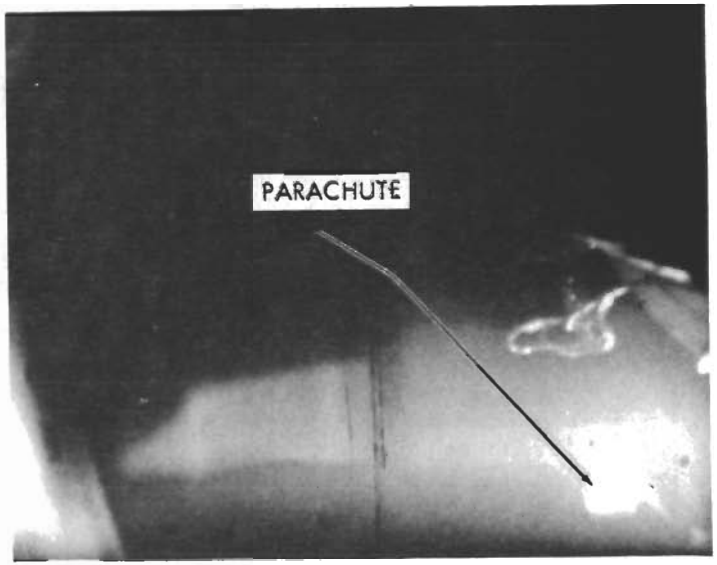

Figure 58. Ancillary Equipment Parachute
at T + 29.79 Seconds

Figure 59. Ascension Balloon
at T + 46.18 Seconds

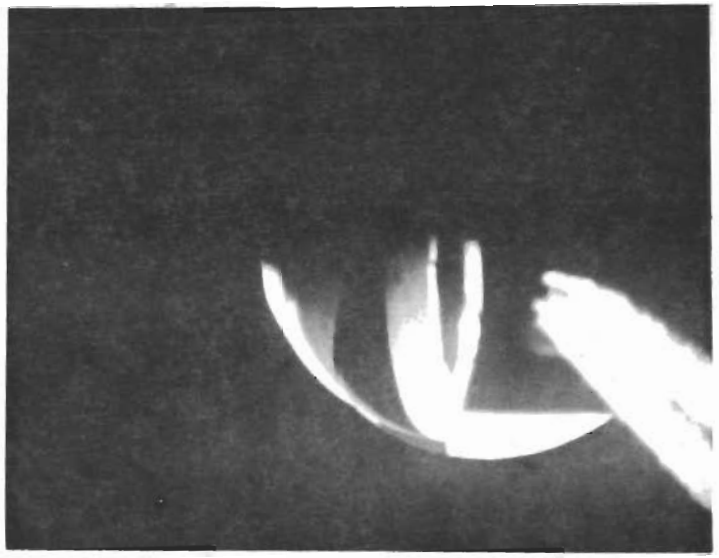

Figure 60. Ballute and Tensiometer at T + 48.46 Seconds

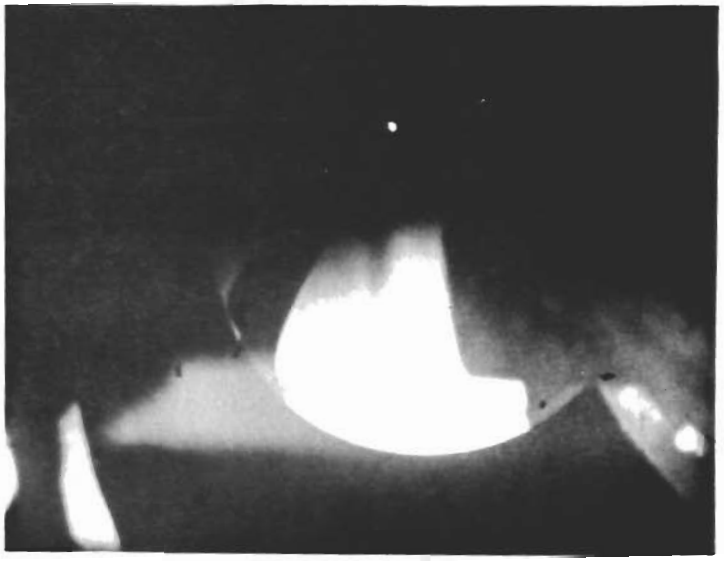

Figure 61. Ballute at T + 51.55 Seconds

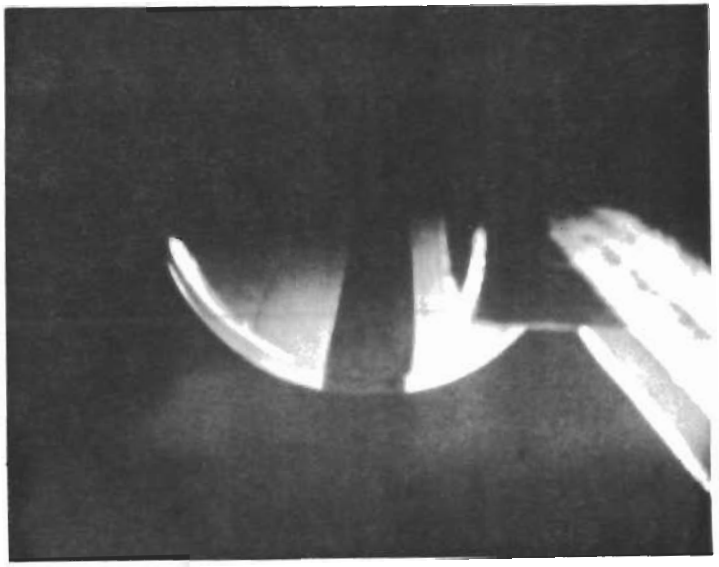

Figure 62. Ballute at T + 51.84 Seconds

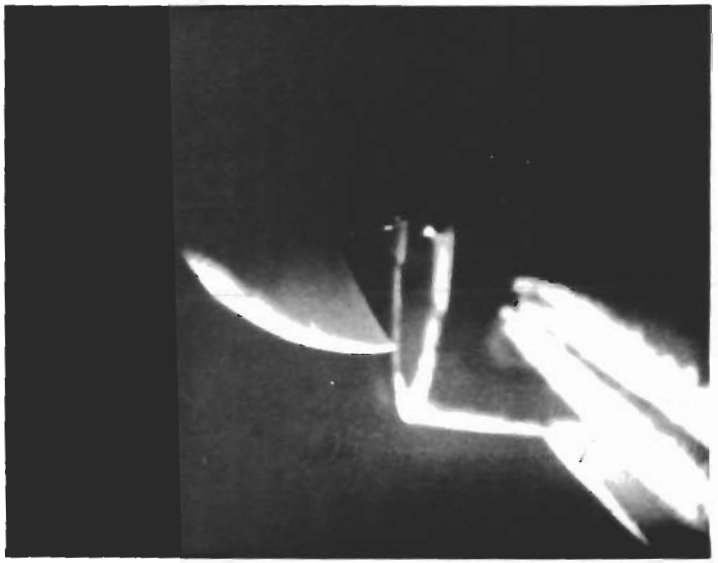

Figure 63. Ballute at T + 53.79 Seconds

SECTION 3

SUPERSONIC FLIGHT TESTS

A. GENERAL

Supersonic flight testing to evaluate the functional and performance characteristics of the Ballute drag device was accomplished at the Air Proving Ground Center, Eglin Air Force Base, Florida. This flight testing utilized a Cree-type, boosted, ground-launched missile as the test vehicle.

B. TEST ITEM DESCRIPTION

The drag device performance characteristics were evaluated during supersonic flight. The drag device is of the inflatable balloon type corresponding to GAC assembly drawing GA482-100. In addition to this drag device, the stowage containers or canisters, inflation components, and suspension hardware were also functionally tested. These units are identical with the items previously tested at AFMDC, Holloman Air Force Base, Alamogordo, New Mexico. A complete description of each of these items and its operation during and after deployment initiation is in Section 2. Two complete and identical systems were required for these tests. The only modification to the inflated drag device for Eglin Air Force Base was the addition of a thermal detector paint to determine the temperature of the surface area of the drag device during the test.

C. TEST EQUIPMENT

1. Test Vehicle

The test vehicles for this project consisted of a Cree test missile and Nike M-5 rocket motors with all units mounted in tandem. Two flight configurations were utilized, one with two Nike motor stages and one with three Nike stages. Figures 64 and 65 show the two-stage configuration on the launcher. Figure 66 is a diagram of the Nike-Nike-Cree II configuration. The three-stage configuration shown on the launcher in Figure 67 contains an additional Nike motor stage and an over-all length of approximately 605 inches.

Standard Ajax fins used on the first-stage motors were modified to provide a cant of 1/2 degree for the two-stage configuration and 1 degree for the three-stage configuration. The second-stage and third-stage fins were the variable incident type and were set for a zero-degree cant (no roll). Further information on this test vehicle and its operation may be found in Reference 4 and in Section 2.

Two Model 60 Cree Type II test vehicles were used to accomplish the test missions. This vehicle contained a five-channel telemetry system, a high-speed motion picture camera, a programming system, a parachute recovery system, a DPN-41 transponder, and a flotation system. A cutway view of the ground-launched Cree missile is shown in Figure 68.

a. Telemetry System. Provisions were made for the following data to be gathered and transmitted by the five-channel telemetry system:

(1) Shock force

(2) Drag force

(3) Acceleration

(4) Differential Pressure

(5) Inflatable Decelerator Internal Pressure

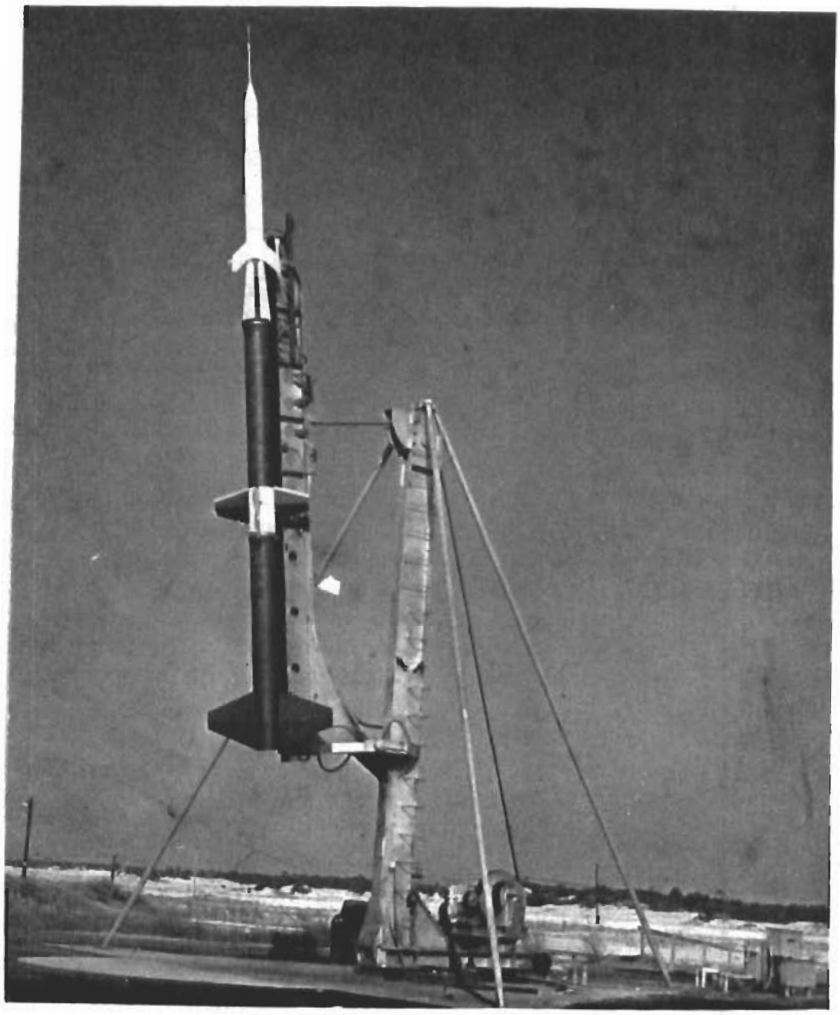

Figure 64. Cree Test Vehicle with Two-Stage Nike Configuration in the Launch Position

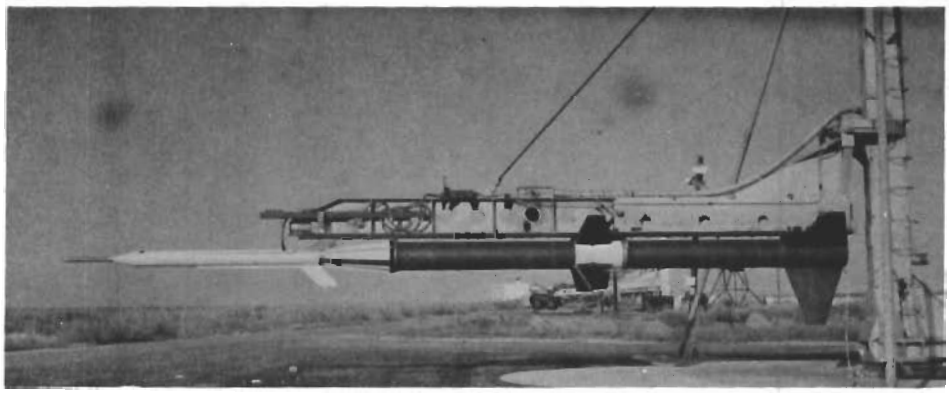

Figure 65. Cree Test Vehicle with Two-Stage Nike Configuration on the Launcher in the Missile Loading Position

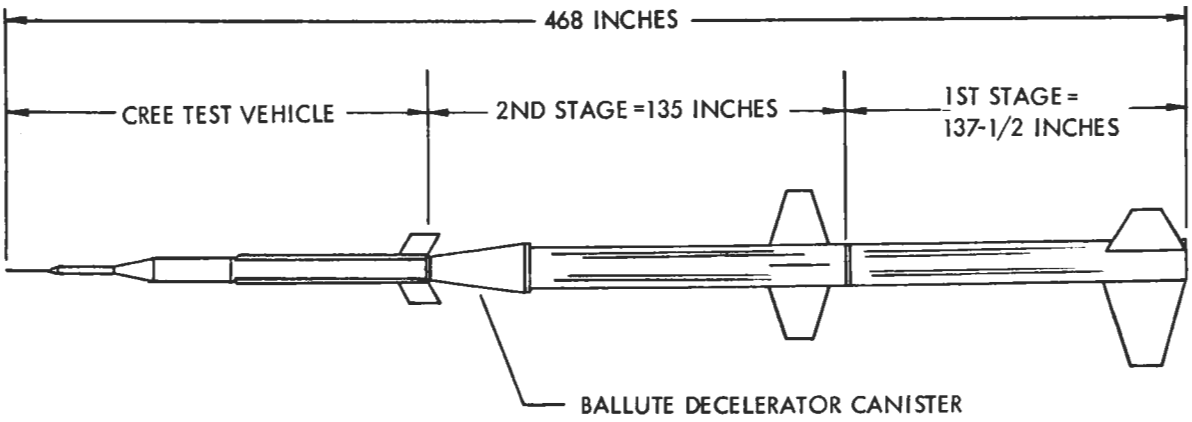

Figure 66. Sketch of the Nike-Nike-Cree II Ballute Configuration

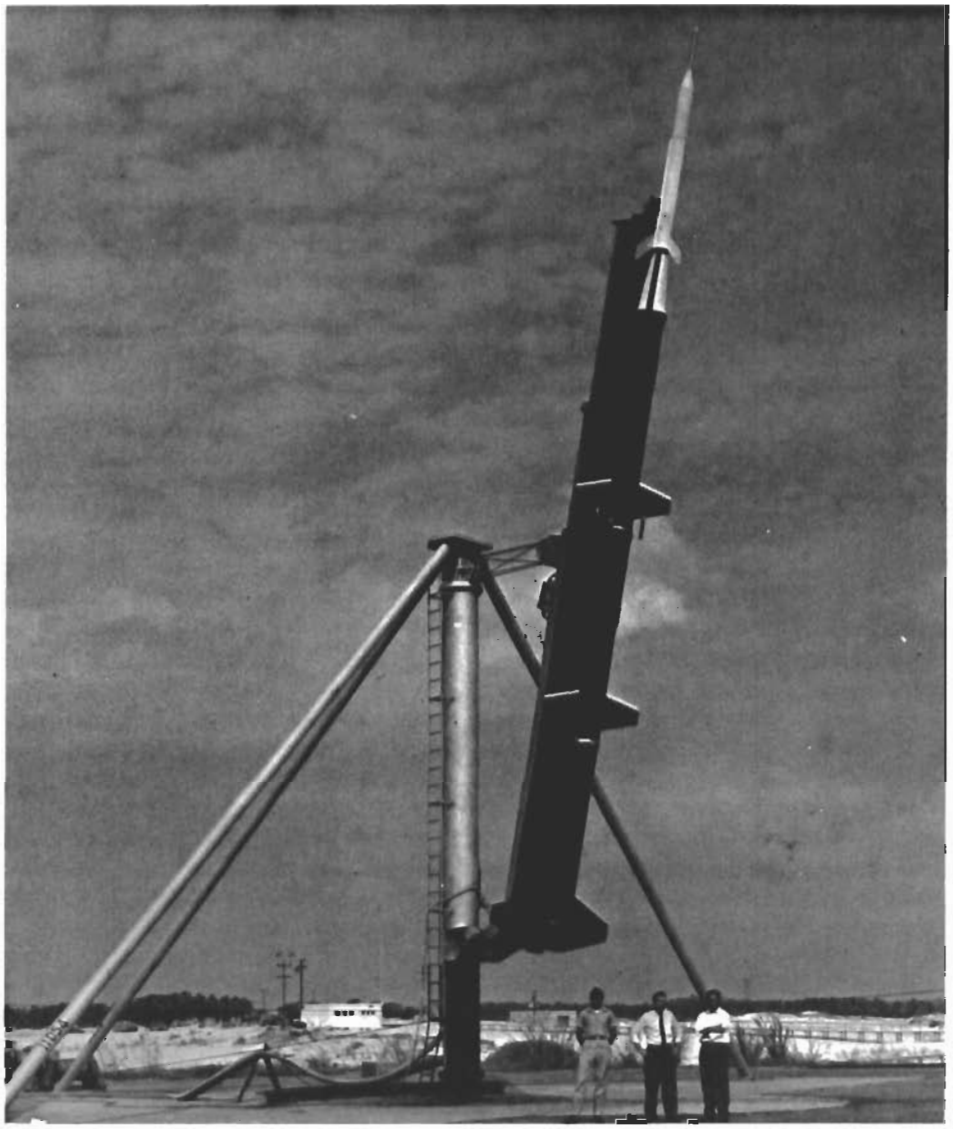

Figure 67. Cree Test Vehicle with Three-Stage Nike Configuration

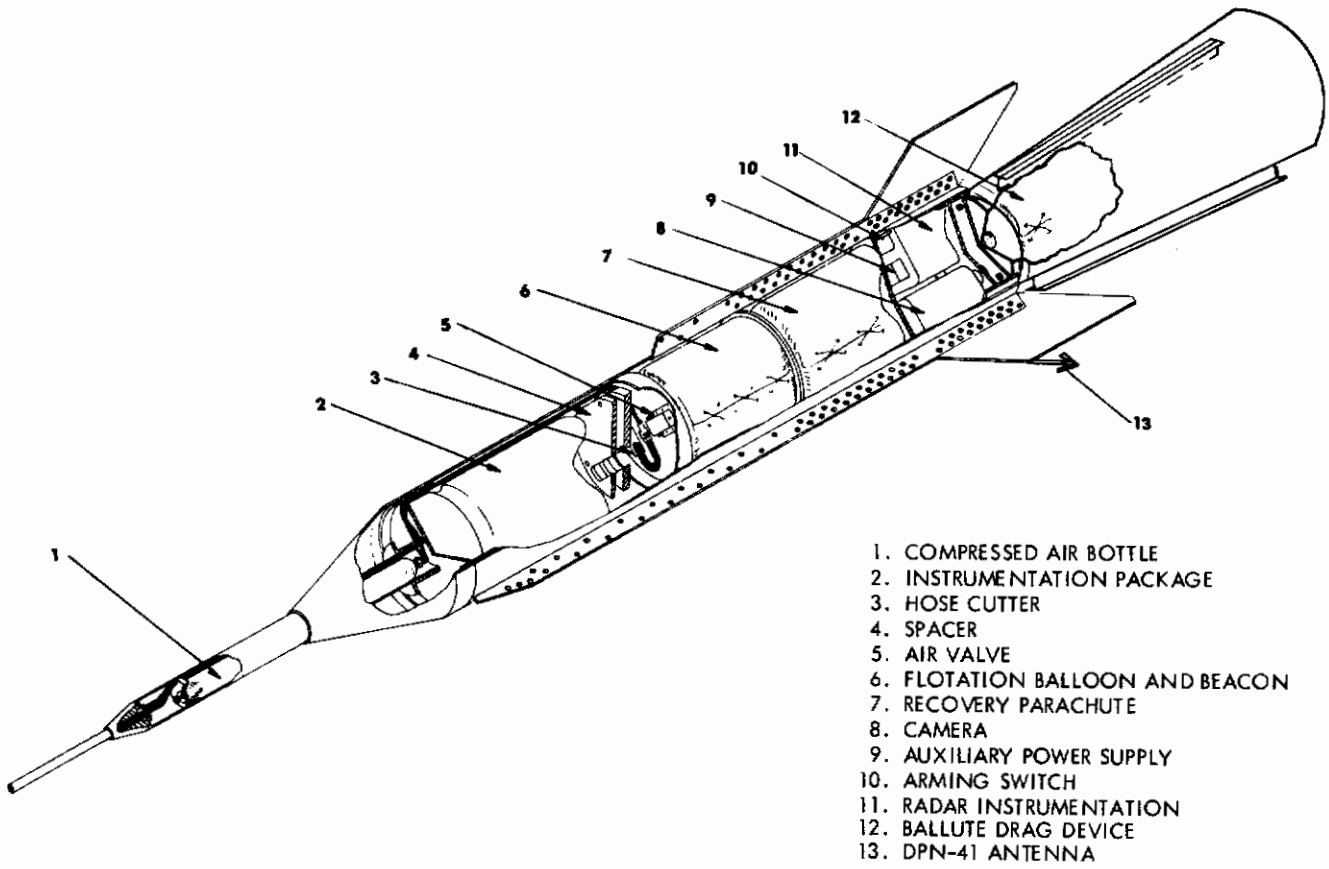

Figure 68. View of Ground-Launched Cree Missile and Ballute Package

A complete description of the instrumentation used to obtain this data is contained in Section 2.

b. Photography. Camera coverage of the deployment and inflation of the decelerator device was provided by a 16-mm motion analysis camera with a spool capacity of 100 feet. The operation principle depends upon a rotating prism by which an image is continuously place on film moving at a specific speed. Figure 68 shows the aft compartment where the camera was mounted and oriented aft to view the drag device being tested.

c. Programming System. The Cree missile programming system consisted of two electromechanical timers. These timers operate independently, have a 120-second capacity, and are capable of controlling a number of functions. The following functions were controlled during these tests:

(1) Booster Separation

(2) Telemetry Calibrate

(3) Camera On

(4) Canister Separation and Ballute Inflation

(5) Parachute Door Opens and Nose Ballast Separates

(6) Parachute Deployment

d. Recovery System. After a suitable test period the programming system initiates the recovery phase. The recovery door is broken open by a pair of blasting caps and a strip of shaped charge. Approximately 1/10 second later the recovery parachute is deployed and the nose weight separates.

e. Flotation System. Since these test missions were conducted over water, flotation equipment was essential for successful missile recovery. The standard Cree Missile recovery equipment was used. Included in this system was a 24-inch-diameter balloon with a nylon drag skirt attached at the equator, a compressed air storage bottle, an ultrasonic marker, marker dye, and shark repellent. The operations were controlled by the sequence timer and initiated by pyrotechnic devices. The recovery sequences were as follows:

(1) The flotation balloon displaces from its compartment as it inflates and remains tethered to the side of the missile until it is completely filled.

(2) After inflation a pyrotechnic-actuated hose cutter frees the flotation balloon so that it will take a position behind the recovery parachute.

(3) Upon impact, a salt-water-activated switch closes a circuit to supply battery power to the ultrasonic marker. The ultrasonic marker operates at a frequency of 37 kc. Deployment of the marker is simultaneous with the floatation balloon. Shark repellent and marker dye are dispersed into the water upon deployment of the floatation balloon.

2. Data Acquisition Equipment

a. Airborne Instrumentation System Description. The airborne instrumentation system employed during the rocket-boosted transonic flight test consisted of the following subsystems and/or components:

(1) FM/FM Telemetry

(2) Program Timer

(3) Radar Tracking Beacon

(4) Camera

(5) Recovery Aids

(6) Power Supply

(1) FM/FM Telemetry. FM/FM Telemetry techniques were used to obtain five measurements of test data. These included dynamic pressure (channel 12), Ballute internal pressure (channel 13), acceleration (channel 14), drag force (channel C), and shock force (channel E). A simplified block diagram of the telemetry system is shown in Figure 69.

(a) Dynamic Pressure. The dynamic pressure data was measured during test No. 1 by using a resistive bridge type pressure transducer with a range of ±2.5 to ±25 psid. Output voltage at full scale is ±10 mv. During test No. 2, a pressure transducer with a range of ± 0.15 to ±0.7 psid was employed to provide greater sensitivity. The output voltage at full scale is ±20 to ±32 mv. A solenoid-operated valve was employed to prevent damage to the diaphragm during the boost phase of the test flight.

(b) Ballute Internal Pressure. A modified potentiometric pressure gage was used to measure the internal pressure of the Ballute. The modification was to permit operation as an absolute gage in the range of 0 to 2 psia. The full-scale output voltage from the gage is 5 volts.

(c) Accelerometer. Accelerations normal to the longitudinal axis of the missile were measured using an accelerometer with the strain gage principle of operation and an output of 20 mv at 50 g's.

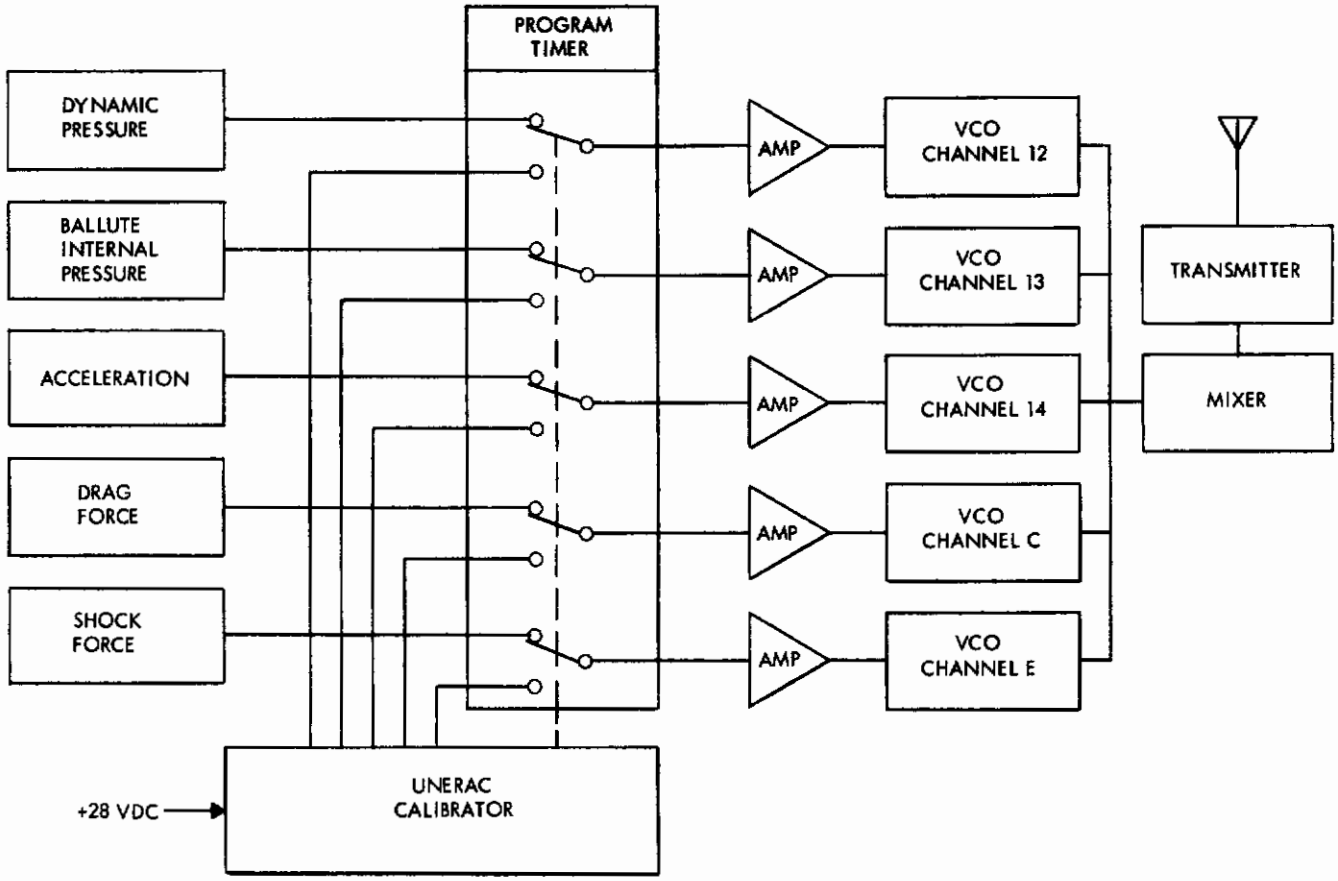

Figure 69. Instrumentation System Block Diagram

(d) Drag Force and Shock Force. The drag and shock force measurements were obtained from a circular ring strain gage tensiometer. This instrument was of the same type that was described for the drop tests in Section 2 of this report.

(e) Voltage Controlled Subcarrier Oscillators. The subcarrier oscillator units of the telemetry system were transistorized units composed of three major functional components: a voltage regulator, a differential amplifier, and a subcarrier oscillator. The units operate with a low-level input signal (±10 mv for full-scale deviation), permitting direct connection to the output of strain gage type transducers.

(f) Transmitter. The transmitter for the telemetry system was a crystal-stabilized type. The power output from this unit is rated at five watts.

(g) Antenna. The antenna system was identical with the system used during the drop tests described in Section 2.

(h) Unerac. Distribution of power, both regulated and unregulated for the transmitter, transducers, and calibration circuits, was provided by a Unerac. This unit is described in Section 2.

(2) Program Timer. An electro-mechanical timer activated the various electrical circuits at particular time intervals. This unit consists of a d-c governed motor which drives a series of cams. The cams in turn actuate corresponding switch closures to complete a particular electrical circuit.

(3) Radar Tracking Beacon. Due to the over-water nature of the flight trajectory and the inherent tracking limitations of the phototheodolite cameras, a DPN-41 radar beacon was employed as a tracking aid to the AN/MPS-19 radar. This was necessary due to the planned trajectory of the test flight and the relatively small physical dimensions of the Cree Missile.

(4) Camera. A motion analysis camera was used to obtain photographic coverage of the aerodynamic decelerator during and immediately after deployment. This unit was identical with the one used for the drop tests.

(5) Recovery Aids. The predicted impact point for the Cree Missile was approximately 17 nmi from point of launch for the first test flight and 30 nmi from point of launch for the second test flight. Since the impact area was in water, a flotation balloon was essential for successful recovery of the missile. In addition to the flotation balloon, other aids were used to direct search and recovery teams to the missile's location. These aids included a dye marker for visual location and an ultrasonic marker for underwater recovery by sound detection. Sound detection equipment was provided aboard the recovery boat.

(6) Power Supply. During the test flights, electrical power to the instrumentation system, pyrotechnic devices, and the radar beacon was supplied from an internal battery pack containing a series of nickel-cadmium cells. In addition, salt-water activated switches were used to supply power for the SARAH beacon ejection after impact.

b. Airborne Instrumentation System Test and Performance

(1) Test Flight No. 1. Four nearly complete instrumentation systems were provided as GFE for contractor's use in performing the free-flight test programs. In order to select the best components available, functional tests were conducted on each component prior to assembly of the instrumentation package. Included in these tests were stability and linearity of the oscillator units, and distortion and power output of the transmitter. The units that most nearly met the manufacturer's published performance specifications were selected to be incorporated into the final system configuration for the first of two test flights.

A modification of the 14.5-kc oscillator unit was necessary to permit reception of its input signal directly from the potentiometric pressure transducer employed to measure the internal pressure of the Ballute. Details of the modification are presented in Figure 70.

The wire connecting pin 8 of the base connector to pin F of the amplifier unit was removed. The wire connecting pin C of the amplifier unit to pin D of the oscillator unit was removed from pin C and soldered to pin 8 of the base connector. This permits the oscillator to receive its input signal directly from the base connector, thereby eliminating the amplifier from the circuit.

Following the functional tests of the components and system assembly, the complete telemetry system was calibrated. This was accomplished by providing the proper stimulus to each transducer and recording the output.

The pre-emphasis for the subcarrier oscillator outputs was established by the procedure described in Section 2. Upon completion of missile and payload assembly, horizontal and vertical on-range checks were conducted. The purpose of these tests was to verify complete compatibility with the booster system, blockhouse control circuits, and satisfactory reception of transmitted signals to down-range telemetry and tracking stations.

During the vertical on-range check, the telemetry signals received at the blockhouse were recorded for each channel during the calibration sequence. Comparison of the on-range checks with records obtained during laboratory systems calibration indicated that the oscillator units for channels 12, 13, and E had drifted beyond acceptable limits. Prior to the final countdown, these units were replaced.

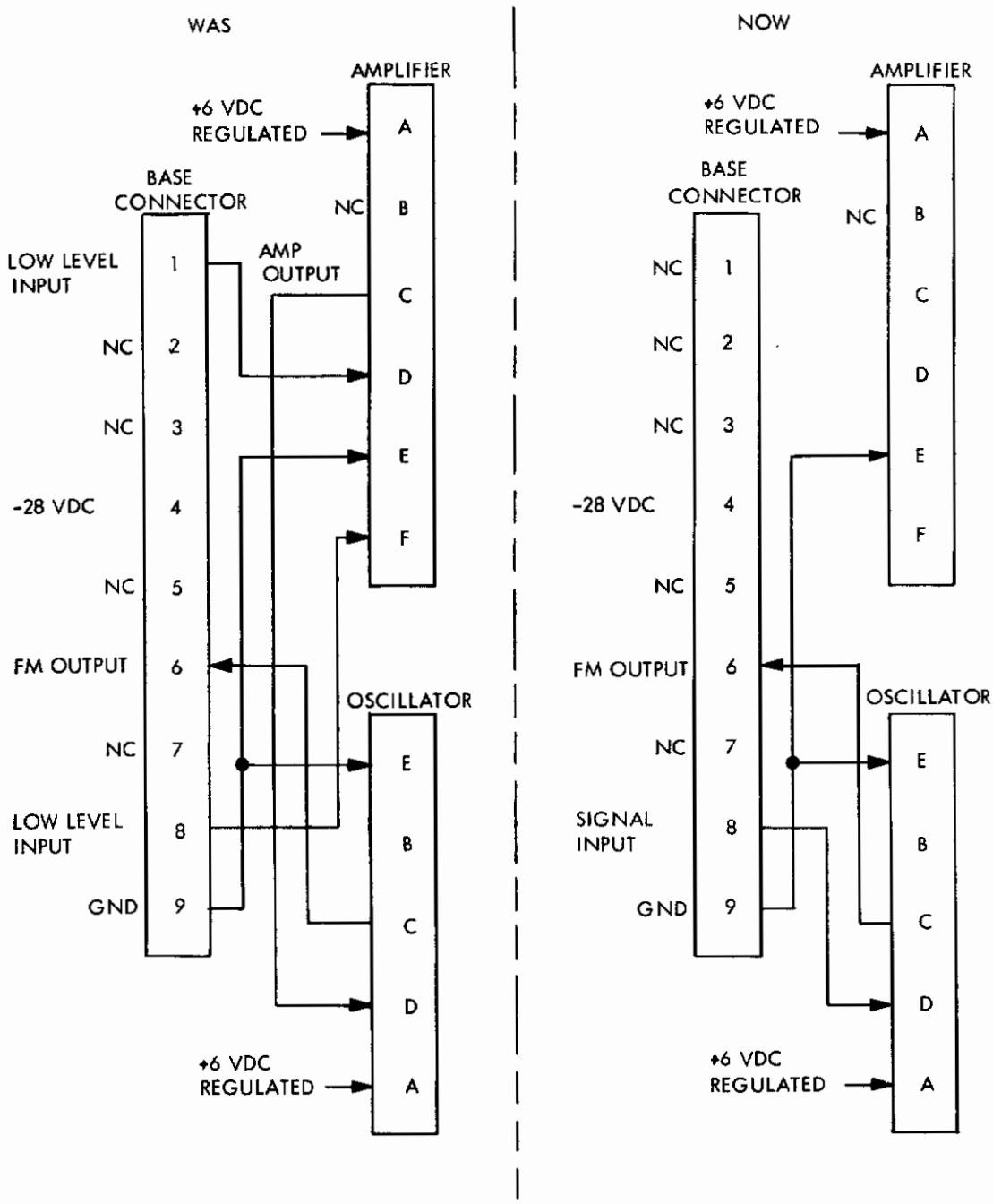

Figure 70. Modifications to Subcarrier Oscillator Unit (14.5 KC)

(2) Test Flight No. 2. Post-flight review of the telemetered data disclosed several descrepancies in the telemetry system. Most prevalent was excessive drift of the oscillator units. In an effort to provide the most reliable components for the second test flight, an extensive component evaluation program was established. As mentioned before, each oscillator unit consists of a voltage regulator, a low-level differential amplifier, and an oscillator. It was decided that all units (20 total) would be disassembled and that each of the three components per unit would be evaluated by itself.

Results of these tests showed that 13 of the 20 voltage regulators failed to perform within acceptable limits of operation. Of the 20 low-level differential amplifiers tested, 11 units were completely unacceptable for use due to low gain, instability, and/or non-linearity. The remaining nine units were non-linear in varying degrees, and all but one were somewhat unstable. Test results from the 20 oscillator units (four units each of five channel frequencies) showed that one channel 12 unit was non-operative, one channel 13 unit could not be adjusted for proper bandwidth, two channel 14 units had very low outputs and considerable drift, three of the channel C units could not be used due to low outputs and excessive drift characteristics, and three channel E units could not be used due to excessive harmonic distortion, instability, and/or excessive drift. Subsequent to the above tests, the best performing components were selected and assembled into the instrumentation system for a complete systems calibration.

D. SUPERSONIC FLIGHT TEST PROGRAM OBJECTIVES

The objective of this test program was to functionally demonstrate the deployment and operation of the inflatable balloon-type drag device. The test conditions programmed were Mach 1.5 at an altitude of 135,000 feet and approximately Mach 4 at an altitude required to develop a dynamic pressure of 10 psf. However, final analysis of the two-stage and three-stage Nike-boosted tests resulted in predicted test points of Mach 1.3 at 124,000 feet and Mach 2.23 at 150,000 feet. These test points were based on the capabilities of the Nike boosters. Boosters with high thrust were not available. See Figure 71 and 74.

In addition to this demonstration of deployment and operation, specific data to include differential pressure, shock force, drag force, test vehicle acceleration, and internal balloon pressure was to be obtained during the test. The data acquired was then to be transmitted to receiving stations for later use in the analysis of these tests and to substantiate the designs of future models.

At the conclusion of these tests, the test vehicle and inflatable drag device tested were to be recovered by an independent parachute recovery system and flotation system.

E. TESTS

1. Two-Stage Nike-Booster Flight

a. Specimen Build-Up. The test specimen build-up for the first vehicle launch began on 18 September 1960. A considerable amount of time was used to check the circuitry at the launch pad and blockhouse and associated launching equipment. The Cree test missile required major refurbishing since its telemetry, timers, and other instrumentaion were as left from a previous Cree test program. The remainder of the time was spent in various coordination meetings with Air Force launch personnel, the project officer, the ASD representative, and the data reduction personnel.

During calibration and telemetry check-out, it was noticed that the subcarrier frequencies had a high tendency to drift. Corrective measures were taken;however, there was no absolute assurance that the telemetry would work during the test.

b. Equipment Check. Table 6 shows the timing sequences that were set on the main and auxiliary programmers to obtain the predicted trajectory shown in Figure 71 .

Table 6. Test No. 1 Timing Sequences - Programmers

SEQUENCE	DESIRED TIME	ACTUAL MAIN (seconds)	ACTUAL AUXILIARY (seconds)
Booster separation	T + 45 seconds	45.12	45.18
Telemetry calibrate	As available	46.47	--
Camera on	T + 69 seconds	68.77	69.23
Canister separation and ballute inflation	T + 71.8 seconds	71.78	--
Parachute door open and nose weight separation	T + 105 seconds	105.15	105.13
Parachute deployment	T + 105.1* seconds	105.25	105.23

*0.1-second time delay used.

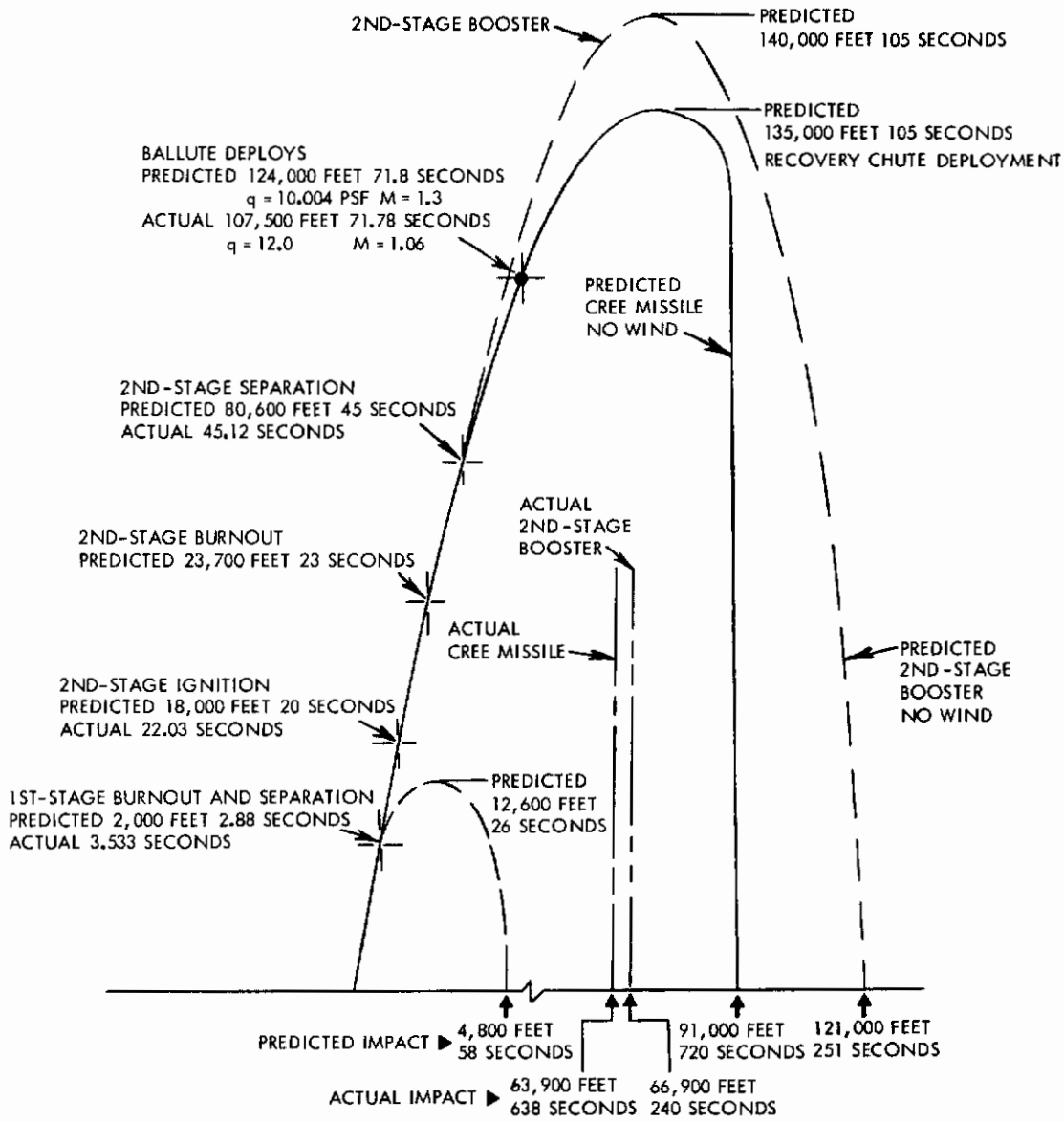

Figure 71. Altitude versus Range - Predicted Trajectory and Radar Plot of Actual Trajectory (Two-Stage Test)

At the conclusion of the bench checks, the test vehicle was moved to the launcher for operational range checking (ORC) with the vehicle in both the horizontal and the vertical positions. Modifications as a result of these checks included relocation of the DPN-41 antenna, relocation of bolts on test item package to match Nike bolt hole pattern, and readjustment of the telemetry carrier frequencies.

c. Launching. The first scheduled launching was to take place on 6 October 1961; however, this mission was cancelled due to weather conditions. Visibility for camera coverage was limited, and vehicle recovery was doubtful because of a sea state reported to be 3. Subcarrier frequencies again appeared to be drifting and require readjustment. As a result, the test specimen was moved to the work area for telemetry check and battery recharge. The rescheduled launch date was 9 October 1961.

This second planned launch date was also cancelled due to a power failure resulting in a complete discharge of the batteries. The mission was then rescheduled for 10 October 1961.

On this third test date, the test vehicle was again placed on the launcher. Vehicle check-out continued until tracking stations A-3 and A-6 could no longer receive the telemetry and beacon signals due to outside interference from an unknown radar source. The countdown was held until this interference reduced to permit reception again at A-6.

At approximately 0925 hours the beacon and telemetry checks were completed, and the reception of these signals at A-3 and A-6 was satisfactory. The phototheodolite stations reported good visibility, and the sea state was calm with the wind at 10 mph.

The missile was launched at 0945 hours on 10 October 1961. Launch position was set at elevation 83 degrees, azimuth 155 degrees. The missile launch appeared normal. A photograph of this launch is shown in Figure 72.

The sequence of events as indicated later by the oscillograph records was as programmed. Telemetry records show that the test period was approximately 37 seconds. Utilizing a ballistic program with corrections drived from the prelaunch wind data, an IBM 7090 computer was used to compute impact point.

d. Recovery. The Ballute package was recovered with the missile by the 3000-pound nylon lanyard. The 15,000-pound strap from the aft end of the missile to the tensiometer had parted during the flight and was not recovered. A majority of the Ballute fabric had been torn away as shown in Figure 73. A review of the film from the camera shows that the Ballute did inflate. The portion of fabric not recovered can be attributed to descent after the test period was over.

2. Three-Stage Nike-Booster Flight

a. Specimen Build-Up. The three-stage launch vehicle also used the Cree-60 missile shell and instrumentation. As a result of the previous firing, several changes were made during the missile build-up in an effort to ensure that the desired test data would be obtained. These changes included:

(1) Installation of a sturdier antenna.

(2) Use of a multi-lap strap for attachment of the tensiometer to the missile.

(3) Confining the Ballute internal pressure transducer wires within the nylon lanyard and the use of rings on the cable to contain the lanyard with transducer wires and prevent them from whipping around after deployment.

(4) An evaluation of transistorized low-voltage control oscillators for each subcarrier frequency. This change was undertaken to obtain better stability and lower noise with the same output. A circuitry change to ground the voltage supply was also made to make the telemetry system less susceptible to interference. A longer warm-up period was also found to be helpful in reducing the drift of the carrier frequencies.

b. Equipment Check. The same procedure was used for the three-stage vehicle as employed on the two-stage vehicle, and all systems were determined to be satisfactory. The timing sequence was changed to comply with the three-stage configuration. The main and auxiliary timer sequences were set as shown in Table 7 to obtain the desired trajectory shown in Figure 74.

During the field checking, the alignment of the Cree/Ballute/Nike was checked. Such a check was felt to be necessary since a photograph of the first test flight vehicle indicated that there may have been some misalignment of the Cree-Ballute as compared to the longitudinal axis of the Nike boosters. A transit was used to check this alignment with the vehicle on the launcher. It was found that in the horizontal position a small deflection was present due to the cantilever effect of the vehicle and the way it is suspended from the launcher.

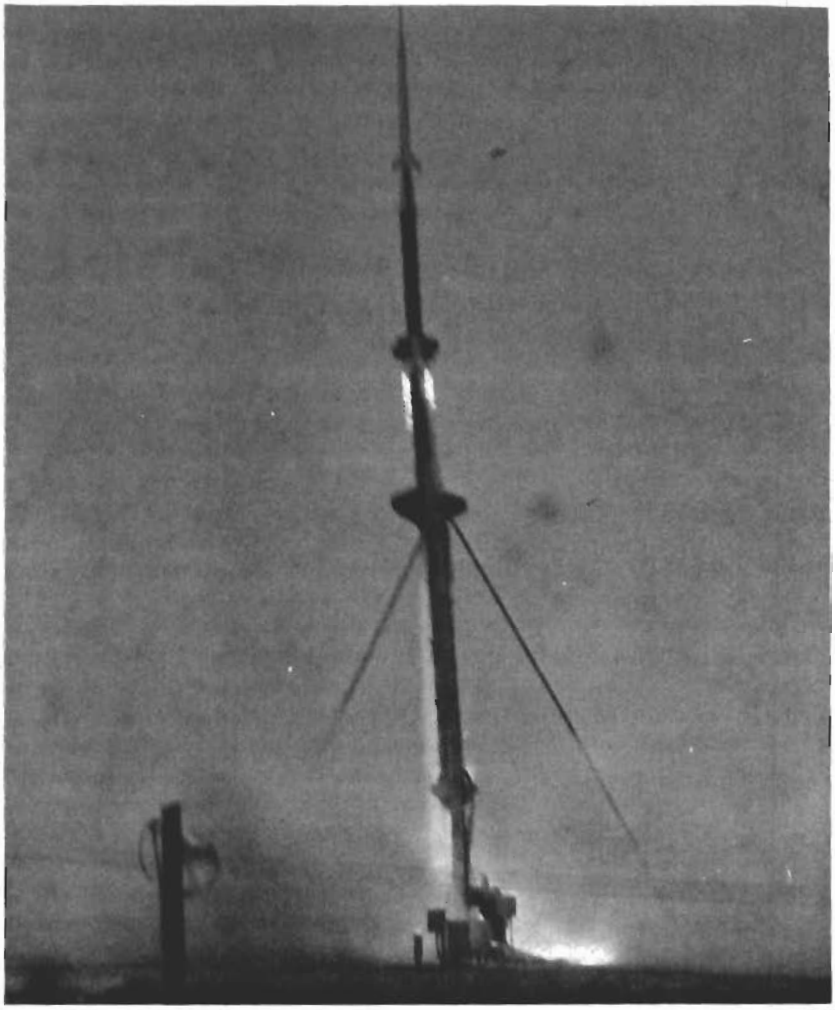

Figure 72. Test Vehicle Launch (Two Stage Booster Configuration)

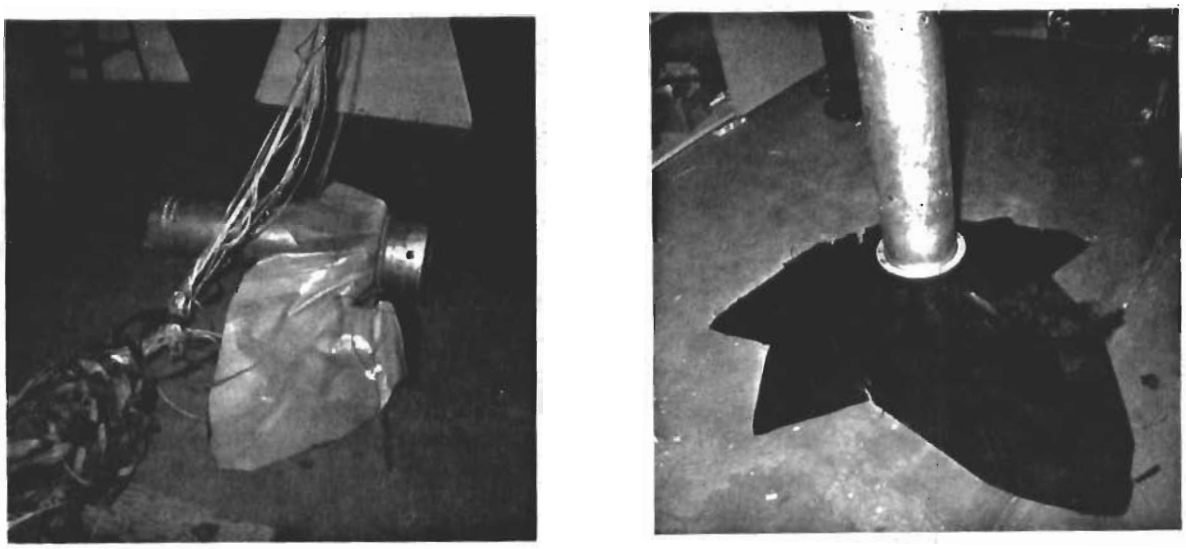

Figure 73. Recovered Ballute Package after Test

Table 7. Test No. 2 Timing Sequences - Programmers

SEQUENCE	DESIRED TIME	ACTUAL MAIN (seconds)	ACTUAL AUXILIARY (seconds)
Booster separation	T + 55 seconds	55.05	55.01
Telemetry calibrate	As available	Not used	57.8
Camera on	T + 78	77.97	78.03
Canister separation and ballute inflation	T + 81.2	Not used	81.09
Parachute door open and nose weight separation	T + 105	105.03	105.37
Parachute deployment	T + 105.1		

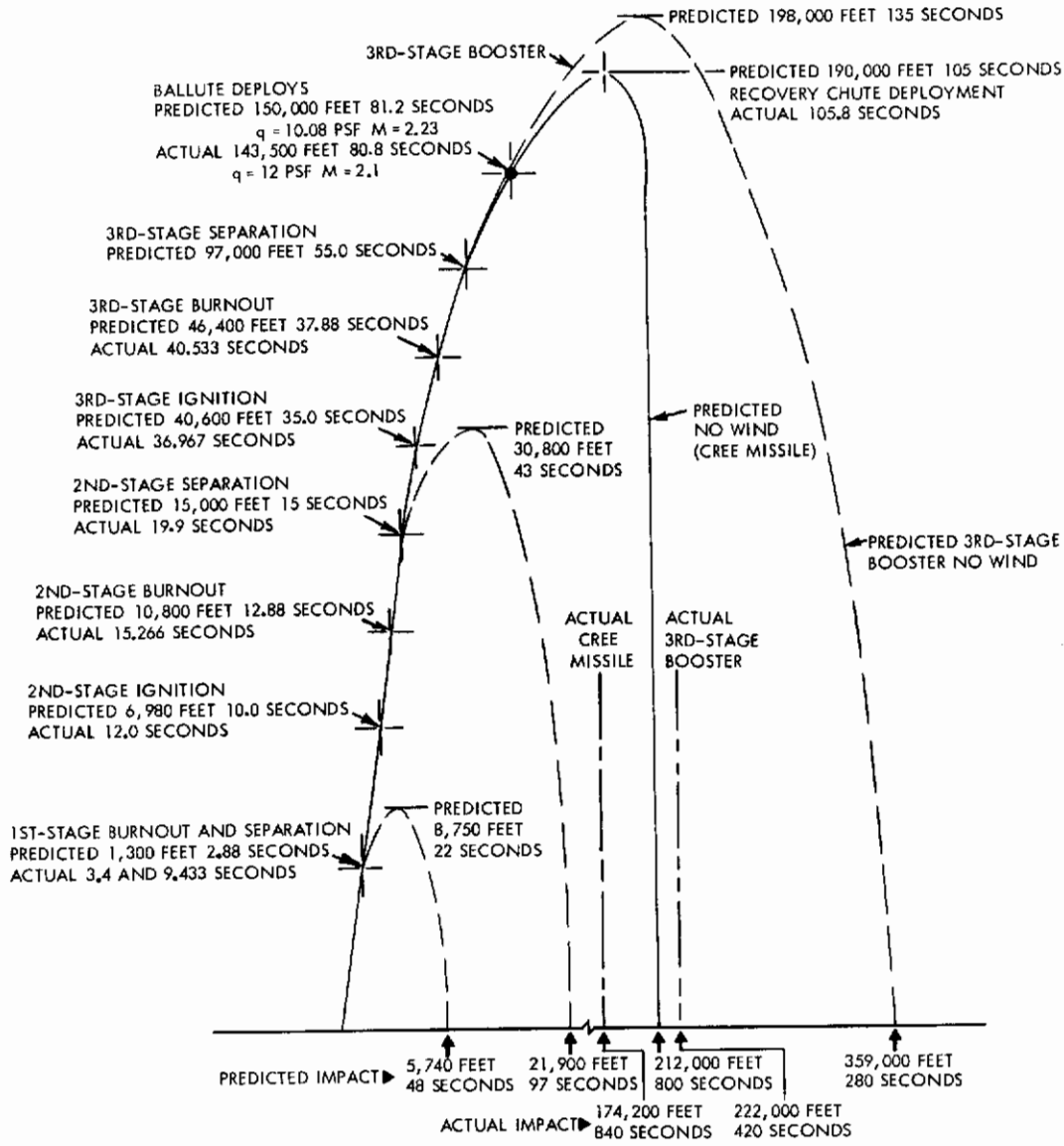

Figure 74. Altitude versus Range - Predicted Trajectory and Radar Plot of Actual Trajectory (Three-Stage Test)

However, when the vehicle was in the vertical position, the alignment was very good.

The telemetry and tracking beacon checked out satisfactorily with the exception of some drifting of the subcarrier frequencies similar to that encountered previously. Firing was scheduled for 25 October 1961.

c. Launching. On the scheduled date, the firing was cancelled due to excessive cloud coverage. Missions were also cancelled on the following dates.

> 26 October 1961 - Cancelled because of sea state 3. Recovery ships reported recovery impossible.
>
> 27 October 1961 - Cancelled because of sea state 3. The missile was moved to the shop area to charge batteries.
>
> 30 October 1961 - Cancelled because of cloud coverage. Sea state of 2+ reported by recovery ships.
>
> 31 October 1961 - Cancelled because of high winds and sea state 3. The missile was again moved to the shop area to recharge the batteries.

On these dates the missile and boosters were assembled on the launcher, telemetry and beacon checks were completed, and the missile was in the fire condition.

On 1 November 1961 the sea state was reported to be calm with a 7-mph wind from the north. The countdown proceeded normally with the scheduled firing to take place at 0800 hours. Shortly before firing, a "hold" was requested by the contractor so that the telemetry could stabilize on the desired carrier frequency. The radar beacon continued to check very good.

The launch occurred at 0843 hours on 1 November 1961. Launch azimuth was 180^{o}; elevation was 79^{o}. A photograph of the launch is shown in Figure 75. By observing the dials of the subcarrier discriminators in the blockhouse, it appeared that the programming sequences functioned properly.

The radar beacon DPN-41 continued operating until T + 160 seconds. From this time on, the missile was skin-tracked, and the radar stations were able to follow the test specimen to impact. Figure 74 shows a calculated trajectory with the actual trajectory superimposed.

d. Recovery. Although radar stations were able to follow the test specimen to impact, the missile flotation equipment did not function properly. The air and sea search could not find any trace of the missile or any trace of dye marker. The missile was fired directly south as required by the Range Safety Officer due to past experiences with three-stage launchings. Therefore, the missile landed in approximately 360 feet of water, preventing recovery by divers.

F. TEST RESULTS

1. Test Data

a. General. Table 8 presents a summary of launch and flight data.

b. Radar Data. Radar position data was computed as the product of the slant range and direction cosines of the line of sight from the radar station to the vehicle with the origin corrected to the launch point. The data was smoothed by a least-squares fit of five consecutive positions to a third-degree polynomial, the midpoint being the desired position. Velocity and acceleration were obtained by evaluating the first and second derivatives of the polynomial.

c. Optical Data. The Davis least-squares method for the N-station solution ($3 \leq N \leq 5$) was used to compute phototheodolite space-position data. This method is a true least-squares adjustment

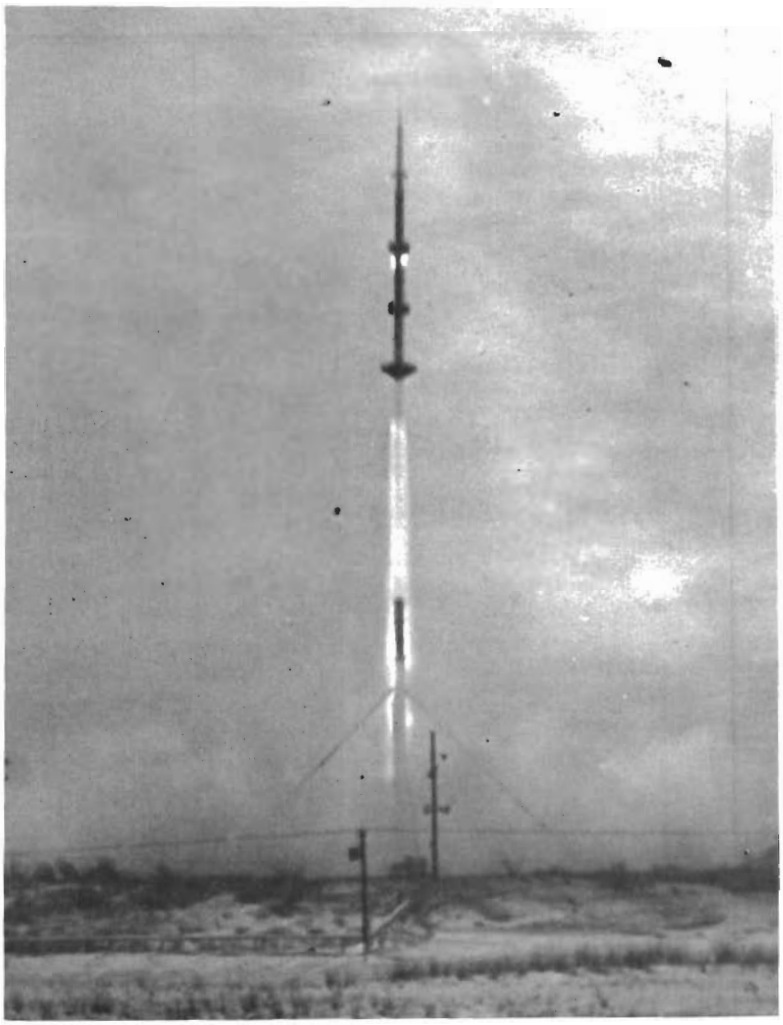

Figure 75. Test Vehicle Launch (Three-Stage Booster Configuration)

which minimizes the deviation in azimuth and elevation readings and yields the best possible solution from the available data. Standard deviations in space position are derived from errors in azimuth and elevation readings from each station. Optical data was smoothed using a five-point program (Reference 5).

d. Data Presentation. Trajectory data for the two flights has been reduced to graphical form and is shown in Figures 76 through 81. Optical data is presented for the first mission, and both radar and optical data are presented for the second mission.

The radar data for the first flight and the radar velocity versus time data for the second flight is not presented in this report, because the data was too rough to be presented graphically.

2. Telemetry

a. Two-Stage Booster Tests. Telemetry data channel assignments were made as shown in Table 9.

Table 8. Launch and Flight Data

Mission		1			2			
Date		10 October 1961			1 November 61			
Launch Time (zulu)		1545:01.168			1453:00.535			
Number Stages		2			3			
Cree Type		II			II			
Launch Elevation (deg)		83			79			
Launch Azimuth (deg)		166			175			
Launch Method		Rail			Rail			
Rail Length (in.)		200			324			
Launch Pad		3			1			
Launch Weight (lb)		3,170			4,450			
Fin Alignment (deg cant)								
1st Stage		1/2			1			
2nd Stage		0			0			
3rd Stage		-			0			
Serial Numbers								
1st Stage		20,138			20,130			
2nd Stage		20,148			20,137			
3rd Stage		-			20,147			
Event Time (sec)		Predicted	Actual		Predicted	Actual		
1st Stage Burnout		2.88	3.533[1]		2.88	3.4[1]		
1st Stage Separation		2.88			2.88	9.433[1]		
2nd Stage Ignition		20.00	22.033[1]		10.00	12.00[1]		
2nd Stage Burnout		22.88			12.88	15.266[1]		
2nd Stage Separation		45.00	45.12[2]		15.00	19.900[1]		
2nd Stage Flight Time		232.	240[3]		97.37	-		
3rd Stage Ignition		-	-		35.00	36.967[1]		
3rd Stage Burnout		-	-		37.88	40.533[1]		
3rd Stage Separation		-	-		55.00	-		
3rd Stage Flight Time		-	-		291	420[3]		
Cree Flight Time		915	638[3]		981	840[3]		
Data (sec)								
Radar - Beacon Track			0-67			0-159.4		
- Skin Tack			67-impact			159.4-impact		
Photothedodolite			0-105			0-66.1		
Recovery			Yes			No		
		No Wind Theoretical	Prelaunch Predicted	Actual	No Wind Theoretical	Prelaunch Predicted	Postlaunch Predicted	Actual
Launch Azimuth (deg true)		180	166	166	180	175	180	175
Launch Elevation (deg)		83	83	83	79	79	79	79
Impact Point		4,809	5,087		5,748	4,961	5,780	
1st Stage (ft) Range[a]		+44	-1,264		+33	+692	+533	
Displacement[b]		20	18.5		3.56	3.07	3.54	
2nd Stage (nm) Range[a]		+0.69	+0.59		+0.03	+0.59	+0.44	
Displacement[b]		-	-		63.75	50.25	55.8	
3rd Stage (nm) Range[a]		-	-		+1.8	+23.5	+17.6	
Displacement[b]		13.19	16.76		44.18	41.50	45.65	
Cree (nm) Range[a]		+0.42	-1.93		+1.17	+11.55	+7.5	
Displacement[b]								
NOTE: Plus signs indicate displacements to the right of the launch azimuth, minus signs to the left.								
1st Stage Impact Azimuth (deg true)								
Range (ft)[c]								
2nd Stage Impact Azimuth			148.7	167.5[3]				
Range (nm)[c]			19.4	11[3]				
3rd Stage Impact Azimuth			-	-		200	197.5	201[3]
Range (nm)[c]			-	-		55.6	58.5	36.5[3]
Cree Impact Azimuth			159.5	174.5[3]		190.6	189.3	187[3]
Range (nm)[c]			16.8	10.5[3]		43	46.3	28.7[3]
Test Points								
Time (sec)		71.81	71.81	71.78[2]	81.20	81.20	81.20	81.2
Altitude (ft/sec)		123,741	124,513	107,500[4]	154,369	163,930	157,010	143,500[4]
Velocity (ft/sec)		1,371.7	1,370	1,035[4]	2,578	2,491	2,554	2,280[4]
Dynamic Pressure (lb/ft^2)		10.0	9.8	12	10.08	6.5	8.8	12

NOTES: 1 - Phototheodolite Film
2 - Telemetry Data
3 - Radar Pen Plots
4 - Graphical Data
5 - Missing times either not applicable or not available

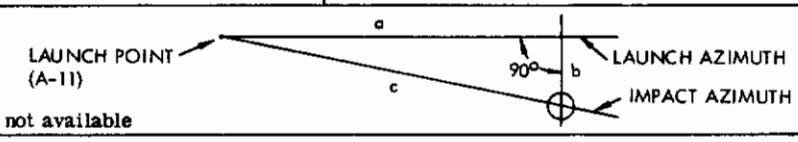

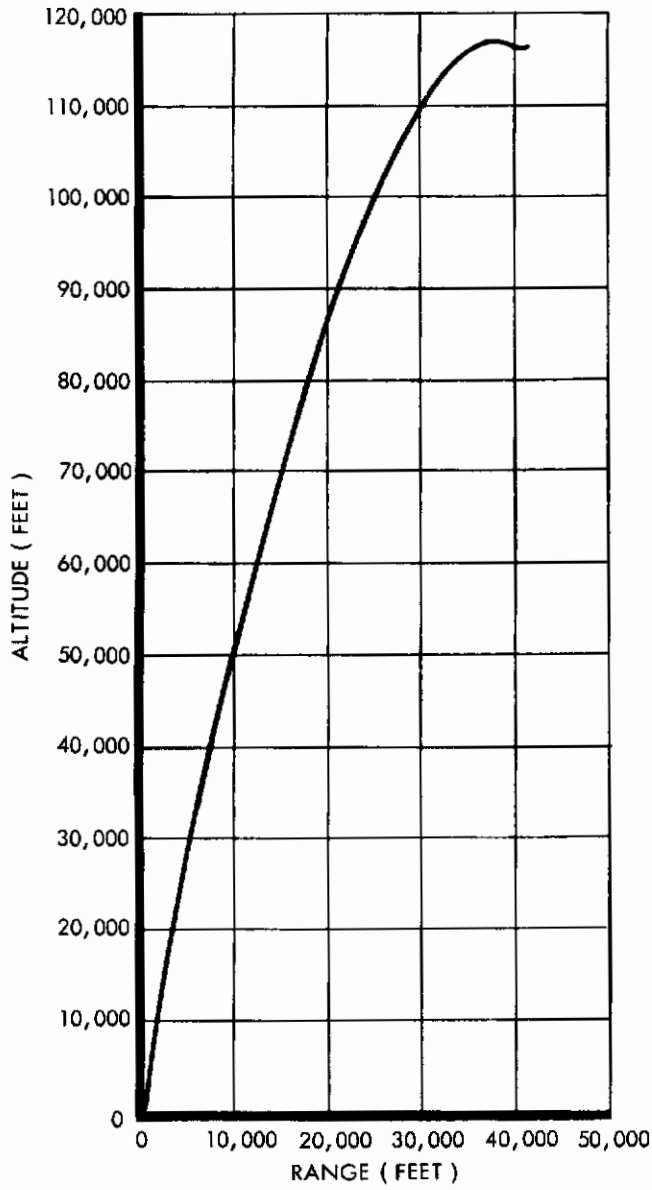

Figure 76. Altitude versus Range (Two-Stage Test Phototheodolite Data)

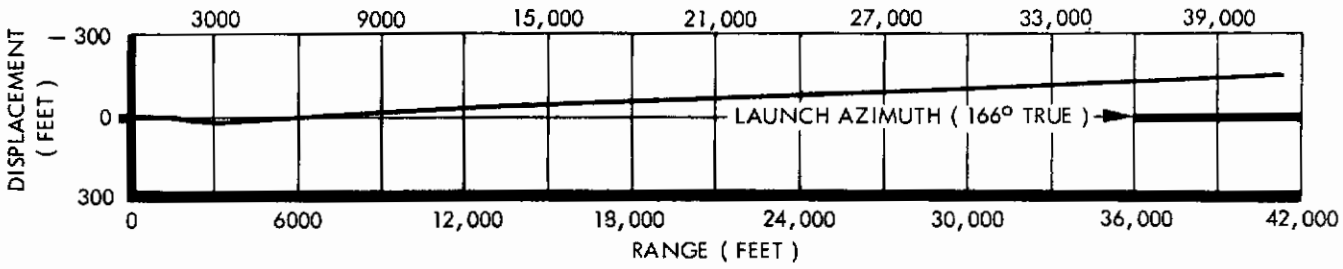

Figure 77. Range versus Displacement (Two-Stage Test Phototheodolite Data)

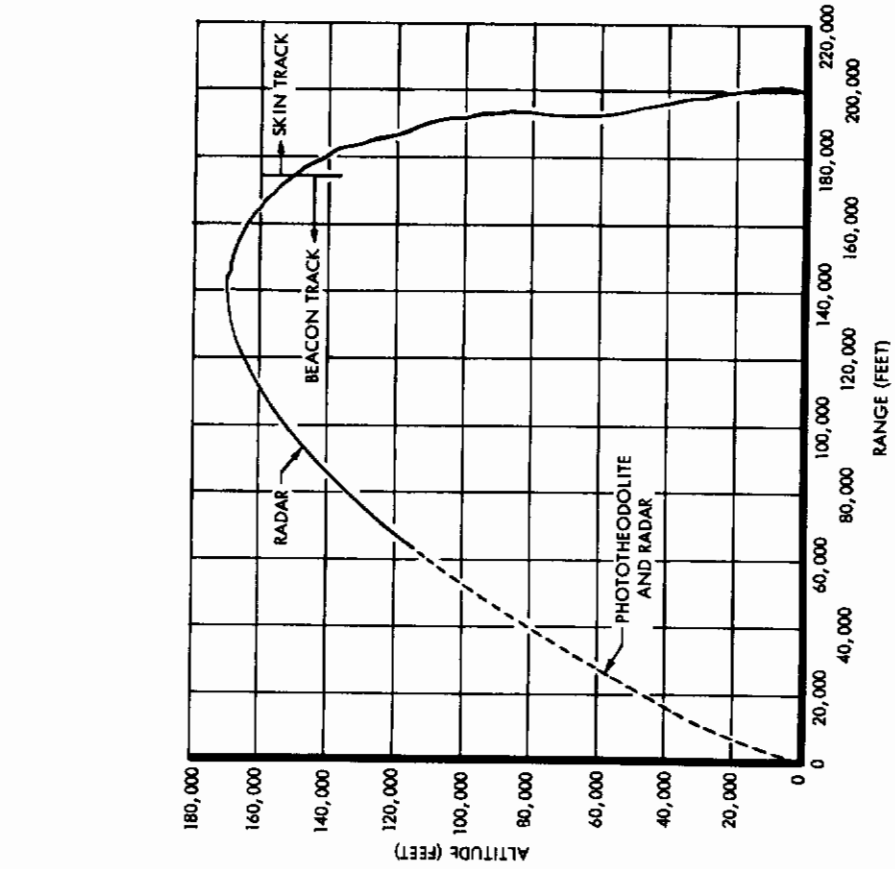

Figure 79. Altitude versus Range (Three-Stage Radar and Phototheodolite Data)

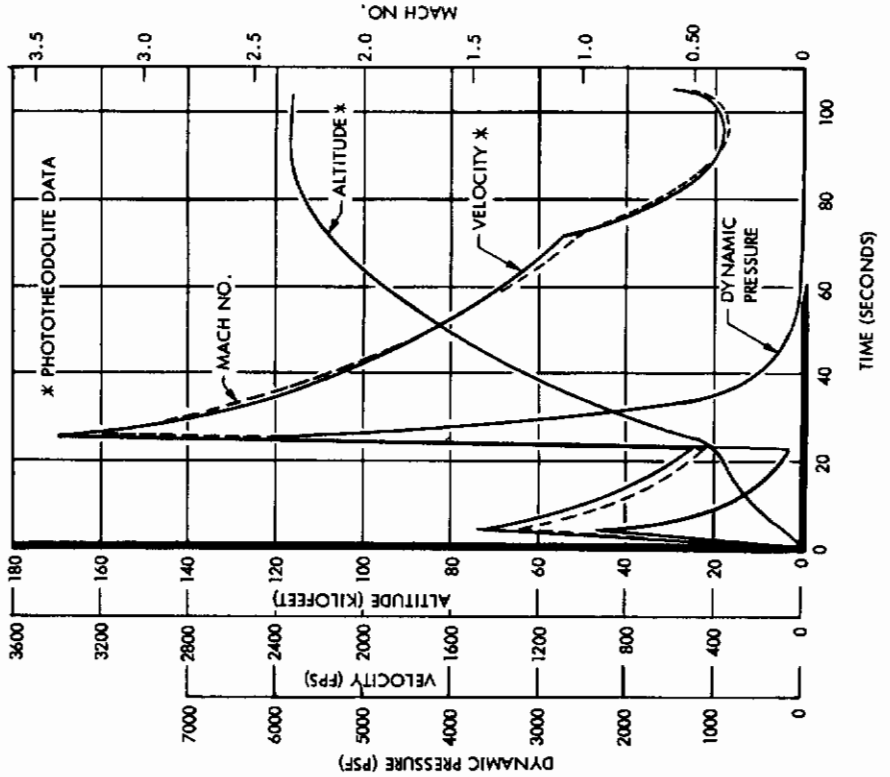

Figure 78. Two-Stage Test Data versus Time

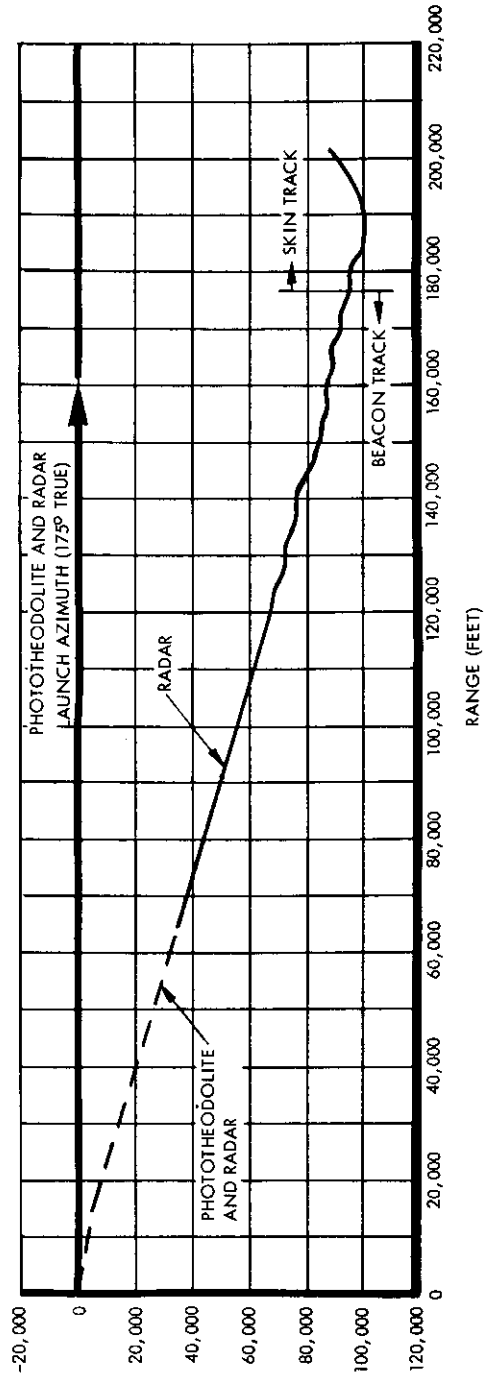

Figure 80. Range versus Displacement (Three-Stage Phototheodolite and Radar Data)

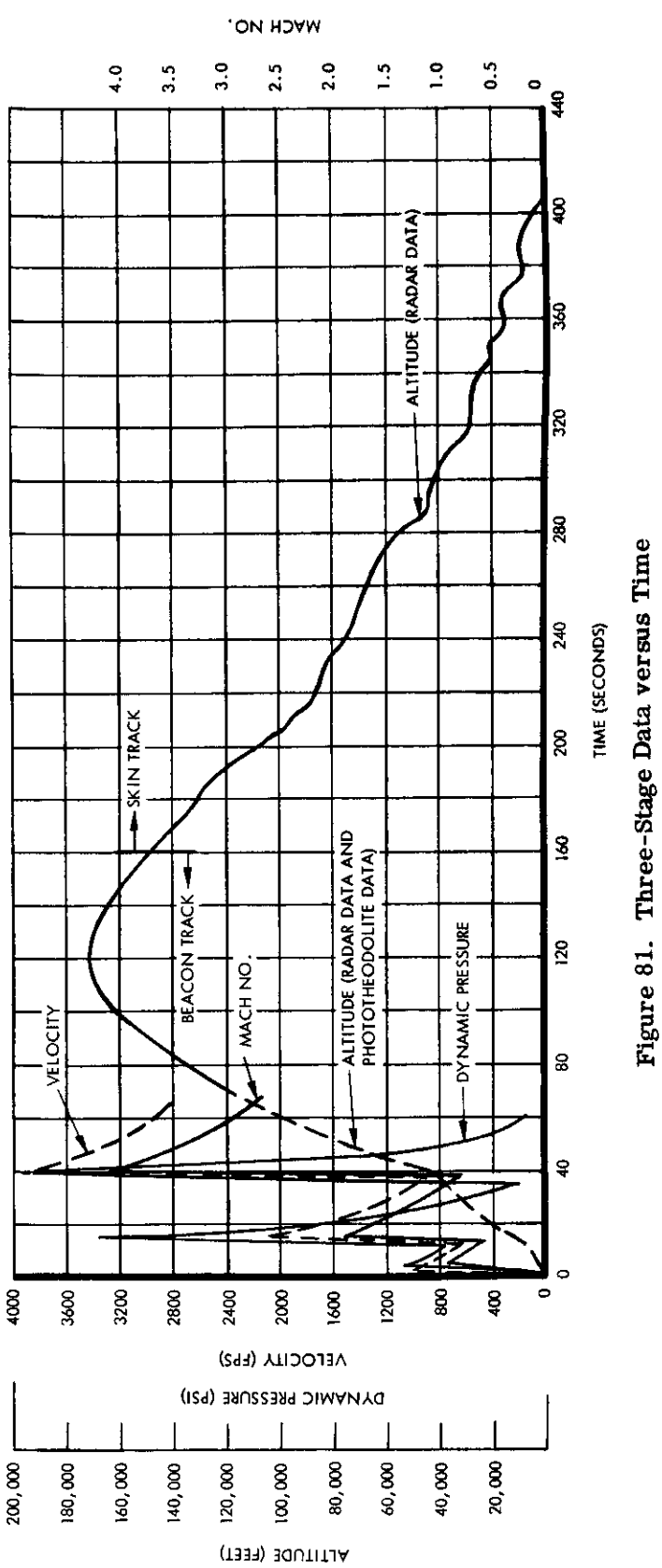

Figure 81. Three-Stage Data versus Time

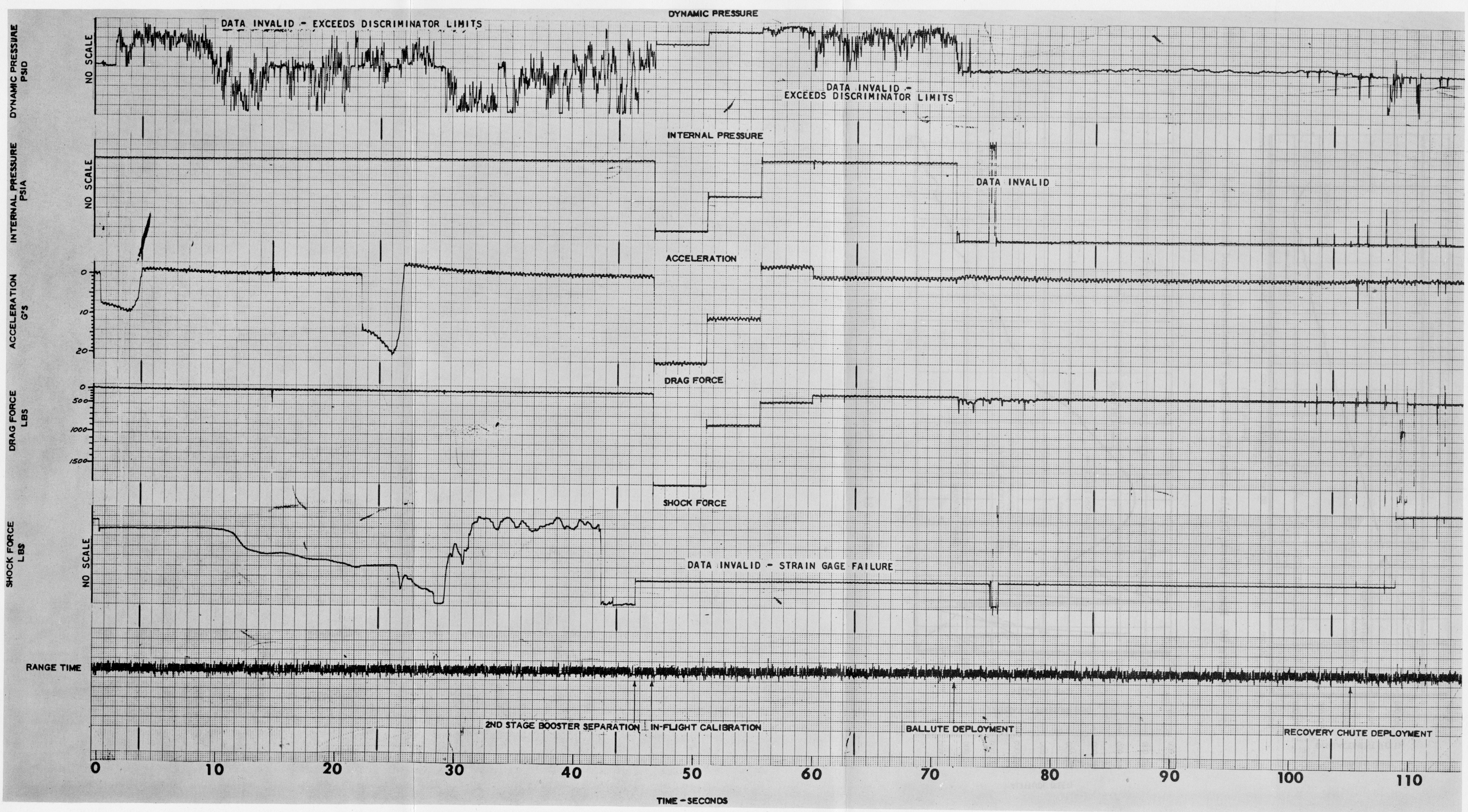

Figure 82. Aerodynamic Decelerator - Two-Stage Test

Table 9. Telemetry Data Channel Assignments - Two-Stage Booster Test

INTER-RANGE INSTRUMENTATION GROUP CHANNELS	NORMAL SUBCARRIER LIMITS			DATA ITEM
	Upper Limit (cps)	Center Frequency (cps)	Lower Limit (cps)	
12	11,288	10,500	9,712	Dynamic pressure
13	15,588	14,500	13,412	Ballute internal pressure
14	23,650	22,000	20,350	Acceleration
C	46,000	40,000	34,000	Drag force
E	80,500	70,000	59,500	Shock force

The telemetry data was received and recorded on magnetic tape at the three separate recording sites designated as A-6, D-3, and blockhouse. All three recordings were of poor quality, having much noise and no usable 100-kc reference signal for WOW and flutter compensation. The blockhouse tape was used for data playout since it was somewhat better than the other two tapes.

A presentation of the telemetered data is given in Figure 82. A panoramic display of the telemetry multiplex signal is given in Figure 83. The panoramic display is very useful in analyzing telemetered signals and provides information concerning telemetry and receiving station performance. A brief discussion of telemetry data follows:

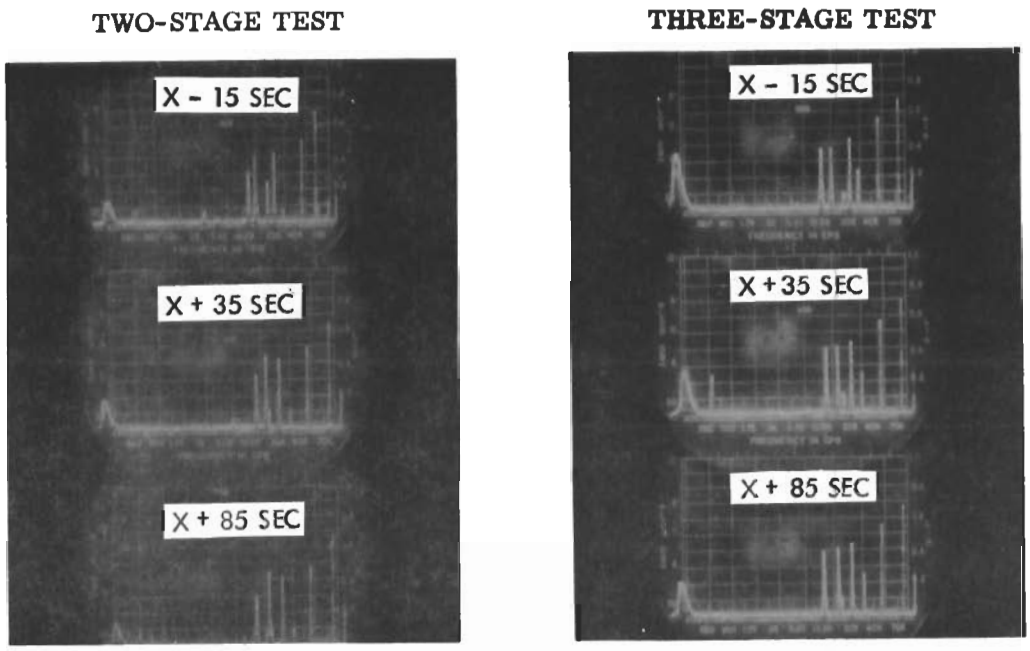

Figure 83. Telemetry Composite Signal Panoramic Displays

(1) Dynamic Pressure - IRIG Channel 12. No useful dynamic pressure data can be obtained from telemetry data because circuit components malfunctioned during flight. As may be noted from Figures 82 and 83, the telemetry signal went out of band limits at approximately two seconds flight time and remained outside until Ballute deployment at 71.78 seconds. At X + 35 seconds, Figure 83 indicates this channel at approximately 13 kc. By detuning ground station playout equipment at GAC, the signal was partially tracked through the inflight calibration. The following is a comparison of preflight and inflight calibration frequencies:

	Preflight cps	Inflights cps
Cal No. 1	10,000	11,760
Cal No. 2	10,680	12,100
Cal No. 3	10,980	12,400
Operate	11,280	12,600 + noise

At Ballute deployment, the signal came back into band limits, but signal drift, noise, and limited transducer resolution caused much uncertainty in the data.

(2) Internal Pressure - IRIG Channel 13. The Ballute internal pressure circuit did not operate properly at Ballute deployment. At deployment the data trace dropped to the zero-volt level (cal step No. 1 level), then dropped to a level 0.5 volts below the zero level. At X + 75 seconds a momentary level of + 5.5 volts was recorded before the trace returned to the -0.5 volt level. These values are not possible under design circuit conditions and seem to require circuit malfunctions to explain the activity.

The high voltage reading could be caused by an open ground circuit within the potentiometer which reduces an 8-volt power supply to 5 volts for the pressure transducer. Such a fault would allow a voltage greater than 5 volts but certainly less than 8 volts, depending on the series resistance of the faulty circuit. Exact values of circuit resistances are not known, so the voltage for this type of fault cannot be calculated. A post-flight circuit check showed that the potentiometer had burned out. The cause, however, was not determined.

The -0.5 volt level of the trace cannot be readily explained by failure of the transducer power supply since all power supply voltages are above zero volts, the ground level. An open or a ground fault in the transducer power lead would produce a zero-volt signal at the oscillator input. A sudden shift in oscillator center frequency is more likely than a negative 0.5 volt signal at the oscillator input. A shift in the center frequency of the oscillator could be caused by a malfunction of the voltage regulator which supplies a nominal 6 volts to the oscillator plate circuit. A voltage less than 6 volts in this circuit could produce the same effect as a negative voltage at the oscillator input terminal.

It is concluded that the telemetry data trace was caused by circuit malfunctions and is not data.

(3) Acceleration - IRIG Channel 14. Acceleration telemetry data was recorded throughout the flight. Accelerations during the first-stage and second-stage boost periods are in general agreement with Cree booster performance. The high g levels recorded during boost make it difficult to read deceleration levels on the same scale, but a change of approximately 1 g can be seen at Ballute deployment.

It is recommended that future measurements of this type be made with a more sensitive accelerometer circuit, including a clamping circuit in the oscillator input to hold the input signal at allowable levels during boost phases. This would yield deceleration resolutions of tenths of g's without difficulty.

(4) Drag Force - IRIG Channel C. The drag force telemetry data is questionable. The channel C oscillator remained about 10 percent above the upper frequency limit of the channel for most of the flight. A few momentary data spikes appear at Ballute deployment, and a small drag force is indicated for approximately seven seconds. The fact that the circuit has an inflight calibration and calibrated during the post-flight check indicates that the strain gain bridge remained intact during the flight. The low-level indication of drag force could be caused by a temporary amplifier malfunction.

(5) Shock Force - IRIG Channel E. No shock force data was obtained during this flight. The data trace indicates amplifier drift or strain gage damage beginning at launch. The absence of an inflight calibrate signal indicates an open strain gage bridge. A post-flight check showed that one of the strain gages was severed.

b. Three-Stage Booster Test. The telemetry data items and channel assignments were the same as the two-stage test.

The recorded telemetry data from this test is much better than two-stage test data. The panoramic display presented in Figure 83 shows a good preemphasis of telemetry signals and very little noise. Two stray signals are noted, however: a strong signal at 30 kc and a low-level signal beginning in the 22-kc band and shifting gradually down into the 14.5-kc band. These signals are sufficiently distinct from the data channels so that interference during playout was not a problem. The data playout is shown in Figure 84. Each data item is discussed briefly as follows:

(1) Dynamic Pressure - IRIG Channel 12. During the boost portion of the flight signal on this channel, the trace had a peculiar appearance which resembles the trace obtained when calibrating a discriminator and recorder. The strange geometry of the trace changed to expected form at the time of inflight calibration. A large frequency shift, approximately one-half the channel band width, was noted between the preflight calibrate and the inflight calibrate. The preflight calibrate had to be used to arrive at a sensible scale for the data. It is concluded that the stimulus that caused the odd trace between zero time and Ballute deployment ceased at Ballute deployment. The data presented is in reasonable agreement with the photometric data.

(2) Ballute Internal Pressure - IRIG Channel 13. Ballute internal pressure data was recorded from the inflight calibrate until shortly after Ballute deployment. At deployment the transducer was suddenly forced against its mechanical stop at two psi. A change occurred in the transducer or its power supply, causing the trace to drop to the zero-volt level, or zero psi. When working properly, the transducer can indicate no more than two psi and no less than ambient atmospheric pressure.

(3) Acceleration - IRIG Channel 14. Acceleration telemetry was recorded throughout the flight. The three stages of boost are clearly shown. A slight deceleration, about 0.5 g, is seen at Ballute deployment. However, the accuracy of this ± 50 g accelerometer is not considered reliable at loads as low as 5 to 10 g's.

(4) Drag Force and Shock Force - IRIG Channels C and E. Drag force and shock force data channels indicate the same forces. The shock force channel has a capability of higher frequency response, but for the playouts presented here, low-frequency filters were used to compress noise.

Drag force and shock force data are essentially the same when played out through a low-frequency response system. In the data presented, a low-frequency playout system was used to suppress noise and to smooth the data to a reasonable degree. An analysis of the high-frequency shock of Ballute deployment is beyond the scope of the present work.

Both data channels functioned satisfactorily, and data was obtained from Ballute deployment through chute deployment. The drag force telemetry data was slightly over the upper frequency limit of C, but the data was recovered by adjusting the playout discriminators.

3. Data Reduction

a. Data Analysis.

The flight test data from two missions have been analyzed to determine an approximate drag coefficient slope through the transonic-supersonic region for a nine-foot-diameter Ballute deceleration system. These missions were a two-stage and three-stage Nike-motor-boosted Cree test vehicle.

Three sources of flight test data were utilized: radar, optical (Askania cinetheodolite), and telemetry (recordings from a strain gage mounted on the cable connecting the Ballute to the Cree vehicle).

The parasite drag of the Ballute deceleration system is approximated directly from acceleration data. The tangential equation of motion of the system was derived as shown in data reduction in Section 2.

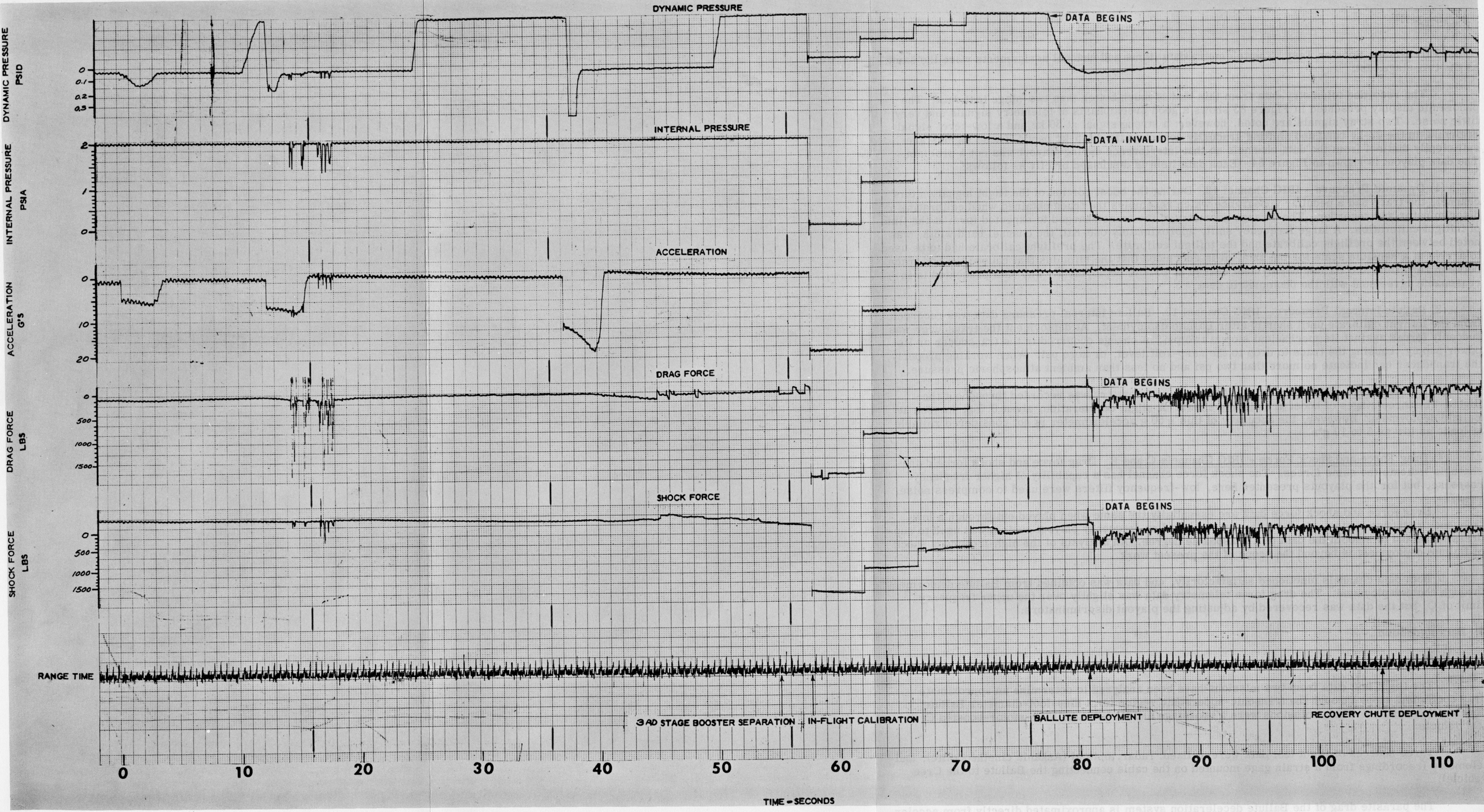

Figure 84. Aerodynamic Decelerator - Three-Stage-Test

Drag data has been derived from telemetry recordings shown in "Data Reduction" in Section 2.

Figures 85, 86, and 87 show the basic flight test data from the two-stage Nike-boosted Cree mission. The drag coefficient slope derived from this data (Table 10) is depicted in Figure 88. Telemetry data was not available from this mission.

Table 10. Parametric Data - Two-Stage Nike-Boosted Cree Flight Test

t	$\dot{V}$	γ^o	D	ρAV^2	C_D	M
72	55.54	62.0	445.52	1502.6	0.593	1.013
74	50.86	59.8	378.35	1184.2	0.639	0.961
76	46.23	57.5	313.79	845.8	0.742	0.806
78	41.65	55.0	250.89	639.1	0.785	0.721
80	37.12	52.3	191.36	477.1	0.802	0.639
82	32.65	48.0	143.46	363.2	0.790	0.571
84	28.22	43.0	103.21	281.9	0.732	0.512
86	23.85	38.0	65.87	224.8	0.586	0.463
88	19.53	31.5	44.49	181.6	0.490	0.420
90	15.26	23.5	39.40	147.0	0.536	0.381
92	11.04	15.0	44.81	129.7	0.691	0.359

Figures 89 and 90 show the flight test data obtained from the three-stage Nike-boosted Cree mission. The velocity history (Figure 91) was determined by taking the derivatives of approximate polynomial fits to this data. This gives an altitude rate ($\dot{h}$) and flight path inclination angle (γ) from which

$$V = \sqrt{\dot{h}^2 + (\dot{h} \cot \gamma)^2}.$$

Acceleration ($\dot{V}$) was then found by taking the numerical differences or slope of the velocity ($\dot{V}$) (see Table 11).

Table 11. Parametric Data - Three Stage Nike Boosted Cree Flight Test

t	$\dot{V}$	γ^o	$(1/2)\rho AV^2$	D*	D**	M	C_D*	C_D**
81.2	35.71	45.3	723.94	203.33	548.89	2.106	0.281	0.554
85	34.96	41.3	643.49	218.22	421.87	1.986	0.339	0.469
90	32.89	37.8	448.39	209.33	342.93	1.814	0.467	0.577
95	29.41	34.4	311.70	178.41	372.51	1.685	0.572	0.870
100	23.47	29.0	223.03	123.82	323.17	1.536	0.555	0.967
105.6	19.94	23.4	160.02	113.70	296.04	1.424	0.710	1.270

The telemetry shock force data for this three-stage Nike-boosted Cree mission is illustrated in Figure 92.

The resulting drag coefficient slopes for these tracking and telemetry data are depicted in Figure 93.

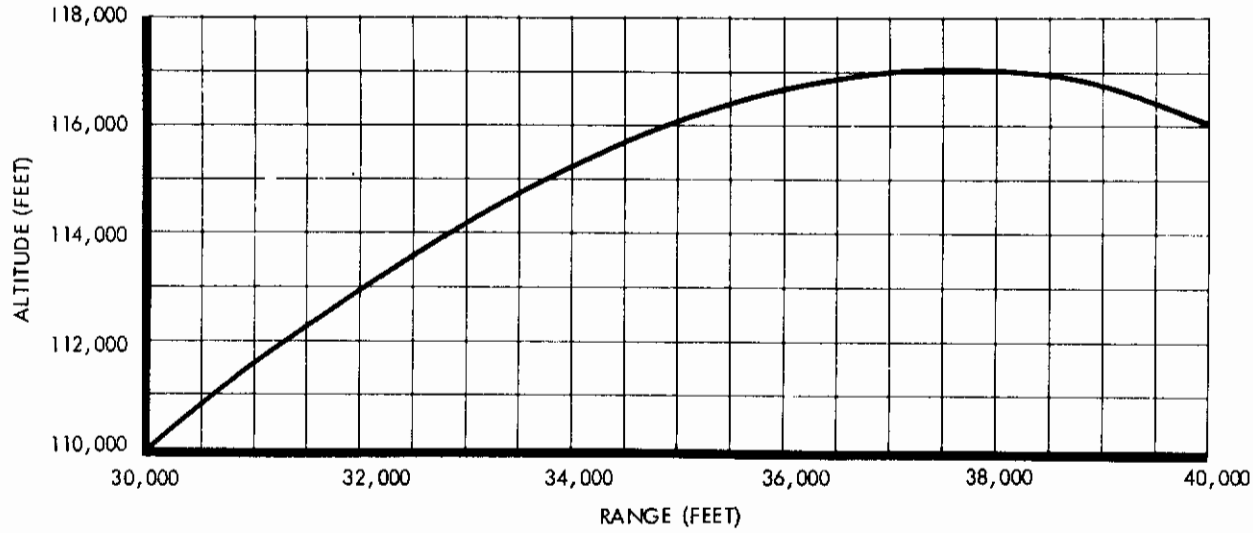

Figure 85. Theodolite Tracking Data - Altitude versus Range - Two-Stage Nike-Boosted Cree Flight Test (Obtained from Reference 4)

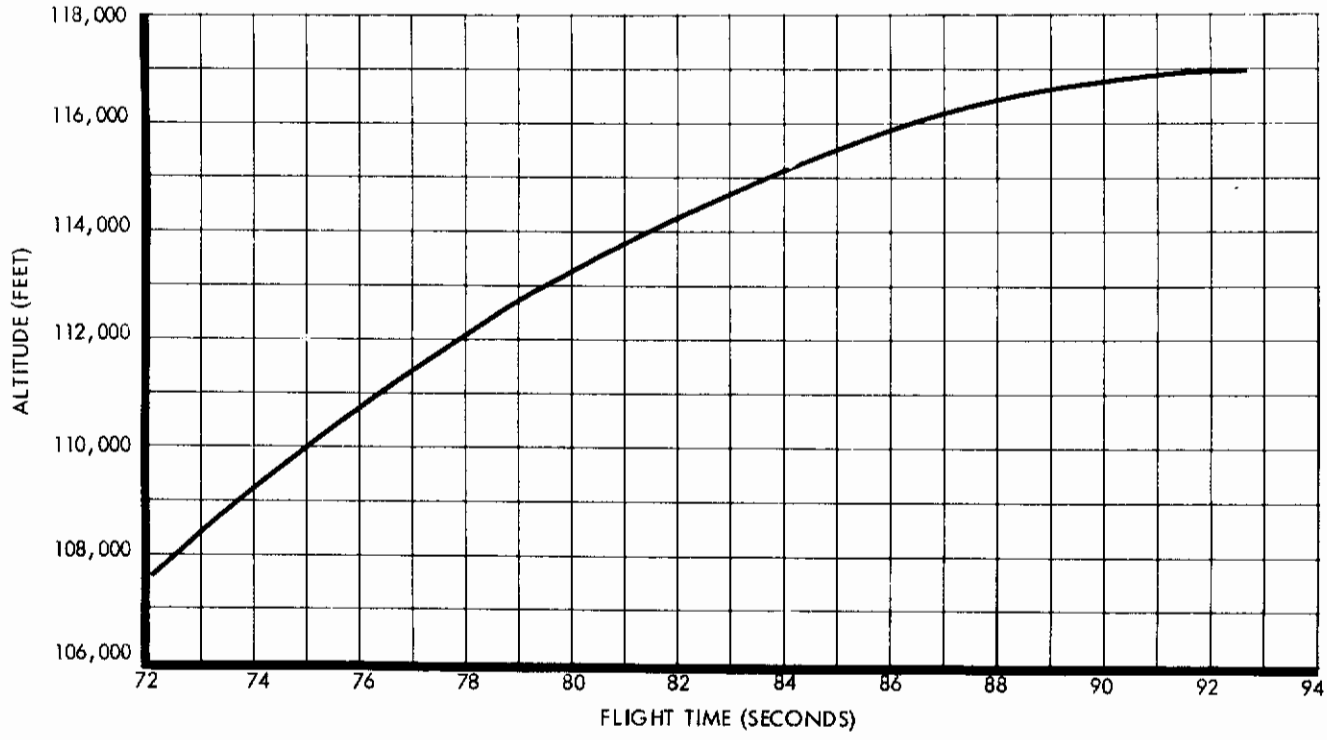

Figure 86. Theodolite Tracking Data - Altitude versus Flight Time - Two Stage Nike-Boosted Cree Flight Test (Obtained from Reference 5)

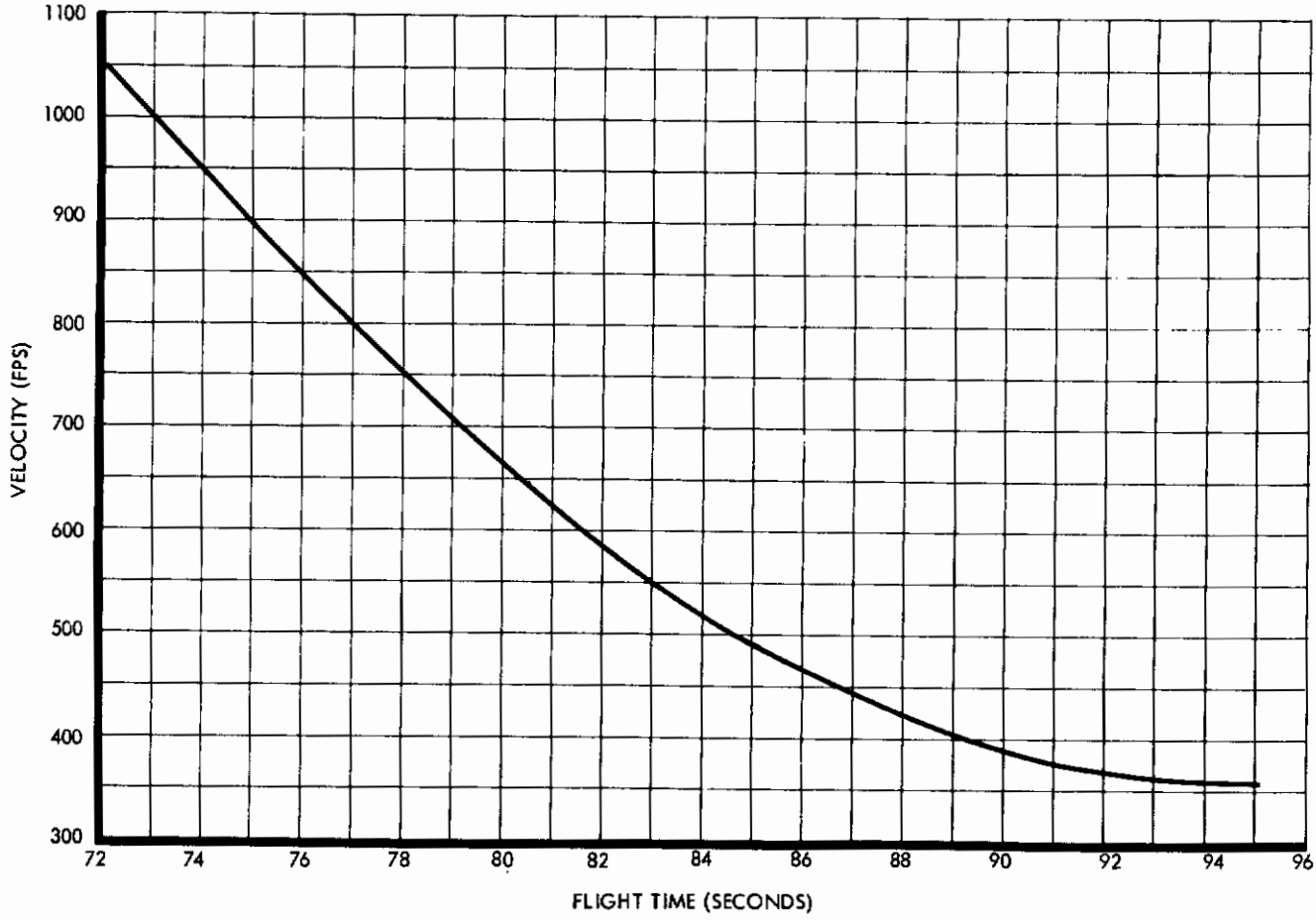

Figure 87. Theodolite Tracking Data - Velocity versus Flight Time - Two-Stage Nike-Boosted Cree Flight Test (Obtained from Reference 4)

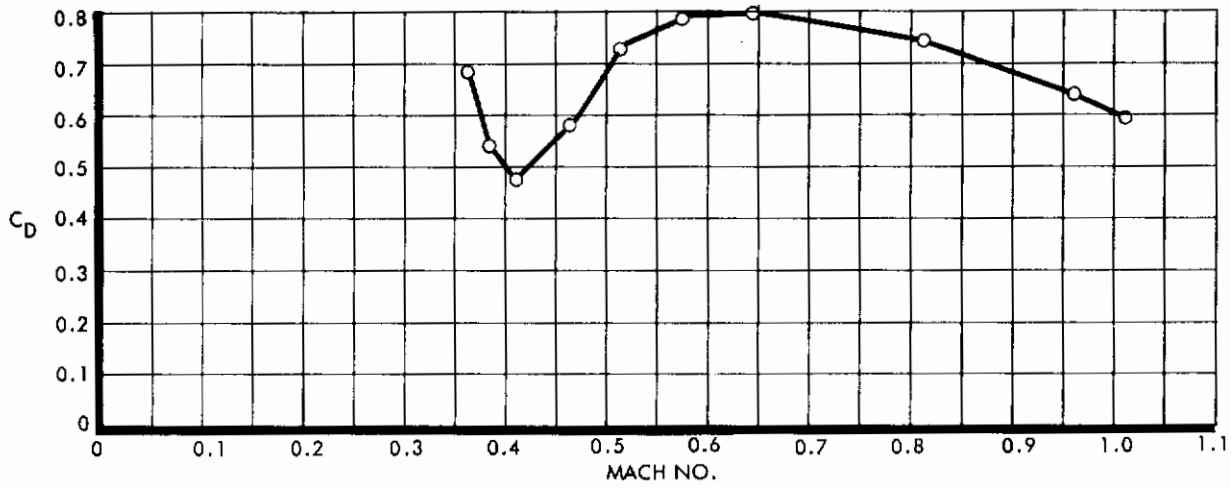

Figure 88. C_D versus Mach Number - Two-Stage Nike-Boosted Cree Flight Test

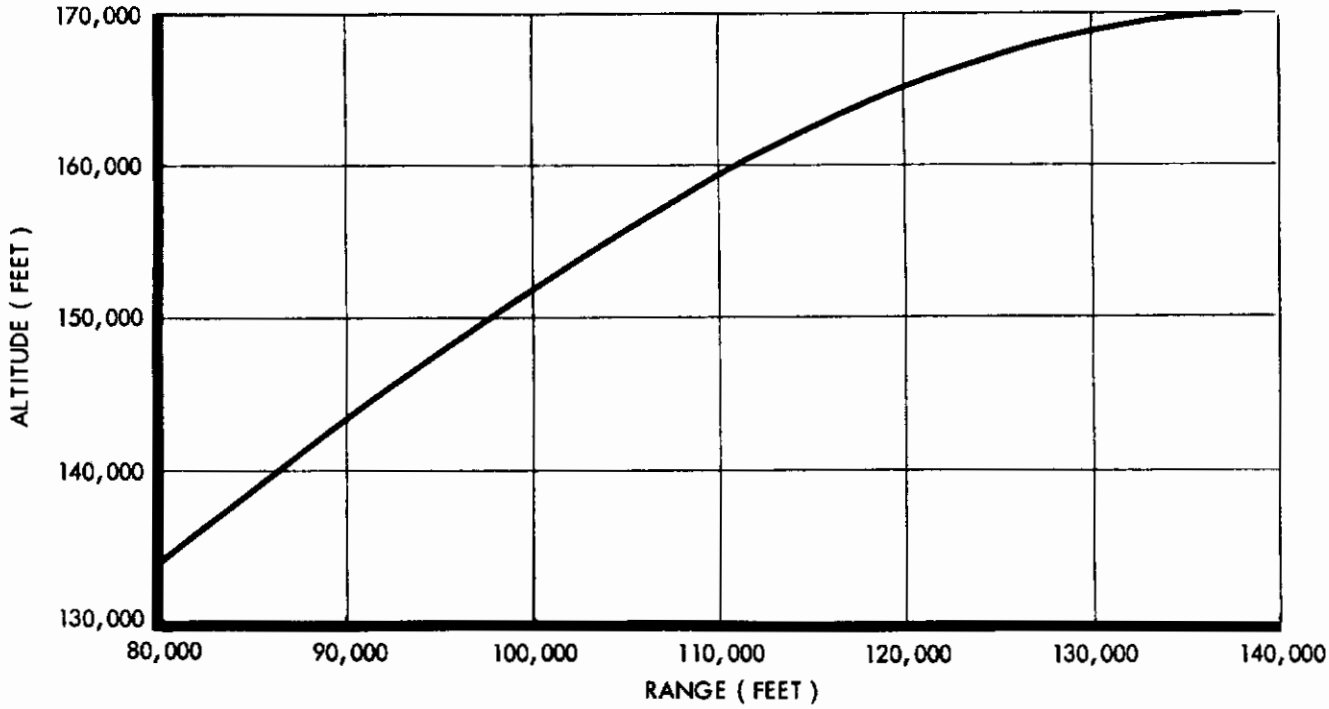

Figure 89. Radar Tracking Data - Altitude versus Range - Three-Stage Nike-Boosted Cree Flight Test (Obtained from Reference 4)

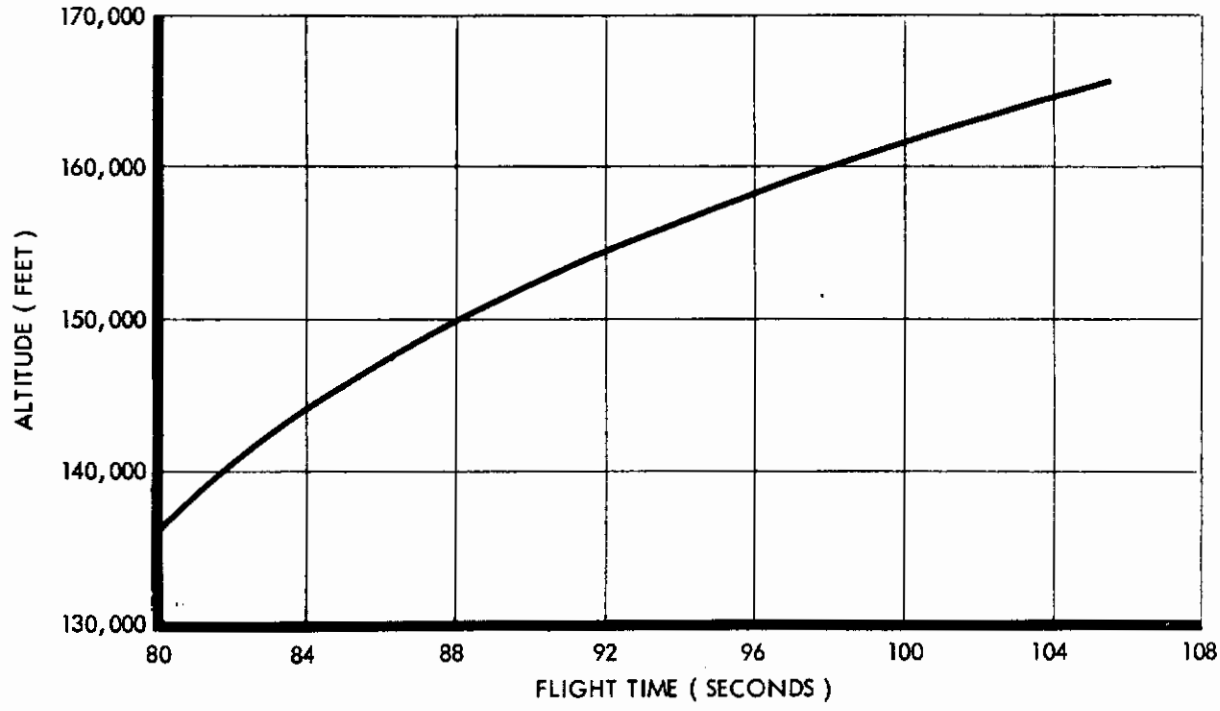

Figure 90. Radar Tracking Data - Altitude versus Flight Time - Three-Stage Nike-Boosted Cree Flight Test (Obtained from Reference 4)

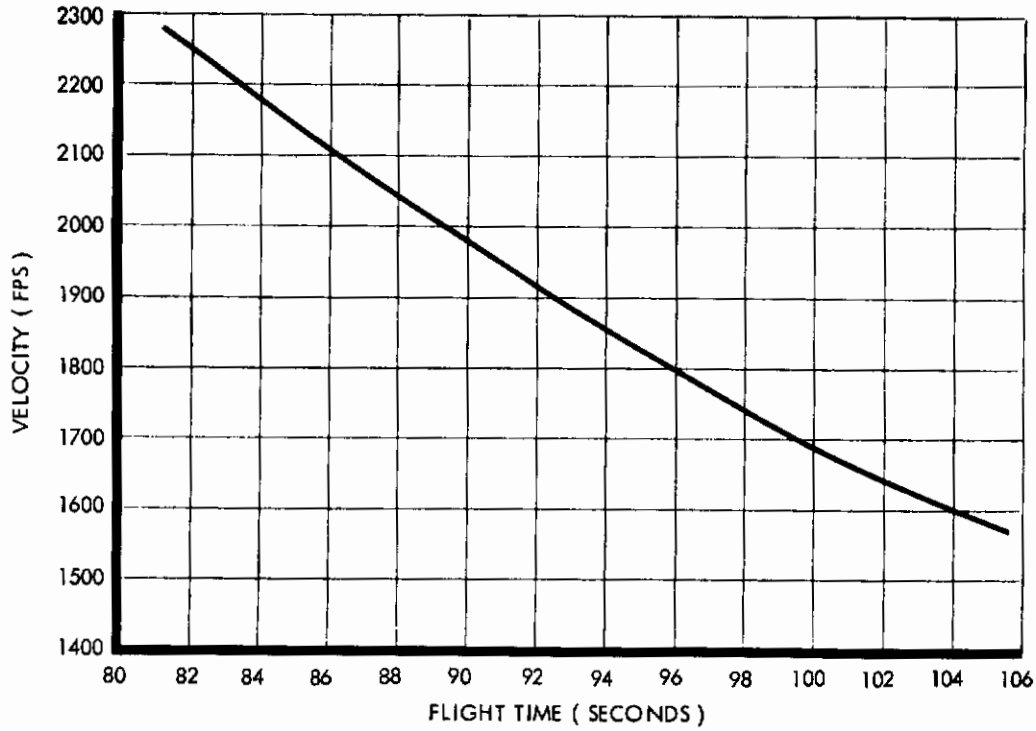

Figure 91. Radar Tracking Data - Velocity versus Flight Time - Three-Stage Nike-Boosted Cree Flight Test (Obtained from Reference 4)

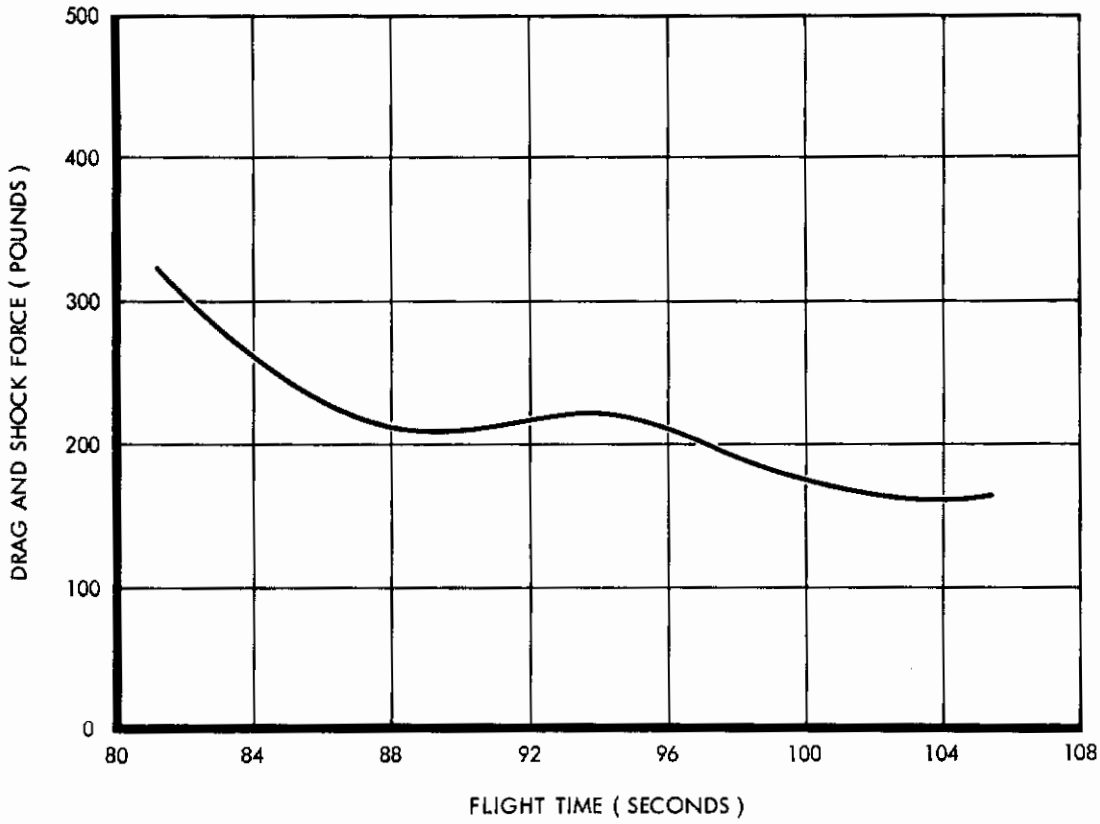

Figure 92. Telemetry Shock Force Data - Three-Stage Nike-Boosted Cree Flight Test

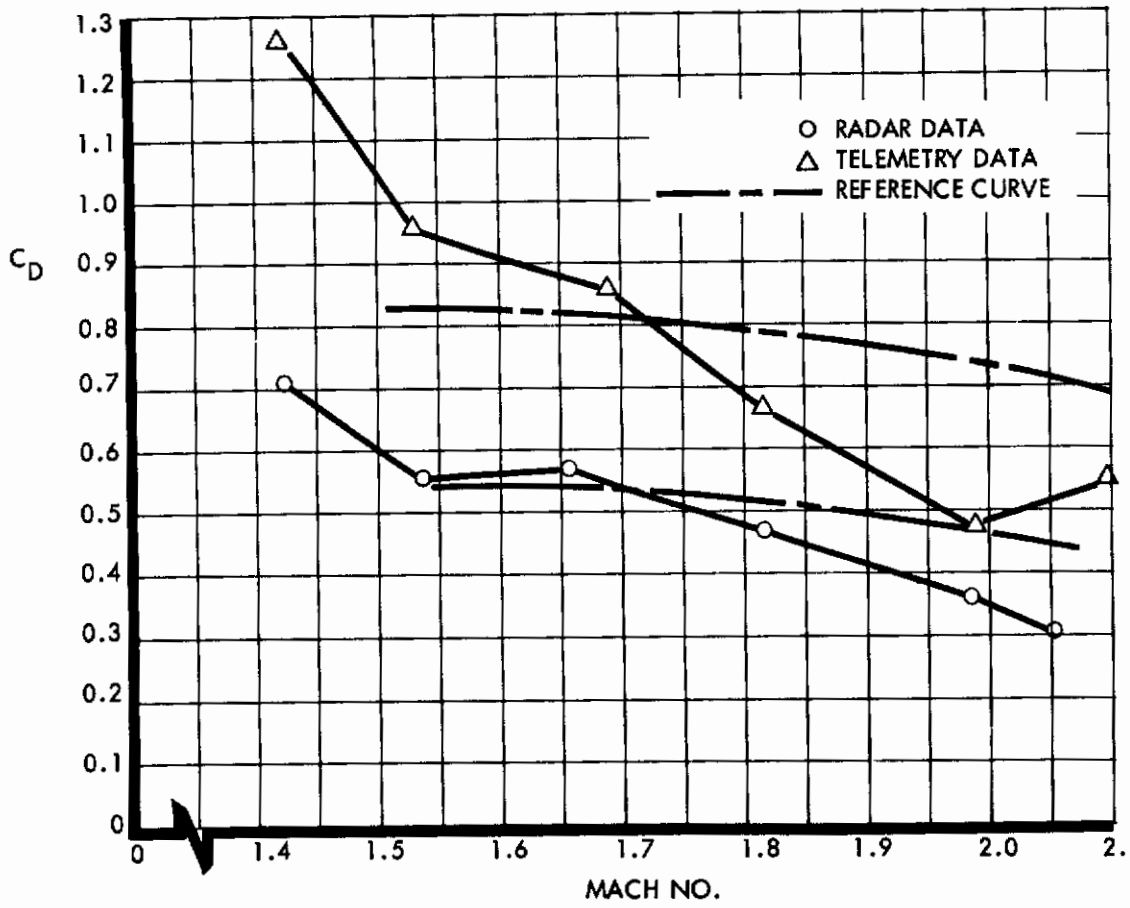

Figure 93. C_D versus Mach No. - Three-Stage Nike-Boosted Cree Flight Test

The accuracy of these solutions is greatly affected by small deviations in the flight test data, especially where more than one interpolation is required as in the three-stage Nike-boosted mission. To illustrate this, reference curves are shown in Figure 93 from Reference 6.

b. On-Board Camera Data. The on-board camera film from the first Nike-boosted test (10 October 1961) was analyzed, and a rather complete definition of the relative movements of the payload-Ballute system was established. Clearly visible in the film are landmarks (Figures 94 through 97) in the vicinity of Eglin Air Force Base which were used as references in the determination of the position of the Cree Missile relative to the flight path. The excursions of the Ballute with respect to the missile were determined by the position and attitude of the Ballute in the field of view of the camera. Figure 98 defines in a dimensionally exaggerated sketch all relative motions for which numerical values have been established (see Table 12).

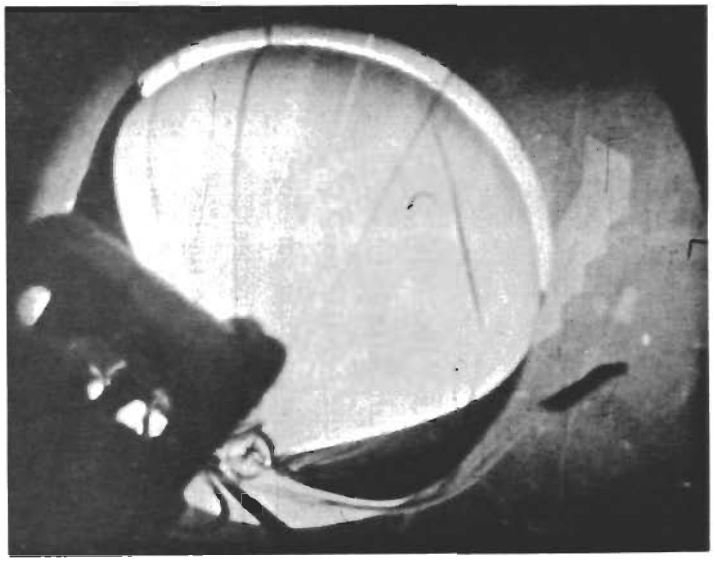

Figure 94. Ballute at Deployment + 7.2 Seconds with Eglin AFB in Background

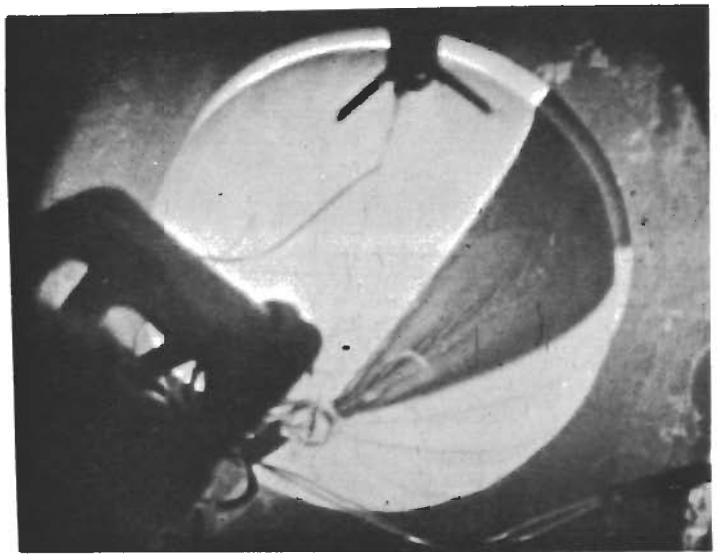

Figure 95. Ballute at Deployment + 8.2 Seconds with Coastline in Background and Cree Shadow on Ballute

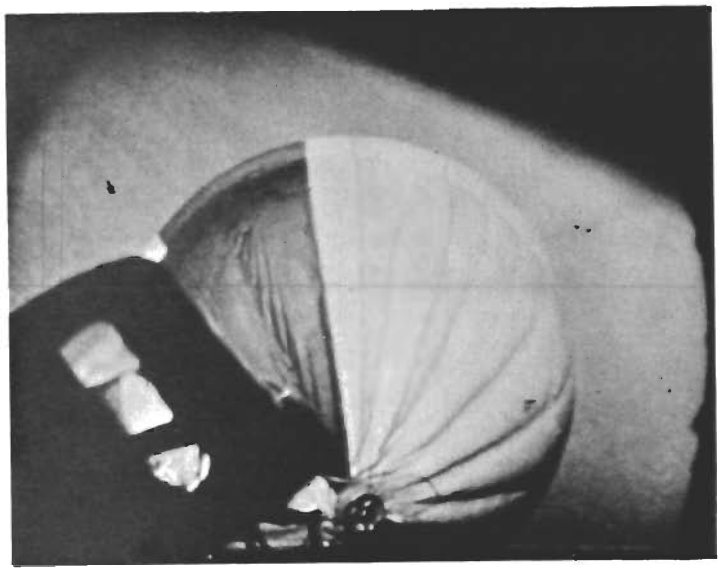

Figure 96. Ballute at Deployment + 12.2 Seconds with Horizon in Background

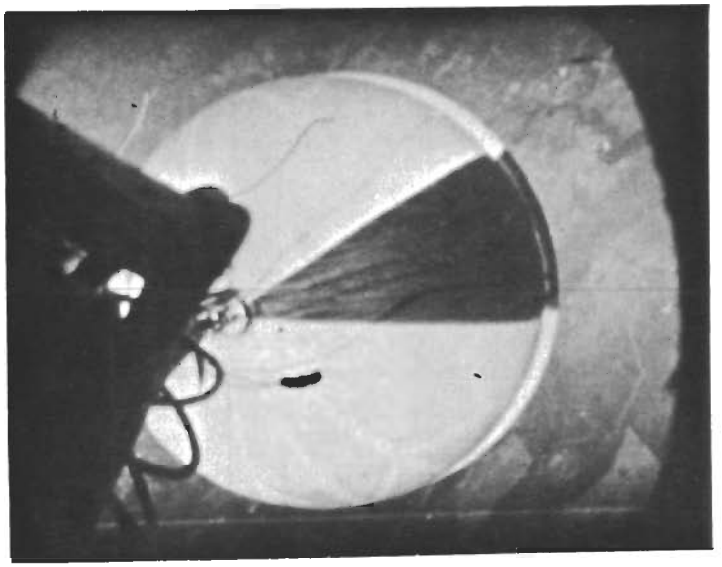

Figure 97. Ballute at Deployment +17.3 Seconds

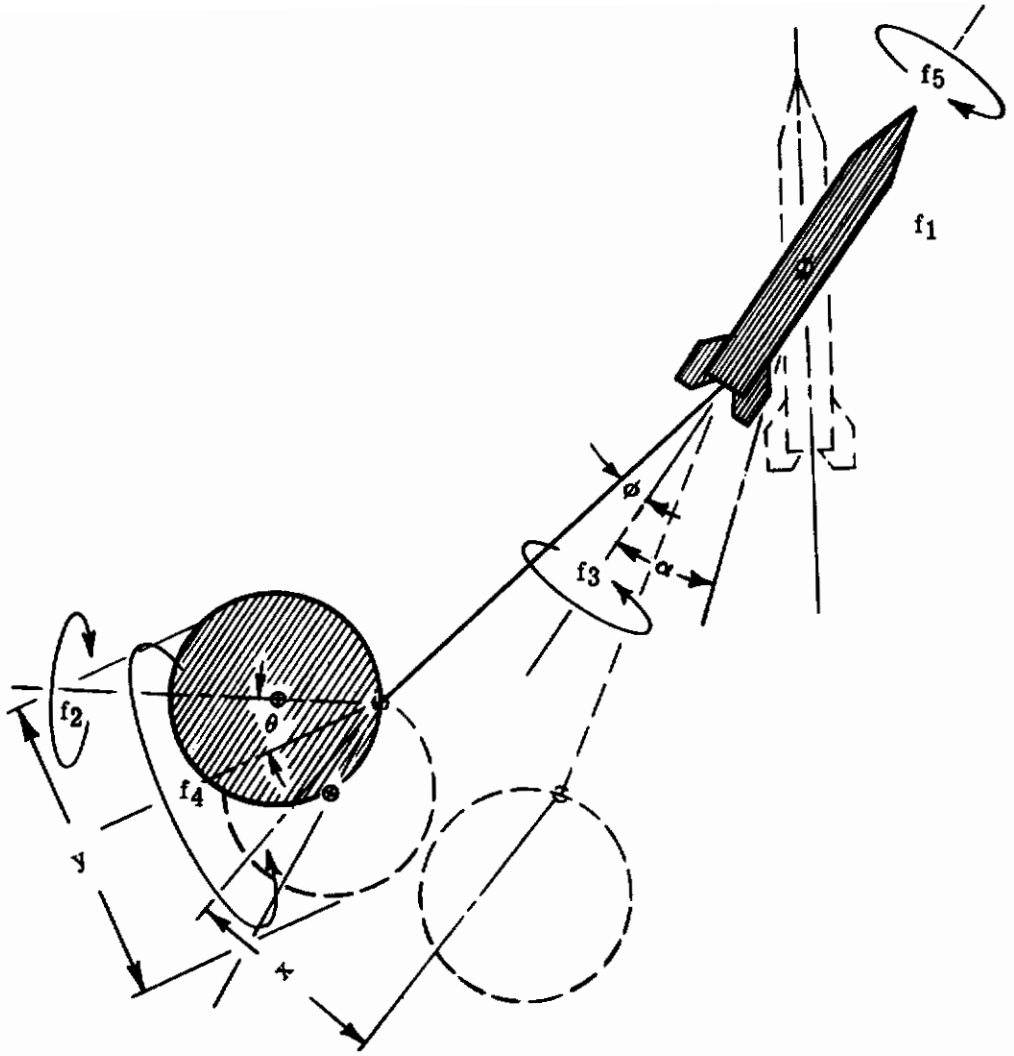

SYMBOL DESIGNATIONS

f_1 = missile rotation rate (cps)

f_2 = Ballute rotation rate with respect to riser line (cps)

f_3 = riser line excursion rate with respect to missile (cps)

f_4 = Ballute excursion rate with respect to riser line (cps)

f_5 = coning rate of missile axis with respect to flight path (cps)

x = amplitude of riser line excursions at Ballute (inches)

y = amplitude of Ballute excursions about riser line (inches)

θ = half angle of Ballute excursions about riser line (degrees)

ϕ = half angle of riser line excursions about missile (degrees)

α = half angle of missile axis deviation from flight path (degrees)

Figure 98. System Motions Schematic

Table 12. Ballute Stability - Nike-Boosted Tests

SYMBOL	VALUE	BASED ON	POSITION REFERENCE
f_1	2.08 cps	6 cycles	Horizon and ground reference
f_2	4.94 cps	10 cycles	Ballute stripes
f_3	0.19 cps	1 cycle	Field of view of camera
f_4	0.87 cps	6 cycles	Field of view of camera
f_5	0.68 cps	1 cycle	Ground reference
x	113.0 inches	6 cycles	Ballute diameter
y	100.0 inches	6 cycles	Ballute diameter
θ	74 degrees	6 cycles	Ballute diameter and position of center riser
ϕ	11 degrees	6 cycles	Riser length and balloon center displacement
α	12 degrees	1 cycle	Ground reference and displacement

SECTION 4

FLIGHT TEST DATA EVALUATION

A. GENERAL

Evaluation of the flight test data for the spherical decelerator requires correlation with data obtained in wind tunnel and analytical data if available. It is desirable to match the test conditions as closely as possible for objective trend judgment.

The objective of the flight test was to determine drag coefficient of the spherical Ballute (with fence), i.e. the effectiveness of this device as a decelerator deployed in the subsonic and lower supersonic Mach number range at altitudes in excess of 75,000 feet.

In general the drag of a spherical object is affected by the Reynold's number, Mach number, air flow turbulence, and surface roughness. The control and recording of these variables are rather difficult to achieve under the actual flight conditions. A brief explanation of how these variables affect the drag of a sphere is offered for proper understanding of this problem.

B. REYNOLD'S NUMBER EFFECT

The magnitude of Reynold's number determines the occurrence of transition from a laminar boundary layer to turbulent flow. This transition is characterized by a decrease in drag due to the fact that turbulent boundary layer possesses high kinetic energy which moves the point of separation further downstream. Thus the wake zone is reduced, and pressure drag is decreased.

Dependence of the drag coefficient on the Reynold's Number is indicated in Figure 99. Due to inherent qualities of each recording system employed (telemetry, theodolite, radar), it is difficult to expect a harmonious compatibility for the limited amount of data points that were obtained. For comparison, two curves (for the applicable regions) of Reference 7 are presented.

In supersonic region, it is shown that the test data (three-stage boost flight) exhibits the same upward trend in C_D as that of Refenece 7 at $R_e > 2 \cdot 10^5$. In subsonic region (drop test No. 4), the test points repeat the trend of Reference 7.

It is noted that only the trends are indicated here with no attempt to pinpoint the critical Reynold's number region for the tested configuration. Consequently it is assumed that the tests were conducted in the non-critical Reynold's number region.

C. AIR FLOW TURBULENCE EFFECT

External disturbance can cause boundary layer to change its state at Reynold's numbers that are lower than those at which transition occurs otherwise.

While wind tunnel turbulence factor is usually known as a function of the air stream velocity, this is not a case for the free-flight test. Although the absolute turbulence is low at altitudes above 75,000 feet, the local disturbances might have been present at the initial time of test or during the descent-ascent phase of the test. External disturbance can influence and explain, to some degree, the spread of points, i.e. the accuracy of data. Although no direct evidence of such a fluctuation is given, the probability of its occurrence is directly proportional to a number of tests.

D. MACH NUMBER EFFECT

The effect of Mach number on the flow around the spherical body is to increase the absolute pressure coefficient. In subsonic region (up to $M \approx 0.5$), the drag coefficient is not influenced by the Mach number significantly. According to Reference 8 at $M = 0.57$ (lower critical Mach number), the drag rises sharply due to a presence of shock waves of increasing strength.

The Reynold's number has a dominating effect in subsonic and partially in transonic regions on the drag,and in the supersonic region the Mach number has the controlling effect. Figure 100 depicts a comparison of drag coefficients obtained from the flight tests with experimental wind tunnel data summarized in Curve A. In addition, Curves B, C, and D show results of fabric covered sphere wind tunnel test, Reference 6. The flight test data for drop test No. 4 indicates general agreement in trend with the wind tunnel testing in M = 0.3 to 0.5 range. At $M \geq 0.5$ the theodolite recordings, which are considered more reliable, indicate the sharp increase in drag to conform with wind tunnel and theoretical results, Reference 8. The left-hand extremes are probably results of cumulative errors of instrumentation.

The two-stage boost theodolite data is also in agreement with drop test data and has the increasing drag trend at lower critical Mach number ($M \approx 0.5$). The three-stage boost flight data is not considered to be reliable especially at initial stages of deployment. Duration of useful tracking was also short; hence the amount of data is limited. The 1.5 to 1.8 Mach number range depicts telemetry data that is indicative for this region. The radar data obtained is questionable because of the rough tracking.

E. DYNAMIC PRESSURE

Based on the available information, the dynamic pressure during the test did not influence the test results significantly because of:

(1) No sharp changes in dynamic pressure were indicated during decelerator deployment and data-producing tracking.

(2) The magnitude of dynamic pressure was small, about 10 psf during two-stage boost.

F. INFLATION TIME

Data to evaluate time of inflation effects are considered inconclusive. Inflation of the Ballute as shown by Figure 44 shows that the Ballute did inflate and maintained inflation.

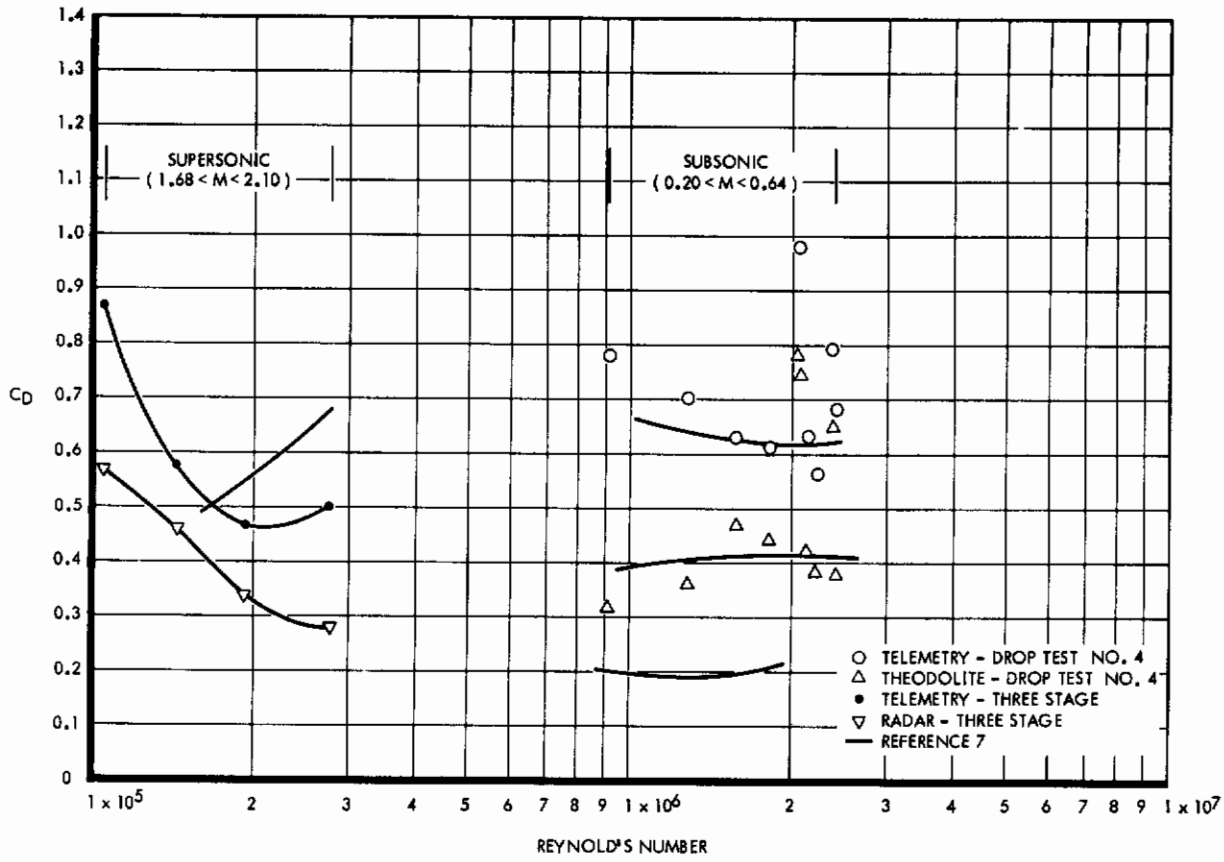

Figure 99. Ballute C_D versus Reynold's Number

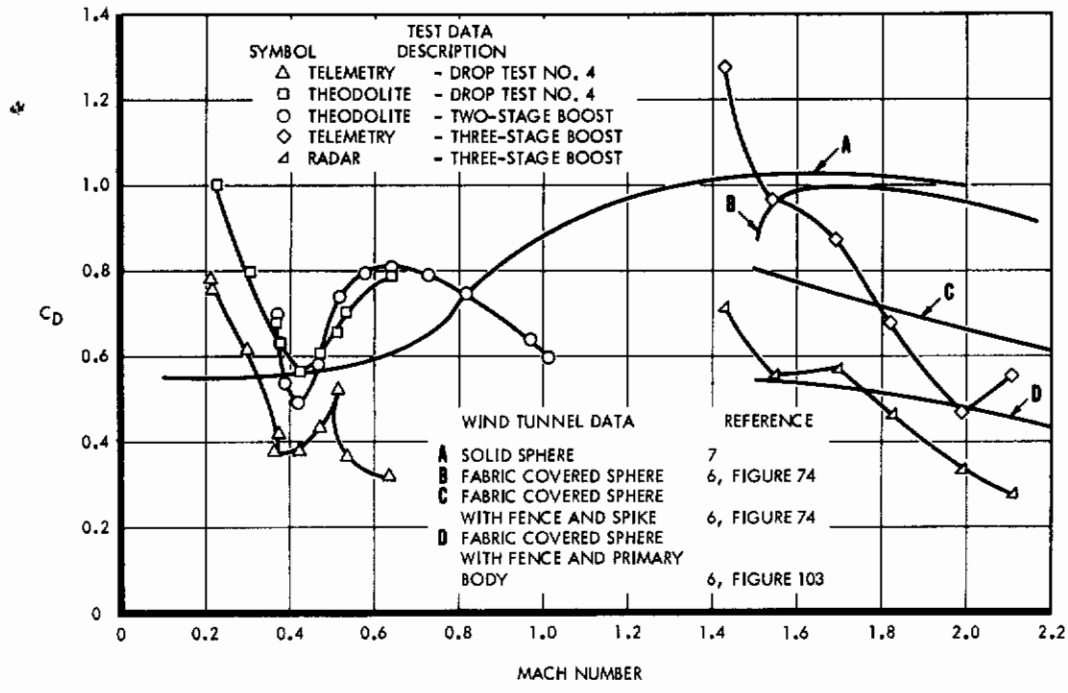

Figure 100. Ballute Flight Test Data Correlation

SECTION 5

CONCLUSIONS AND RECOMMENDATIONS

A. CONCLUSIONS

Examination of test data and over-all results of both the stratosphere balloon-launched test and the Nike-boosted test lead to the following:

(1) The objective of the free-flight full-scale tests to functionally evaluate the performance of the Ballute as an initial recovery device was accomplished.

(2) The performance of the Ballute as an inflatable drag device was considered adequate. However, improved stability of the system can be achieved by removal of the metal canister, inflation bottle, etc from within the Ballute. The vehicle used for these tests did not have space to store the inflation hardware due to the location of the camera and tensiometer. Satisfactory drag characteristics were demonstrated. The coefficient of drag, C_D, compares very well in the lower Mach number range of 0.25 to 0.80 to the wind tunnel test data. In the higher Mach number range up to Mach 2, the coefficient of drag does not compare quite as well to the wind tunnel test data as the lower Mach data. However, these C_D values were derived from only one test, and as previously mentioned the tracking for this test was considered very rough, resulting in scattered test points.

B. RECOMMENDATIONS

For further demonstration of the feasibility of the Ballute system for initial recovery applications, it is recommended that additional free-flight tests be conducted. Consideration should be given to a rocket boosted program that will encompass demonstration of the drag device at Mach 2.5 to 10 at altitudes from 200,000 feet to 250,000 feet with payloads in the range of 250 to 500 pounds.

The Ballute design should incorporate ram-air inflation with preinflation for high-altitude deployment. The ram-air will provide positive inflation throughout the free-fall down to impact.

APPENDIX I

THERMAL ANALYSIS OF BALLUTE CANISTER

A. DISCUSSION

The purpose of this analysis is to determine whether the Ballute container wall temperature could be controlled to the extent that at the time of deployment the Ballute fabric would be between -25^{o} and $+160^{o}F$.

In view of the Ballute package within the canister, the following assumptions were then made:

(1) The portions of the Ballute that are in contact with the container wall will be at the container wall temperature.

(2) Heat absortion at altitude will be greater than heat lost during ascent.

B. ANALYSIS

A heat balance was made based on a solar exposed, non-rotating cylindrical container. The following equations were set up based on an average ascent of 1200 feet/minute up to about 80,000 feet and then one hour above 80,000 feet prior to release from 100,000 feet. The ascent to 80,000 feet was taken for cooling by which time convection becomes negligible, and the hour from 80,000 to 100,000 feet was taken for radiation heating.

1. Cooling

$$WC_P \frac{dt}{d\theta} = h\,(T-T_a)$$

where

C_P = specific heat of container wall, BTU/lb - ^{o}R

h = convective heat transfer coefficient, BTU/hr-ft^2 - ^{o}R

T = container wall, temperature, ^{o}R

T_a = ambient temperature, ^{o}R

W = unit weight of container, lb/sq ft

dt = change in wall temperature, ^{o}R

$d\theta$ = change in time, hr

The heat transfer coefficient, h at sea level for 1200 feet/minute air velocity, is approximately 4 BTU/hr-ft - R^{o}, and it was scaled for altitude from

$$h = h_0 \left(\frac{\rho}{\rho_0}\,\frac{\mu_0}{\mu}\right)^{0.75}\,\frac{K}{K_0}$$

ρ = air density (from Reference 3)

μ = viscosity (from Reference 3)

K = thermal conductivity

Table 13 shows the heat transfer coefficient and ambient temperatures at altitudes to 100,000 feet.

Table 13. Heat Transfer Coefficient and Ambient Temperatures at Altitudes (Properties from Reference 3)

ALTITUDE (Z) (ft x 10^{-4})	0	1	2	3	4	5	6	7	8	9	10
h	4	2.5	1.5	0.85	0.45	0.19	0.10	0.05	0.025	0.012	0.005
T_a	520	483	448	412	390	390	390	390	390	403	420

2. Heating

Neglecting heat interchange between the container and the earth (direct earth radiator and scattered solar reflectivity), the following equations were applied:

$$Q_1 = Q_2$$

$$Q_1 = \frac{2}{\pi} C_s \alpha$$

$$Q_2 = F \epsilon \delta \left(T^4_c + T^4_h \right)$$

and

$$F \epsilon \delta \, T^4_c = \frac{Kt}{144} (T_h - T_c)$$

where

Q_1 = heat absorbed
Q_2 = heat radiated
C_s = solar constant, BTU/hr-ft^2
F = view factor (approximately 0.5)
K = thermal conductivity BTU/hr-ft^2 - ^oR/in.
L = length, ft
T_c = average temperature of cold side, ^oR
T_h = average temperature of hot side, ^oR
t = wall thickness, in.
α = solar absorptivity
ϵ = emissivity
δ = Stephan-Boltzman constant
π = 3.14.

This results in the following two equations:

$$T_h = T_c + \frac{144 \, F \delta \, L}{Kt} \left(\frac{T_c}{100} \right)^4$$

$$T_c = 100 \left(\frac{2 C_s \alpha}{\pi F \delta \epsilon} - \left\{ \frac{T_c}{100} \left[1 + \epsilon \left(\frac{T_c}{1000} \right) \right]^3 \right\}^4 \right) \quad .$$

These equations were solved graphically.

3. Cooling After Drop

The equation used for the cooling is applied:

$$WC_P \frac{dT}{d\theta} = h(T - T_a).$$

The convection heat transfer coefficient (h) is corrected for velocity by

$$h_a = h \left(\frac{V_a}{V_0} \right)^{0.75}$$

where

V = velocity, feet/minute

h_a = heat transfer coefficient at altitude and 1200 feet/minute.

and

a = condition.

C. RESULTS

Using an emmissivity of 0.9 flat paint (black or white) and a solar absorptivity of 0.25 for flat white and 0.90 for flat black and selecting the upper temperature limit for the hot side (160°F), the area ratio is about 40 percent black. Considering the diffusivity of the container material and the thickness, alternating 1/2-inch black strips and 3/4-inch white stripes should be adequate for temperature limits.

D. CONCLUSIONS

The Ballute material will have small areas that will drop below -25°F temporarily on the way up and then will rise to temperatures between 40 and 160°F at altitude. When the Ballute is dropped, there will be no noticeable change in temperature on the Ballute fabric until the container is ejected. Neglecting solar radiation during the drop, it will take about 10 seconds for the Ballute material to reach -25°F, after which it will probably approach -40 to-50°F at 55,000 feet.

The leading edge ring of the Ballute canister, which surrounds the reel, was painted black. The purpose of this was to keep the reel oil temperature in the vicinity of 30°F. Since the reel is housed in a non-sealed area, no analytical attempt was made to determine the reel oil temperature.

APPENDIX II

REFERENCES

1. Wakefield, Treon, and Knechtel, Effects of Centerbody Length and Nose Shape on the Transonic Characteristics of Low-Fineness Ratio Bodies of Revolution with a Flared Afterbody, NASA TMX-366, May 1960. (CONFIDENTIAL Report)

2. Krause, R., and Haldeman, W. F., Vertical Descent Trajectories Including Re-entry into the Atmosphere, AFMDC TR 58-4, March 1958.

3. The ARDC Model Atmosphere, 1959, AFCRC-TR-59-267, Air Force Surveys in Geophysics No. 115, August 1959.

4. Vickery, W.K., Cree II Vertical Probe Firing Report, APGC TN 61-36, September 1961.

5. Askania Cinetheodolite Reduction Procedures, APGC-TR-57-114(U), dated November 1957, reprinted January 1960, ASTIA Document No. 142376.

6. Nebiker, F.R., Feasibility Study of an Inflatable Type Stabilization and Deceleration System for High-Altitude and High-Speed Recovery, WADD TR 60-182, Goodyear Aircraft Corporation, November 1961.

7. Sabin, C.M., The Effects of Reynold's Number, Mach Number, Spin Rate, and Other Variables on the Aerodynamics of Spheres at Subsonic and Transonic Velocities, BRL, Memorandum Report No. 1044, November 1956.

8. Shapiro, A.H., The Dynamics and Thermodynamics of Compressible Flow, Vol I, 1953.